MASTER

An analysis of the performance of a thermal conductivity detector

Dassen, A.G.M.

Award date:
1990

AN ANALYSIS OF THE PERFORMANCE OF A THERMAL CONDUCTIVITY DETECTOR

by

A.G.M. Dassen

Afstudeerhoogleraren:	Prof.dr.ir. H.L. Hagedoorn
	Prof.dr.ir. C.A. Cramers
Coaches:	Dr.ir. C.H. Massen
	Dr.ir. J.A. Rijks

Afstudeerverslag, TUE

Oktober 1990

The author wishes to thank Dr. Leon Blumberg of Hewlett Packard, Avondale, PA, USA for the fruitful discussions we had during my visit at the HP plant. Also the assistance of Dr. A. Hirschberg of Aeroacoustic/Gas Dynamics group of the Eindhoven University of Technology is gratefully acknowledged.

ABSTRACT

Considering the Minimum Detectable Concentration, the actual performance of all Thermal Conductivity Detectors (TCD) used in Gas Chromatography is far from theoretical expectations. In this theoretical concept the thermal noise of the sensing element, the filament, is assumed to circumscribe the fundamental detection limit.

So far, the achieved Minimum Detectable Concentration is approximately 100 PPB. This is 2 orders of magnitude above what can be calculated as the theoretical detection limit for this type of detector.

It is tried to estimate the influence of several processes that occur in an operating TCD cell on its Signal to Noise Ratio. It is shown that (statistical) fluctuation in the heat conductivity of the gas in a μl–volume cell and the influence of filament vibrations are negligible. The influence of an unsteady wall temperature of the block (which forms the cavity which contains the filament) is a parameter which has to be investigated further although it is possible to eliminate its influence by applying precise thermal control systems.

In this report, the influence of the flow in the cell on the Signal to Noise Ratio is dealt with profoundly. One of the phenomena which is connected with flow in a heated cell is convective heat transfer because the gas entering the cell will be heated up. Although convective heat transfer will have an negligible effect on the response of the filament it can be the main source of noise in case of flow fluctuations and so limit the Minimum Detectable Concentration. The convective heat transfer is correlated with the speed and the heat conductivity of the gas as well as with the density and the viscosity of the gas. An expression for the (flow) noise as a function of these parameters is suggested. This is done by considering the flow of helium in a 3.5 μl cell (HP 5890 A TCD, Avondale PA, USA). From an analytical

solution of the mass, momentum and energy equations for the flow in the cell it can be concluded that 0.3% of the applied heat is transferred by convection if the flow is 10 ml/min. For that, some appropriate simplifications and assumptions for the flow had to be made. After solving the mass, momentum and heat equations of the flow in this cell numerically, it was found that approximately 0.08% of the applied heat is transferred by convection if the flow is 10 ml/min. This result was accomplished by using a software package which applies the Finite Elements Analysis method to solve flow problems. The amount of convected heat is approximately found to be directly proportional to the flow rate for both concepts.

The flow noise of this cell was determined by monitoring its filament signal in three different ways. A lock-in amplifier, oscilloscope and spectrum analyzer were used for this purpose. Although the result obtained with the frequency analyzer are the most accurate the three results show reasonable agreement. From the measurement of the filament noise with the frequency analyzer, caused by known (5 Hz) fluctuations in the flow rate, it appears that 0.01% of the applied heat is transferred by convective heat transfer if the flow is 10 ml/min.

As an additional result of the numerical simulation it can be shown by plots of the flow that the thermal and hydrodynamic entrance lengths for the actual flow rates in the cell exceed the theoretical values obtained with the boundary layer theory, many times. This could be expected since the boundary layer theory is useless for small (<10) Reynolds numbers.

The developed regions, where the flow has established temperature and velocity profiles, are however at least 15 times larger than the entrance regions, where the flow has unestablished profiles. This implies that the temperature of the gas which reaches the part of the cell which contains the filament will be at the temperature of the wall of the block. Assuming that helium is an ideal gas, so it will expand according to the ideal gas law, the energy density of the carrier gas (helium) in the cell (the energy per unit of cell length) is constant in the entire cell. This implies that the mean velocity of the flow only increases in the thermal entrance region where the gas is heated up. Consequently the thermal heat conductivity is the only gas parameter affecting the total transferred heat in the developed region. Here the cell operates like an ideal Thermal Conductivity Detector, assuming uniform filament temperature and block temperature.

CONTENTS

Symbols and Values

The Cell

A = cross-sectional area of the cell ($2.8\ 10^{-7}\ m^2$)

A_F = surface area of the filament ($5.1\ 10^{-7}\ m^2$)

C_F = heat capacitance of the filament ($4.34\ 10^{-6}$ J/K)

G = geometrical factor ($\simeq 1.63$)

G_H = heat conductance of the cell ($G\lambda L_F$) ($4.06\ 10^{-3}$ W/K at 453 K)

i = current through the filament (0.16 Amp)

L_F = length of the filament ($1.27\ 10^{-2}$ m)

P_0 = input power applied to the filament (0.45 W)

P_C = power conducted by the carrier gas (W)

P_{CV} = power dissipated by convective heat transfer (W)

P_F = power dissipated by mass flow (only in chapter 2) (W)

P_R = power dissipated by radiation (W)

R_0 = resistance of the filament at 273 K (9.41 Ω)

R_F = resistance of the filament at 550 K (17.7 Ω)

r_F = radius of the filament ($6.35\ 10^{-6}$ m)

r_W = inner radius of the block ($3\ 10^{-4}$ m)

T_F = temperature of the filament (550 K)

T_W = temperature of the block (440 K)

V = voltage across the filament (2.81 V)

α = temperature coefficient of resistivity of the filament ($1.61\ 10^{-3}\ K^{-1}$ at 550 K)

ϵ = emissivity of tungsten (0.06)

ρ_F = density of tungsten ($19.3\ 10^3\ kg/m^3$)

Helium

c_p = *specific heat* ($5.192\ 10^3$ J/K)

η = *viscosity* ($4.17\ 10^{-8}T+7.56\ 10^{-6}$ kg/m s if $270\ K \leq T \leq 550\ K$)

λ = *heat conductivity* ($3.38\ 10^{-4}T+4.24\ 10^{-2}$ J/m s K)

ρ = *density* ($49/T$ kg/m^3)

ρ_0 = *density at 273 K* (0.179 kg/m^3)

Dimensionless Numbers

Re = *Reynolds number* ($ur_W\rho/\eta$)

Pr = *Prandl number* ($\eta c_p/\lambda$)

Nu = *Nusselt number* ($\alpha_T r_W/\lambda$)

Constants

k = *Boltzmann constant* ($1.38\ 10^{-23}$ J/K)

σ = *Stephan-Boltzmann constant* ($5.67\ 10^{-8}$ J/m^2 s K^4)

Others

C = *electrical capacitance* (C/V)

f_1 = *end frequency of the sweep signal* (Hz)

f_0 = *start frequency of the sweep signal* (Hz)

f_p = *peak frequency* (Hz)

Δf = *bandwidth* (Hz)

F_V = *volumetric flow* (in ml/min)

F_V' = *volumetric flow* (m^3/s)

H = *plate height* (m)

l_{MF} = *mean free path* (m)

L_C = *length of the column* (m)

L_{EH} = *hydrodynamic entrance length* (m)

L_{ET} = *thermal entrance length* (m)

m = *mass of a propane molecule (kg)*

n = *density of propane molecules* (m^{-3})

p = *pressure* $(kg/m\ s^2)$

R = *electrical resistance* (Ω)

t_M = *time constant of the Lock-in Amplifier (s)*

t_S = *time the sweep lasts (s)*

T_C = *detector fill time (s)*

T_{AV} = *average temperature (K)*

u = *velocity (m/s)*

V_{F0} = *amplitude of the filament signal (only in paragraph 9.2) (V)*

V_{LIA} = *output of the Lock-in Amplifier (V)*

V_{REF} = *voltage of reference signal (V)*

V_{REF0} = *amplitude of the reference signal (only in paragraph 9.2) (V)*

x = *molefraction of propane in a helium-propane mixture*

α_D = *molecular thermal diffusity* (m^2/s)

α_T = *heat transfer coefficient (J/s K)*

∇ = *differential operator* (m^{-1})

θ = *temperature above ambient (or block) temperature (K)*

σ = *effective collision cross-section* (m^2)

σ_K = *peak standard deviation (s)*

τ_H = *time constant (s)*

GENERAL INTRODUCTION TO GAS CHROMATOGRAPHY

Gas chromatography is a technique widely used in the field of analytical chemistry for the separation and measurement of the constituents of a gaseous sample.

A gas chromatograph consists of three main components: a sample injection system, a long narrow separating column and the output detector, as shown in Fig. 1.

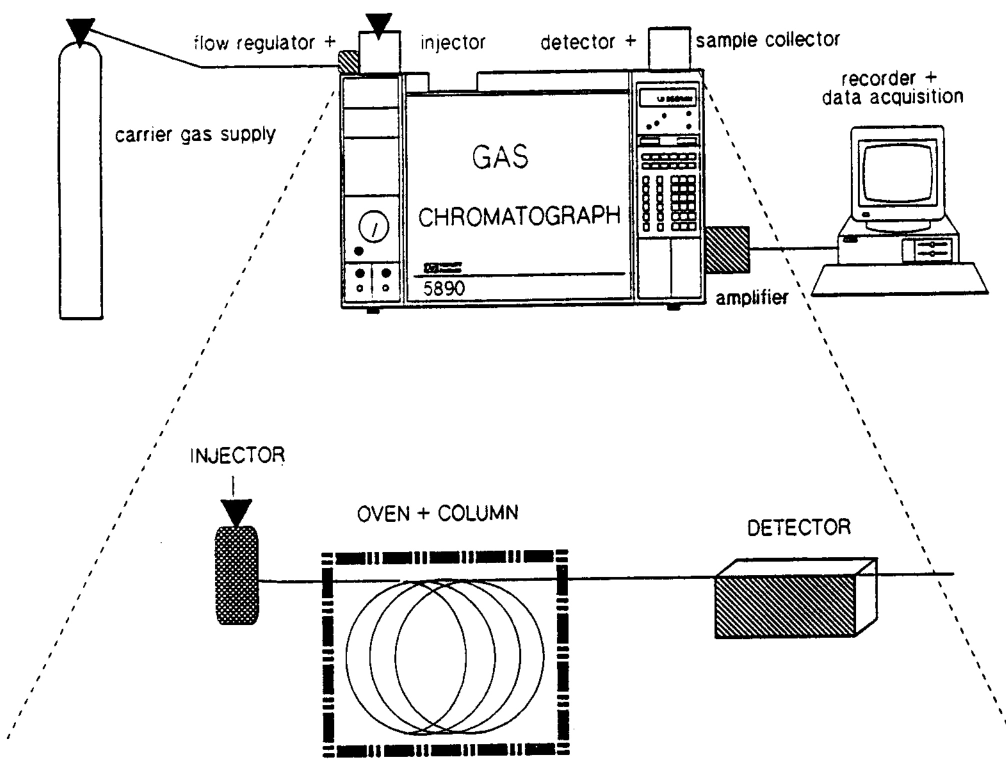

Fig. 1 Schematic design of a Gas Chromatograph.

Separation of the sample vapours is achieved via their differential migration rates through a (capillary) column. The sample vapours are introduced at the column inlet and are swept through it by an inert carrier gas. The column is lined with a (liquid) stationary phase, a substance capable of absorbing and desorbing each of the constituents of the gaseous sample.

The migration rate of each individual vaporized component of the sample matrix along the column depends on the carrier gas velocity and the degree to which the vapour is solved in or absorbed by the stationary phase. In order to affect the degree of absorbtion and so the migration rates, the column is placed in an oven.

The migration rates can be affected by setting or programming the oven temperature (rate). The mixture of sample gas vapours, injected into the column almost as a single pulse, is separated into components as it travels through the column. Each component travelling at a different rate and emerging at a specific time. The output of the column is thus a series of vapour peaks separated by regions of pure carrier gas. The output gas stream is then passed by a detector which measures a specific property of the gas stream, such as the thermal conductivity, which can be related to the concentration or the mass of the sample gas in the carrier gas.

The detector output signal, or chromatogram, is also a series of peaks which can be analyzed to determine the identity and the concentration of the component vapours in the injected sample.

The identity of the compound is determined from the retention time of that gas and the concentration or quantity of the gas is typically found by integration of that output peak.

1 Introduction

The use of capillary columns (less then 50 μm inner diameter) in gas chromatography makes it possible to separate components within a time less then a few seconds. The sample capacity of these columns is in the order of a few μlitres, the peak widths of the eluted substances is the order of tenths of a second.

These narrow peaks require compatible cell detector volumes, in order to avoid peak distortion.

Even though the various ionization detectors are generally considered to be more sensitive, the Thermal Conductivity Detector (TCD) seems to have lower detectivities when we are moving towards miniaturized systems.

The sensing element of a TCD consists of a resistor with a relatively high temperature coefficient of resistivity. The detector is operated by heating this resistor by applying electrical power. The resistor reaches an equilibrium temperature by balancing the applied power and the power which its dissipates through the carrier gas output stream. Any change in the concentration of the gas mixture, which means a change in the heat conductance, is reflected in a change in the filament temperature. This causes a change in the filament resistance, so in the one or the other way this produces an electrical treatable signal.

The detector is preferably operated in a constant temperature configuration in order to reduce the temperature effects of gases and the detector support and to protect the detector from thermal runaway.

The sensitivity of low-volume or miniaturized TCD's is not as low as what is expected from some (simple) theoretical considerations. The gap between the practical achieved Minimum Detectable Concentration (MDC) and the theoretical calculated MDC is roughly more than 2 orders of magnitude.

The main goal of the research was to get insight in all processes which take place in a Thermal Conductivity Detector in order to find the cause of the practical achieved Signal to Noise Ratio.

The TCD considered in this report has an internal volume of 3.5 μl. It is not what is called a Micro TCD or miniaturized TCD. These TCD's have internal volumes in the order of nanolitres.

Its small time constant makes it, however, possible to deal with peaks with a width in the order of a second, without significantly increasing the width of the output signal.

The TCD considered is designed by Hewlett Packard. According to its manual its MDC is less then 400 picograms propane per ml of carrier gas which is here helium.

The reason why the HP 5890 A detector was taken as an example of a detector which matches with the use of capillary columns is twofold.

One reason was because of the special design of the cell and the easy handling of the detector when it is used as the output detector on the HP 5890 Gas Chromatograph. The design of this cell is different compared to other actual TCD designs. It provides us of the opportunity to perform experiments concerning the influence of the flow on the (noise) signal.

The co-operation between the Avondale division of Hewlett Packard and the group of Instrumental Analysis of the Eindhoven University of Technology on the area of developing smaller and faster analysis methods and equipment formed another reason. Because of the mutual interest, all the information concerning this cell, was accessible.

2 The TCD Response

2.1 Introduction

This chapter will develop a theoretical basis for predicting the performance of the detector. The theory is used to predict the response, sensitivity and signal to noise ratio of the detector as a function of its quantities and the flow quantities.

This chapter will first discuss a thermal model which is appropriate to use to handle the thermal characteristics of the detector structure. The assumption here is that the detector is always in thermal equilibrium with the carrier gas stream.

The model will be applied to the constant temperature driving circuit, and the response of the detector in this configuration will be determined. The HP detector operates in this mode, the response of the cell in this mode will be compared to the magnitude of the fundamental noise.

This will finally yield a form for the theoretical signal to noise ratio of the cell. This theoretical signal to noise ratio will be compared to what is achieved in practice. The thermal model will also provide the possibility to derive an expression for the thermal time constant of the cell.

2.2 Thermal Model

In order to calculate the operating point and operating point characteristics of the detector it is necessary to formulate a thermal and electrical model of the detector structure. For this, appropriate simplifications and approximations are applied to the model to allow the calculation of the desired quantities. Fig. 2 shows a schematic idea of a heated TCD-filament. It is assumed in the sequel of this report that the cell consists of two exact concentrative cylinders.

The filament is heated up by applying electrical power. The resistor reaches an equilibrium temperature by balancing the applied power and the power it dissipates. For the HP cell, the temperature difference between filament and block is kept fixed after the filament temperature is chosen. According to the manual this difference is 110 K when the filament has a temperature

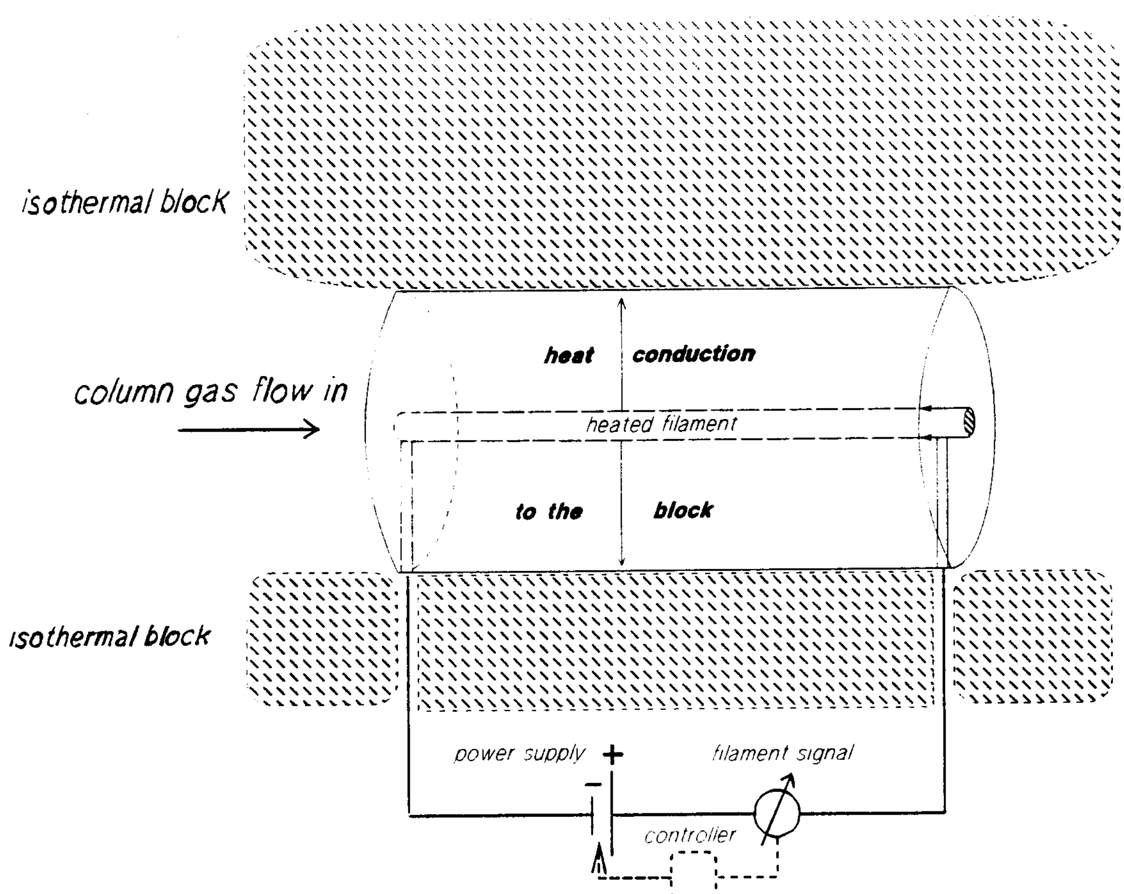

Fig. 2 Schematic idea of a Thermal Conductivity Detector

of 550 K which is a normal temperature to operate on.

The input power to the filament is given by:

$$P_0 = i^2 R_0 (1+\alpha T_F) \tag{1}$$

Where i is the current through the filament, R_0 the filament resistivity at 273 K and α is the temperature coefficient of the wire at its operating temperature.

Fig. 3 shows an electron microscope picture of a part of the filament, 2000 times expanded. This picture is made by a member of the group of Physical Chemistry of the Eindhoven University of Technology. It was confirmed by a X-ray diffraction measurement that the filament consists for about 97% of tungsten and for about 3% of rhenium.

The resistance of the passivated filament at 273 K, R_0, is 9.41 Ω, its temperature coefficient, α at 550 K is 1.61 10^{-3} K^{-1}.

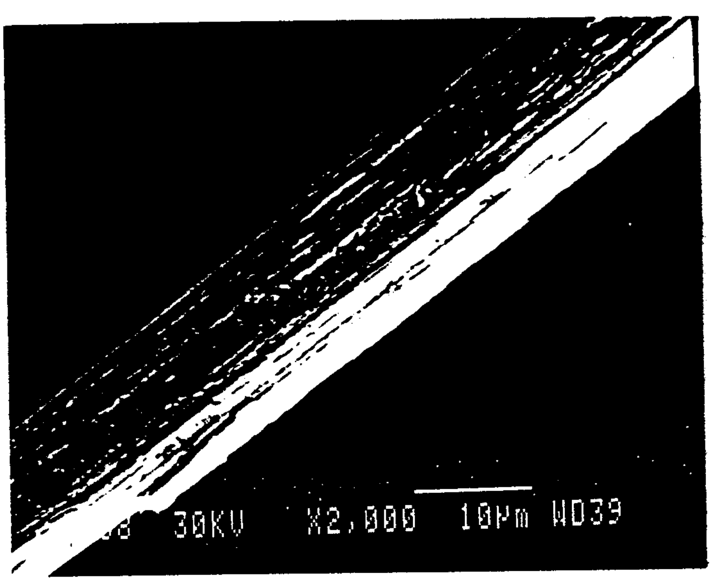

Fig. 3 Electron microscope picture of a part of the Rhenium-Tungsten filament, 2000 times enlarged.

The power conducted by the carrier gas is given by:

$$P_C = G\lambda L_F(T_F - T_W) \quad (2)$$

where λ is the heat conductivity of the carrier gas (helium), L_F is the length of the filament (1.27 10^{-2} m for the HP filament) and G is a dimensionless geometrical factor. T_F is the filament temperature and T_W is the block temperature.

The heat conductivity of helium for temperatures between 450 K and 550 K is given by (1):

$$\lambda = 3.38\ 10^{-4}T + 4.24\ 10^{-2} \quad (\mathrm{J/m\ s\ K}) \quad (3)$$

where T is the temperature at which the helium is.

The geometrical factor for the heat conductance between two coaxial cylinders is given by:

$$G = 2\pi/\ln(r_W/r_F) \quad (4)$$

where r_W is the radius of the outer cylinder, the block, and r_F is the radius of the inner cylinder, the filament.

The total heat conductance, $GL_F\lambda$, at an average gas temperature of 453 K is 4.05 10^{-3} W/K. The power transferred by heat conduction is equal to 0.45 Watt.

As a first approximation it will be assumed that the power transferred by mass flow (convection) and by radiation will be negligible. We will justify this approach by calculating its magnitudes.

The power transferred by radiation is given by:

$$P_R = \sigma\epsilon A_F(T_F^4 - T_W^4) \tag{5}$$

where σ is the Stephan-Boltzmann constant, A_F is the area of the filament and ϵ is the emissitivity of the material the filament is made of.

All filaments used in TC cells are made of a material with a high temperature coefficient and a high melting point. Of all common metals, nickel, iron and tungsten have the highest temperature coefficients and the highest melting points. The HP filament consists for 97% of tungsten. The emissitivity of tungsten is 0.06. Its melting point is 3400 K.

The power transferred by radiation is about 9.3 10^{-5} Watt.

As a first approximation, the amount of power transferred by mass flow from the detector is given by:

$$P_F = \rho c_p \theta F_V \tag{6}$$

where c_p is the heat capacity of the helium carrier gas, ρ is the density of helium, θ is the average helium temperature above its temperature before it enters the cell, and F_V is the carrier gas volumetric flow rate.

It is calculated in chapter 7 of this report that the average temperature of the helium is about 13 degrees Kelvin above the temperature it had before it entered the cell. It will also be shown that its temperature is equal to the block temperature right before it enters the cell.

Concerning its heat capacity, helium behaves like an ideal gas over a wide range of temperatures. This means that its specific heat per mole at constant pressure is approximately equal to:

$$c_p = 5/2\ R \tag{7}$$

Where R is the molar gas constant (8.134 J/mole K). It remains constant with temperature up to 6000 K or more. This because helium is a monatomic gas and the molecules posses translational energy only. The molar weight of helium is 4 gr so the heat capacity at constant pressure is found to be $5.192\ 10^3$ J/kg K.

According to Gay-Lussac's law, which says that in a gaseous system at constant pressure, the product of the temperature of any ideal gas and its volume is a constant, the density of helium as a function of its temperature can approximately be written as:

$$\rho(T) = \rho_0 T_0/T \tag{8}$$

where ρ_0 is the density of helium at a certain temperature T_0 (in Kelvin). In this report T_0 is 273 K. The density of helium at this temperature is equal to the molar weight (4 gr) divided by the molar volume at this temperature (22.3 l). For the density of helium as a function of its temperature in degrees K can be found:

$$\rho(T) = 49/T \tag{9}$$

At a flow rate of 10 ml/min ($1.7\ 10^{-7}$ m^3/s), which is high for the considered cell, the detector would only lose $1.2\ 10^{-3}$ W by mass flow. This effect is relatively small, but can be important in certain circumstances which will be discussed in the following chapters.

Finally, the current through the filament and the voltage drop across it, can be calculated. If the total power dissipated is 0.45 W if the cell is in thermal equilibrium and the electrical resistance at 550 K is 17.7 Ω, the voltage drop across the filament is 2.81 Volts and the current through it is 0.16 Amp.

2.3 The heat conductivity of a binary mixture

In the previous paragraph it is made acceptable that the power applied to the filament is almost completely transferred by heat conduction to the wall.
The energy necessary to keep the filament at a fixed temperature above the block temperature is thus approximately only a function of the heat conductivity of the gas in the cell and a function of the geometry of the cell.
So, the heat conductivity of the carrier gas has to differ as much as possible from the heat conductivity of the sample gases.
The signal change has to be as large as possible whenever a sample gas with a different heat conductivity as the carrier gas enters the cell. The heat conductivity of some common gases are listed in table 1 (1).
It can be seen that the heat conductivity of hydrogen and helium is at least 3 times larger than the heat conductivity of all other gases. Although

TABLE 1

Heat Conductivity of some common gases at 300 K (J/m s K)

Gas	λ (J/m s K)
Hydrogen	0.1815
Helium	0.1499
Neon	0.0493
Argon	0.01772
Nitrogen	0.02598
Oxygen	0.02674
Benzene	0.0104
Carbon dioxide	0.01662
Methane	0.0343
Ethane	0.0218
Propane	0.0183
n-Butane	0.01599

the heat conductivity of hydrogen is about 20% higher than the heat conductivity of helium, helium is the most commonly used carrier gas because of its inertness and safety.

So, when another gas than helium enters the cell the heat conductivity will decrease which means that the power supplied to the filament has to be adjusted in order to keep the cell in thermal equilibrium.

Before the response of the detector can be determined a relation has to be derived between the thermal conductivity of the gas in the cell and the concentration of sample in the carrier gas.

Fig. 4 shows the heat conductivity of a helium-propane mixture at a temperature of 328.4 K. It can be seen that the change in concentration is not linear with the change in concentration. This is only true if the mole fraction of propane is smaller than 0.05. A general expression for the heat conductivity of a binary mixture is given by (2):

$$\lambda = \lambda_1/(1+A_{12}x_2/x_1) + \lambda_2/(1+A_{21}x_1/x_2) \tag{10}$$

where λ is the thermal conductivity of the mixture, λ_1 and λ_2 are the thermal conductivities of the components, x_1 and x_2 are the volume fractions of the two components, and A_{12} and A_{21} are coefficients which can be derived from knowledge of the masses, diameters and other properties of the gases.

Touloukian (1) gives numerous data for the heat conductivity of binary mixtures at several temperatures. Unfortunately, the heat conductivity of a helium-propane mixture is only shown for 328.4 K (page 346). The heat conductivity of a helium-nitrogen mixture at several temperatures is shown on page 342 and for a helium-oxygen mixture on page 344.

Studying these figures, it can be found that the ratio of the derivative of the heat conductivity and the heat conductivity itself is approximately independent of the temperature. Assuming that the behaviour of the thermal conductivity of a helium-propane mixture is no exception to this rule, it can be found that:

$$\frac{\Delta\lambda}{\Delta x}\frac{1}{\lambda} = 3.44 \quad (\text{for} \quad x < 0.05) \tag{11}$$

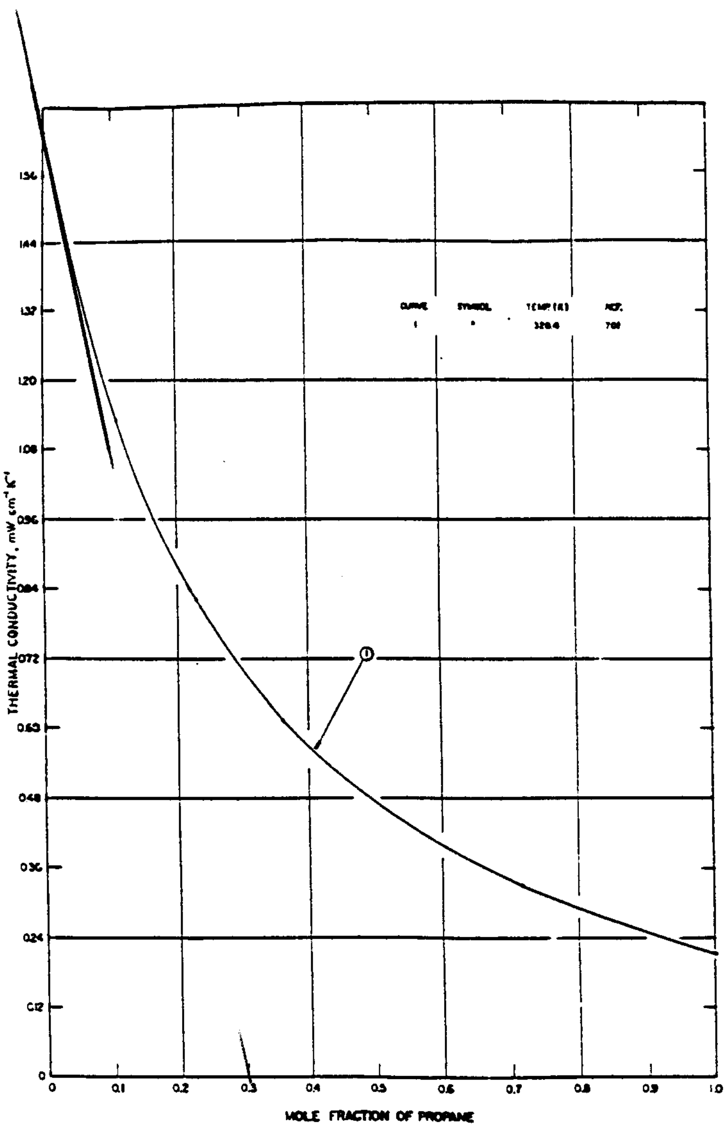

Fig. 4 Heat Conductivity of a helium-propane mixture at 328.4 K.

(Source: Thermophysical Properties of Matter, Vol. 3, Therm. Cond., Y.S. Touloukian).

Where x is the mole fraction of propane. It is further assumed that this relation is true for all temperatures the detector operates on.

2.4 The Constant Temperature Mode

The constant temperature configuration is the most straightforward mode to analyze, since the resistance of the filament becomes constant. Because analysis of this mode also provides us with a way to get the best insight in the connection of all the quantities influencing the response of the TCD, this mode is considered in this report. The response of the detector, meaning the ratio of the change in output voltage to the concentration change, can be derived as follows.
The voltage across the filament is given by:

$$V = (P_0 R_F)^{1/2} \tag{12}$$

where P_0 is the supplied power and R_F is the resistance of the filament. In paragraph 2.2 it is already derived that P_0 is 0.45 W and that R_F is 17.7 Ω. When sample gas enters the cell, the voltage across the filament will adjust in such a way that thermal equilibrium is established. The voltage in case of the presence of sample gas, V_S, will be:

$$V_S = (P_S R_F)^{1/2} \tag{13}$$

Where P_S, the new supplied power, can be written like:

$$P_S = P_0 - \frac{\Delta\lambda P_0}{\lambda} \tag{14}$$

$\Delta\lambda$ is the change in heat conductivity of the gas caused by the presence of sample gas.

Subtracting eq. 12 and eq. 13 and combining the result with eq. 14, the change in voltage across the filament shows to be:

$$\Delta V = (P_0R_F)^{1/2} - (P_0R_F - \frac{\Delta\lambda}{\lambda}P_0R_F)^{1/2} \qquad (15)$$

Using eq. 11 the voltage change can be written like:

$$\Delta V = (P_0R_F)^{1/2} - (P_0R_F)^{1/2}(1-3.44\Delta x)^{1/2}$$

and by using $(1-x)^{1/2} = 1-x/2$ for $x<<1$, it can be derived that:

$$\Delta V = (P_0R_F)^{1/2}\,\frac{3.44\Delta x}{2} \qquad (16)$$

With the already mentioned values for the power and resistance of the HP cell the response is found to be:

$$\Delta V = 4.85\Delta x \quad \text{(in Volts)} \qquad (17)$$

Eq. 16 shows that the response of a TCD cell can be increased by increasing the supplied power. Because the actual 12 µm diameter filament will burn through in case its temperature exceeds 400°C, the supplied power cannot be increased that much. It is however possible, by adjusting the geometry, to increase the supplied power without significant rise of filament temperature. It may be clear that a larger cell has to be used in order to attain that goal. In chapter 4 will be shown that filament volume as well as the cell volume are limited by the total time constant of the cell.

3 Fundamental Noise

3.1 Thermal Noise

Thermal noise (also called Johnson noise) is due to the random motion of carriers in any conductor. As a consequence of this random motion a fluctuating electromotive force is developed across the terminals of the conductor.

The fluctuation in the voltage caused by the thermal noise of the resistance R can be calculated using the equipartition theorem.

This theorem states that the average energy per degree of freedom is $\frac{1}{2}kT$. k is the Boltzmann constant, T is the temperature of the resistance.

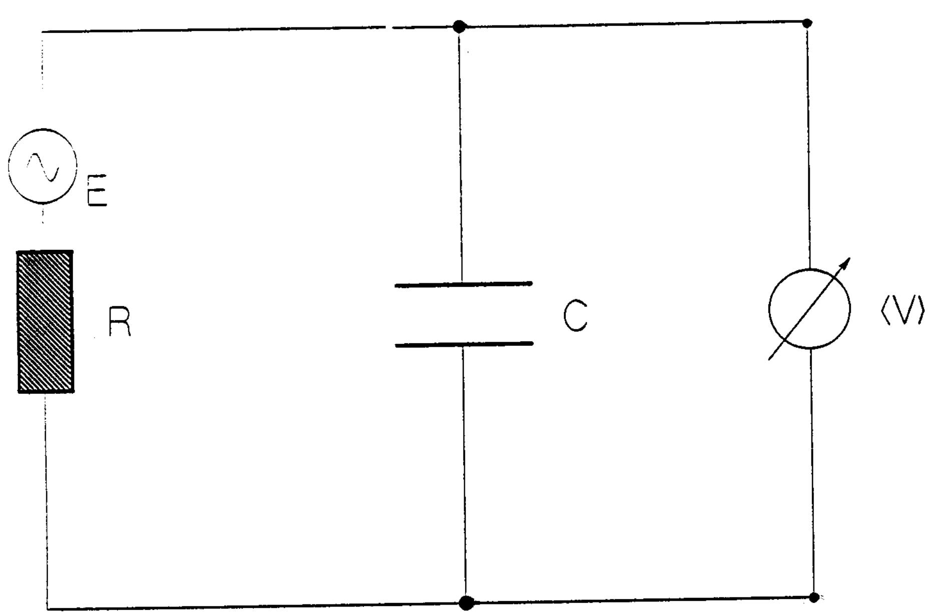

Fig. 5 Thermal noise voltage.

An expression for the thermal noise voltage (<V>) can be calculated considering a white noise source (E) in series with an ideal resistor (R) and parallel with an ideal capacitor (C).

Any resistor has a shunt capacity associated with it. Across the terminals of the resistor we have the noise voltage. The energy associated with the voltage variation is stored in the electric field of its capacitance. The energy content of the capacitor due to the thermal noise voltage of the resistor is equal to $\frac{1}{2}CV^2$. C is the capacitance.

Fig. 5 shows the electrical circuit considered to derive an expression for the magnitude of the thermal noise.

This means that the energy content of the capacitor is generated by the random motion of the carriers in the resistors.

$$\tfrac{1}{2}CV^2 = \tfrac{1}{2}kT \tag{18}$$

By using Parceval's theorem and assuming that the spectral density of the noise is independent of the frequency (white noise), it can be calculated (3) that the mean square voltage of the noise is equal to:

$$\langle V^2 \rangle = 4kTR\Delta f \tag{19}$$

where Δf is the frequency bandwidth with which the thermal noise is measured. Using $T_F = 550$ K and $R_F = 17.7\ \Omega$ for the HP cell the RMS value of the noise voltage per unit of squareroot of bandwidth is:

$$\langle V^2 \rangle^{1/2} = 7.3\ 10^{-10}\ \text{Volts}/\sqrt{\text{Hz}} \tag{20}$$

3.2 Filament Temperature Fluctuation Noise

A value for the temperature fluctuation noise of a thermal detector is given by an expression which can be derived in the same way as the expression for the thermal noise in an electrical resistor is derived.

Temperature fluctuation noise will always occur because of the fundamental fluctuation in the heat conduction caused by the random motion of the heat carriers.

In Fig. 6 the detector is modeled as a thermal resistor parallel to a heat capacitor. The circuit is driven by temperature fluctuations across the thermal resistance.

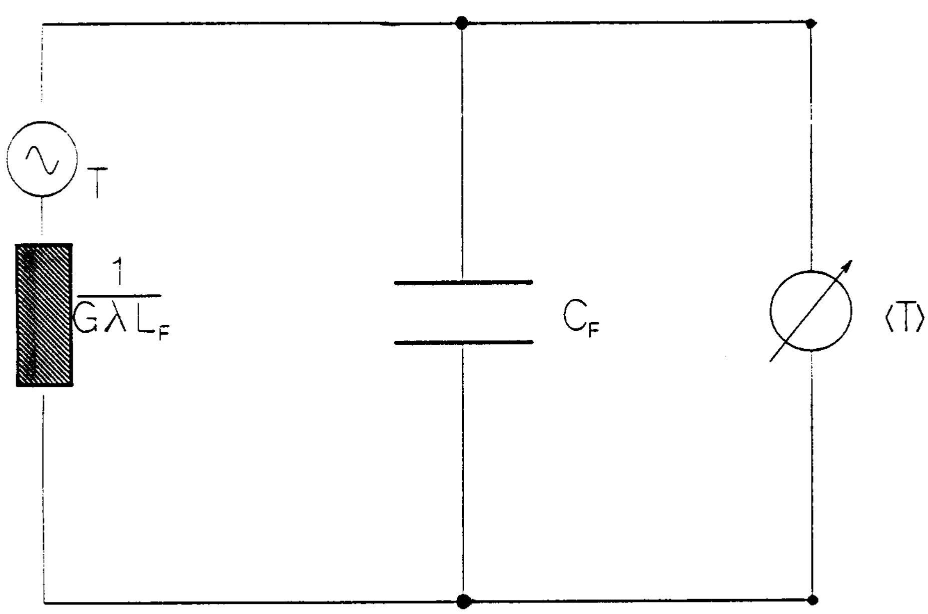

Fig. 6 Thermal model of the detector and temperature fluctuation noise.

An expression for the temperature fluctuation noise (<T>) can be calculated considering a white noise source (T) in series with an ideal thermal resistor ($1/G\lambda L_F$) and parallel with an ideal heat capacitor (C_F).

The noise, which can be expressed as a fluctuation in the filament temperature, is given by:

$$<T^2> = 4kT^2\Delta f/G\lambda L_F \tag{21}$$

where Δf is again the frequency band width with which the temperature fluctuations are measured. An expression for the geometrical constant, G, is already given in eq. 4.
Using $T_F = 550$ K, $G = 1.63$ and $\lambda = 0.195$ J/m s K, the RMS value of the temperature noise per unit of squareroot of bandwidth is:

$$<T^2>^{1/2} = 6.4\ 10^{-8}\ \text{Kelvin}/\sqrt{\text{Hz}} \tag{22}$$

From the above considerations about the thermal (voltage) noise and the temperature noise of the detector it may be clear that both noise sources are basically the same. Electrical voltage, resistance and current are connected to thermal voltage (temperature difference), thermal resistance (one over the conductance) and heat (energy) current (dissipated heat per second) by eq. 2. This means that expressing voltage noise in temperature noise, or the other way around, will give the same results for the noise level or signal to noise ratio, assuming the same bandwidth.

4 The Signal to Noise Ratio

4.1 Introduction

Before a theoretical detection limit or minimum detectable limit (MDC) can be determined a minimum signal to noise ratio (SNR) has to be defined.
It is commonly used in chromatography that noise peaks in the chromatogram with a width or height 4 times or more smaller than the height or width of the real peaks are neglected when determining the minimum detectable level. In that case, noise peaks and real peaks are assumed to be of the same (gaussian) shape. Since the peaks where is dealt with, in practice, have a width of 0.25 s or more, the width of the noise peaks of interest is 62.5 ms or more.
The HP TCD, however, can only handle peaks with a width of 1 second or more because of its special design. According to its manual the minimum detectable concentration for this cell is approximately 400 picograms of propane per ml of carrier gas, helium. This is equal to 350 PPB at a gas temperature of 453 K and a pressure of 1 bar.
Its MDC is determined by considering all noise peaks occurring in the chromatogram. Because of the special design of this TCD the filament signal has a major noise component with a frequency of 5 Hz. A description of the operation of this cell is given later on in this report and the 5 Hz noise is here considered more profoundly.
One of the operations done on the filament signal before it becomes GC output is digital filtering. This digital filter has a bandwidth of 2.7 Hz. This means that 5 Hz noise of the filament signal will be subdued considerably before it becomes the GC output signal.
Fig. 7 shows a GC output signal when a TCD is used as the column output detector. It can indeed be seen that no significant 5 Hz noise component

occurs in the chromatogram. It is shown in this chromatogram how the MDC is determined.

If a random noise signal is considered and the RMS value of that signal is determined, it can be proved that 68 percent of all the (positive and negative) noise peaks is between the negative and positive RMS value. The positive RMS value is shown in Fig. 8 and so 68 percent of the positive peaks will be lower than this level. It can further be shown that 95 percent of all noise peaks will be within a 4 times RMS wide band around the baseline and 99.7 percent will be within a 6 times RMS wide band around the baseline.

This means that there is a very slight change (0.4 percent) that a noise peak which contributes to the RMS value of the noise, with a peak to peak value of 6 times the RMS level occurs in the chromatogram. For that it can be easily stated that a peak in the chromatogram with a peak to peak value of 12 times or larger the RMS value of the noise is a real peak.

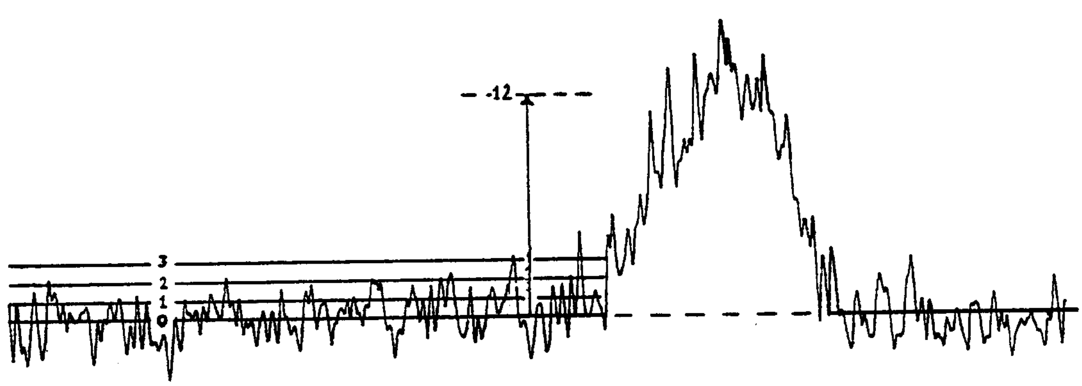

Fig. 7 GC output signal and the definition of the Minimum Detectable Level. 68% of the peaks is within the RMS value (line 1) of the noise, 95% is within two times the RMS value (line 2) and 99.7% is within 3 times the RMS value (line 3). A peak having a height of 12 times the RMS value is considered to be a real peak.

4.2 The Minimum Detectable Concentration

The theoretical MDC can be found using eq. 16 for the response of the cell and eq. 20 for the RMS value of the noise.

The signal to noise ratio in units of squareroot of bandwidth is:

$$SNR = \frac{P_0^{1/2}}{(kT)^{1/2}}(3.44/4)\Delta x \quad (\text{in } \sqrt{Hz}) \tag{23}$$

where P_0 again is the supplied power, k the Bolzmann constant and T the resistor (filament) temperature.

Requiring a SNR of 12 the minimum detectable concentration per unit of squareroot of bandwidth becomes:

$$MDC = \frac{48(kT)^{1/2}}{3.44(P_0)^{1/2}} \quad (\text{in } 1/\sqrt{Hz}) \tag{24}$$

It is already discussed that the HP 5890 A detector requires very accurate filtering because of the its special design. It will be made acceptable in chapter 8 that there is a large 5 Hz noise component in the filament noise spectrum because of this design. This is recognized by the designers who tried to match the GC filter bandwidth in such a way that this noise would be filtered out. For that a 2.7 filter bandwidth was chosen. Taking 2.7 Hz for the bandwidth, eq. 24 gives the theoretical MDC for propane of the HP cell.

$$MDC = 3.0\ 10^{-9} \quad (3\ PPB) \tag{25}$$

According to the manual, the practical achieved MDC is 400 picograms of propane per ml of helium. At an average gas temperature of 453 K and at a pressure of 1 bar this equals 0.33 PPM.

This implies that there is roughly a difference of an order of 2 in magnitude between theoretical and practical level.

5 The Detector Time Constant

5.1 Introduction

Considering the detector voltage peaks to be of gaussian shape, the observed peak standard deviation, σ_{OBS}, may have received contributions from all portions of the chromatographic system.

The contributions of n independent factors can be treated as additive in their second moment of variances, so that the observed second moment, σ_{OBS}^2, is the summation (4).

$$\sigma_{OBS}^2 = \sum_{k=1}^{n} \sigma_K^2 \qquad (26)$$

In an ideal case the contributions to the final standard deviation from the injection pulse and the detector time constant are negligible. In that case the observed standard deviation is only due to column lining.

In order to find out whether the detector time constant of our cell contributes to the observed standard deviation we first have to consider the peak broadening caused by the column lining.

One of the classical measures of the performance of the column lining is the plate height, H, which is defined by:

$$H = L_C(\sigma_C/t_R)^2 \qquad (27)$$

where L_C is the length of the column and t_R is the retention time of the gas peak. The more efficient the column, the smaller is H, and thus the standard deviation of the output peak is reduced.

For the columns which match with a μl-TCD cell, $L_C = 10$ m, $t_R = 10$ s and $H = 6$ mm. This means that $\sigma_C = 0.25$ s. The present column linings are not optimum, however, and increases in lining performance will further decrease H.

It seems even well within the limits of performance to expect that the plate height for capillary columns will decrease to about 0.05 mm (L_C = 1.5 m, t_R = 1.5 s, σ_C = 10 ms).

Accepting a 5% increase in the column standard deviation caused by the time constant of the detector as not noticeably degrading the column performance the time constant can be found using eq. 26.

$$\sigma_{DET} = \sqrt{(\sigma_{TOT}^2 - \sigma_C^2)} \tag{28}$$

where σ_{TOT} is the standard deviation of the detector output peak.

If $\sigma_{TOT} = 1.05\sigma_C$ and $\sigma_C = 0.25$ s is substituted, the magnitude of σ_{DET} is found to be 56 ms.

This means that for the actual case in point, the detector time constant must be less than 56 ms.

Substitution of σ_C = 10 ms gives σ_{DET} = 3 ms.

5.2 The detector fill time

The detector fill time is not contributing to the total variance of the peak width as is assumed in eq. 26. Its value is, however, important. In case the fill time exceeds the width of the peak eluting from the column peak broadening will occur.

The detector fill time is found by taking the detector volume and dividing by the flow rate:

$$T_C = V_C/F_V' \tag{29}$$

Where V_C is the volume (3.5 μl) and F_V' is the flow rate (in m^3/s). If we consider a capillary column with an inner diameter of 25 μm, the column flow rate for the above example (t_R = 10 s, L_C = 10 m) shows to be 0.5 ml per second.

Substituting this in the above equation gives T_C = 7 s.

This value for T_C shows that the volume of this cell doesn't match with the use of capillary columns. It will be shown later in this report that extra gas has to be added to the column flow in order to decrease the detector fill time.

5.3 The detector thermal time constant

Because of the thermal resistance of the gas in the cell and the heat capacitance of the filament, the detector is also affected with a thermal time constant.

Like in the electrically analogy the (thermal) time constant is equal to the (thermal) resistance times the (heat) capacitance.

$$\tau_H = C_F/G_H \tag{30}$$

where G_H is the heat conductance of the cylindrical cell when containing helium and C_F is the heat capacitance of the filament. G_H is equal to $G\lambda L_F$. The values for the HP cell substituted gives τ_H = 1.1 ms which is much smaller than the 56 ms detector time constant which causes a 5% peak broadening. Even in case the lining performance increases up to the values mentioned in paragraph 5.1, the thermal time constant of this detector won't limit the performance of the entire GC set-up.

6 Other losses and noise sources

6.1 The heat conductivity of the gas

The equations in the former chapters used to derive an expression for the response and MDC are only valid if the heat conductivity of the gas in the cell behaves like it is assumed paragraph 2.5. In the following paragraphs the behaviour of the heat conductivity of the gas in a μlitre TCD cell will be looked more closely at.

6.1.2 The mean free path of the gas molecules

The heat conductance in a cylindrical cell can only be described in the way it is done in chapter 2 if the heat conductive gas can be treated like a continuum. This implies that the mean free path of the molecules has to be smaller than the heated objects from which the heat is dissipated.
Only in this situation a local temperature equilibrium can be defined because many collisions between many molecules take care of the kinematic heat transfer so, of the heat conductance.
If the mean free path becomes larger than the dimensions of the objects the heat is dissipated from, the heat conductivity of the gas will drop rapidly. This means that the filament response decreases.
A gas in which the mean free path of the molecules is larger than the dimensions of the enclosure which surrounds it, is called a Knudsen gas in literature.
The mean free path, l_{MF}, can be calculated using:

$$l_{MF} = 1/4n\sigma \qquad (31)$$

Where n is the total density of the molecules (in molecules/m^3) and σ is the effective collision cross-section of the molecules. The mean free path of the helium molecules at a average temperature of 453 K is about 0.15 μm ($\sigma \approx 1\ 10^{-19}\ m^2$).

Since the diameter of the wire is 12 μm the ratio of mean free path and diameter is small enough to consider the gas as a continuum. If this ratio nears 0.1 (for example when the pressure in the cell decreases) the gas will run into a state of transition between the continuum behaviour and the Knudsen gas behaviour. This means that decreasing the pressure in the HP cell below roughly 0.12 bar will slowly result in a lower signal.

This explains the decrease in thermal conductivity van Es (6) already noticed when increasing the detector sensitivity by decreasing the TCD outlet pressure. It is confirmed in his experiment that the decrease in thermal conductivity is manifested at pressures below 0.1 bar. The somewhat lower pressure at which the influence of the decreased pressure is manifested can be explained by the used cell. A Varian constant temperature TCD (Varian, Walnut Creek, USA) was used in this experiment. The diameter of the heated filament of this cell is 10 μm.

Decreasing the pressure in the cell can be useful in case the volumetric time constant of the cell is limiting the magnitude of the peak widths which with the cell can cope without deforming the peak shape.

So, decreasing the pressure is a way to expand the peak width of the column output peaks in order to make these compatible with the filling time of the cell. In case that the heat conductivity of the gas doesn't drop no sensitivity loss will occur, because the concentration of sample gas in the carrier gas is constant.

On the other hand, eq. 30 shows that in case the heat conductivity of the gas in the cell decreases, the thermal time constant of the cell will increase. So, decreasing the pressure is only useful in case the filling time of the cell is much larger than the thermal time constant of the cell.

Other effects where have to be paid attention to are effects caused by thermodiffusion. Thermodiffusion can cause separation of the mixture at low pressures.

6.1.3 The statistical fluctuation in the heat conductivity

The HP cell has an internal volume of 3.5 μl. This means that at a pressure of 1 bar and at an average gas temperature of 453 K, about 6 10^{16} molecules will be in the cell. The number of molecules colliding with the filament per second can be written as:

$$N = nA_F(3kT_F/m)^{1/2} \tag{32}$$

Where N is the number of molecules colliding per second, n is the density of molecules, A_F is the filament area, T_F is the filament temperature and m is the mass of a molecule.

At the theoretical MDC level of propane, which is calculated to be 3 PPB, the density of propane molecules is 5 10^{16} molecules per cubic meter.

At this temperature the number of propane molecules colliding with the filament per second is 3 10^{12}. Because of the statistical fluctuation in this number the heat conductivity of the sample gas will also fluctuate. The statistical fluctuation in this number is equal to the squareroot of the total number.

Within the considered bandwidth of the cell, which is 2.7 Hz, the relative fluctuation is:

$$\Delta N/N = \surd(1/2.7\ 3\ 10^{12}) = 3\ 10^{-7} \tag{33}$$

This fluctuation in the number of molecules at the theoretical MDC level will cause a change in the thermal conductivity of the same order. It may be clear that such a change in the heat conductivity is of no importance whenever it is at the MDC level.

6.2 Vibration of the filament

It is easy to show that vibrations of the filament can be a source of noise. When the wire is forced to vibrate simply by knocking on the top of the detector the baseline shows greater noise.

When the filament is vibrating the cell constant for the radial conduction is affected. It is already mentioned that the cell constant is given by:

$$G = 2\pi/\ln(r_W/r_F) \qquad (34)$$

if the axes of the block and the filament coincide.

The cell constant changes if the axis of the cell and the axis of the filament do not coincide.

This means that the heat conduction from the filament to the wall will change periodically if the distance between the wire axis and the wall changes periodically.

Tye (5) gives an expression for the cell constant of two parallel but eccentric cylinders of uniform surface temperatures.

$$G = 2\pi/\ln \frac{\{r_F^2((r_W/r_F)+1)^2-b^2\}^{1/2} + \{r_F^2((r_W/r_F)-1)^2-b^2\}^{1/2}}{\{r_F^2((r_W/r_F)+1)^2-b^2\}^{1/2} - \{r_F^2((r_W/r_F)-1)^2-b^2\}^{1/2}} \qquad (35)$$

where b is the normal distance between the middles of the two axes. If it is assumed that the axes coincide in the steady state an estimation of the change in heat conduction can be made in case both axes do not coincide as a result of filament vibrations. Because the deflection of the wire is a function of the mass, length, tension of the wire and perpendicular forces working on it, it was tried to determine the deflection, experimentally. This was attempted by stroboscopic flashing of the vibrating filament. For this purpose the detector was opened and placed under a microscope. In order to attain a regular deflection and frequency of vibration the filament was forced to vibrate by blowing air towards it by means of a fan. The maximum deflection in the middle of the filament was about equal to the diameter of the filament.

Also the vibrational frequency plays a role when determining the influence of the vibration on the change in the heat conduction.

The frequency of the filament vibration is a function of its density, length and tension.

$$f = \frac{1}{2L_F}\sqrt{(T/\rho_F)} \tag{36}$$

Where ρ_F is the density of the wire meaning the mass per unit of length, T is the tension of the filament. The tension of the HP filament is approximately $1\ 10^{-2}$ kg m/s^2 and the density is $4\ 10^{-6}$ kg/m. Substituting these values in eq. 36, the vibrational frequency shows to be 2.5 kHz.

Assuming that the average deflection of the total wire is half the deflection of the wire in its middle, so $b = r_F$, we can calculate the change in the heat conductance. For the relative change in the heat conductance, if the wire has its maximum deflection can be found:

$$\frac{\Delta G}{G} = \frac{\Delta G_H}{G_H} = 7\ 10^{-5} \tag{37}$$

Regarding the deflection of the filament harmonically, the deflection as a function of the time can be written like:

$$D(t) = D_0 \sin(2\pi ft)\sin(\pi x/L_F) \tag{38}$$

where t is the variable for the time and x is the variable for the length coordinate. D_0 is the maximum deflection in the middle of the wire and is equal to $2r_F$.

The fluctuations in the heat conductance caused by the vibrations are, however, always positive and can be written like:

$$G_H = G_{H0}|\sin 2\pi ft| \qquad (39)$$

Where G_{H0} is the maximum change in the heat conductance caused by an average (maximum) deflection of the wire of r_F.

This has as a result that the vibration will always cause a raise in the heat conductance for the time the vibration lasts regardless of its vibrational frequency.

Assuming the time the vibration lasts to be much greater then the filament thermal time constant the average change in the heat conductance is given by:

$$\sqrt{<G_H^2>} = G_{H0}\frac{1}{T}\int_{-T/2}^{T/2} \sin^2(2\pi ft)\, dt \qquad (40)$$

where T is the time one vibrational cycle takes.

The average change in the heat conductance is $\sqrt{2}G_{H0}$. This means that the relative change in the dissipated heat will be approximately $4\ 10^{-5}$.

For small relative changes in the dissipated power and small relative changes in the voltage across the filament the relative change in the dissipated power is twice as large as the relative change in the voltage across the filament.

$$\frac{\Delta P}{P_0} = 2\frac{\Delta V}{V} \text{ (for } \Delta V << V \text{ and } \Delta P << P_0) \qquad (41)$$

Using this relation it is shown that vibration of the filament with a deflection of the order of the filament radius itself can increase the MDC to about 20 PPM.

It is already mentioned that the deflection of the wire is a function of (the ratio of) the external forces working perpendicular on the wire and the tension of the wire.

In the experiment done, where the filament was forced to vibrate by blowing air towards it, the external forces will exceed the external forces working on the filament when it is operating in a closed cell, many times.

The only forces working on an operating filament are viscous forces caused by the flow. These forces are parallel to the wire in case the flow is laminar with a symmetric velocity profile.

It is therefore very unlikely that the filament will endure deflections of the magnitude described when it is operating in the cell.

It is, however, important to clench the filament tightly between its points of support in order to increase its tension. For that it is also important to choose materials for the block and the filament with almost the same coefficient of expansion.

Whenever this is not taken into account the filament tension will either get to low or the filament will crack, when increasing the cell temperature.

6.3 Temperature of the cavity wall

The TCD requires accurate control of the cavity wall temperature for proper operation and any fluctuation in this parameter can cause noise in the operation of the system.
The temperature of the block is tried to kept constant at a fixed temperature below the filament setting temperature. This is done by implementing the block with a temperature sensor and a backcoupled heater close to the sensor. This prevents the block from cooling-down because of the lower ambient temperature. Because block temperature tends to decrease the heater will switch on and off driven by the sensor and controller.
For that, different types of controllers can be chosen in order to achieve a steady temperature. However, due to the fluctuating operating heater, temperature fluctuations will occur close to this heater. These temperature fluctuations will be subdued because of the large heat capacitance of the block.
Recalling eq. 1 it can be proved that a 0.3 degrees K increase in the block-wall temperature will result in a 1 nV filament voltage change. This change in the filament voltage equals the magnitude of the thermal noise voltage. In practice it is, however, very well possible that this noise exceeds the thermal noise level. Some shallow studies recently attempted to estimate the influence of the periodically heating of the block on the actual noise level. It could not be proved explicitly that this is in practice the main source of noise.
To describe the magnitude of the thermal mismatch of the cavity wall temperature has not been attempted to achieve in the scope of this research. Further investigations have to be made on the thermal control system for the TCD and until that is performed this parameter cannot be forgotten.

7 The flow in the cell

7.1 Introduction

In the ideal case, the signal of a TCD should only vary in case the heat conductivity of the gas in the cell varies. It is already mentioned, however, that the total transferred heat changes in case the flow in the cell changes. In spite of the fact that only a small percentage of the total supplied energy is transferred by convective heat transfer, it can become important whenever this heat loss source fluctuates in time.

These fluctuations will cause noise on the baseline because the total transferred heat is not a function of the heat conductivity of the gas in the cell only.

A schematic idea of a TCD cell is already given in Fig. 2. The inner cylinder represents the filament, the outer cylinder represents the wall of the block. The filament is heated up to the preset value, the block is kept at a constant temperature, being approximately 110 K below the filament temperature. The inlet of the cell in this picture is at the left side of the cell. It is here that the cell is connected to the column by means of an interface.

7.2 Hydrodynamic and thermal entrance lengths

If 25 μm is taken as the inner diameter of a capillary column and 1 ml/min (equal to approximately 1.6 10^{-8} m^3/s) for the column flow the Reynolds number for the flow in the column is 0.3. The Reynolds number is based on the viscosity and the density of helium and on the diameter of the column. This Reynolds number implies a laminar flow in the column.

When the flow enters the interface (and finally the cell) the laminar pattern will be disturbed because of the abrupt change in the geometry. The flow in the cell tends to develop towards a laminar flow pattern if the Reynolds number is below 2300.

The inner diameter of the HP cell is 0.3 mm, its internal volume is 3.5 μl. Whenever this TCD is used as the output detector of capillary columns some extra carrier gas has to be supplemented to the column flow in order to increase the gas velocity in the cell. Addition of extra carrier gas makes the volumetric time constant of the cell match with the narrow peak widths of the capillary column output peaks. On the other hand it will cause loss of signal because the sample gas concentration will decrease.

According to its manual the performance of this TCD is optimal if the flow through the cell is 5 ml/min when using capillary columns. This means that 4 ml/min has to be added to the column flow in case this flow is 1 ml/min.

The Reynolds number for the flow in the cell is 0.4.

Fig. 8 gives a schematic idea of the flow in the cell. The disturbed region at the inlet of the cell is called the entrance region (region 1 in Fig. 9), its length the entrance length. After the entrance region the flow pattern will become independent of the length coordinate (region 2).

The entrance length for the velocity profile, called the hydrodynamic entrance length L_{EH} is a linear function of the Reynolds number (7).

$$L_{EH} = 0.03 Re r_W \quad (42)$$

Here, the Reynolds number for the flow in the cell is defined by $Re = u r_W \rho / \eta$.

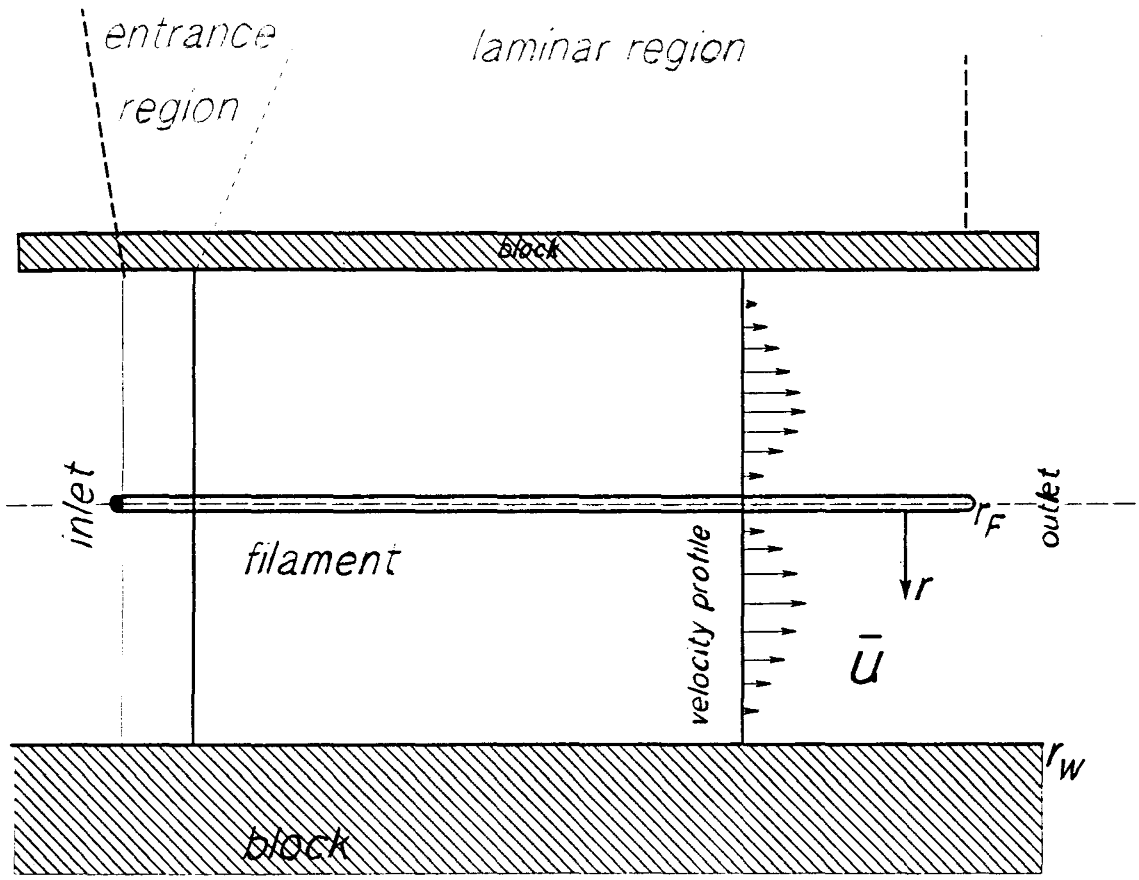

Fig. 8 Schematic idea of the behaviour of the flow in the cell.

r_W is the radius of the cell, u is the average velocity of the flow, η is the dynamic viscosity and ρ is the density of the gas.

In case the gas is heated up, the length needed to establish the temperature profile is called the thermal entrance length, L_{ET}. It is a function of the product of the Reynolds number and the Prandl number (Pr) (7).

$$L_{ET} = 0.1RePrr_W \tag{43}$$

The Prandl number is merely a gas property parameter defined by $Pr = \eta C_p/\lambda$. Where C_p is the specific heat of the gas at constant pressure and λ is the heat conductivity of the gas.

The above equations show that L_{EH} is about 0.015 times the radius of the cell and L_{EH} is about 0.04 this radius.

7.3 Heat transfer

The scope of this chapter is to find an expression for the ratio of the heat transferred by conduction and the convective heat transfer as a function of the flow in the cell. Mainly because the Reynolds number of the flow in the cell is very small the approach using dimensionless numbers is not very valuable.
For that reason some efforts will be made later in this chapter to find this expression by solving the momentum and energy equation for the flow in the cell.

7.3.1 Dimensionless numbers

In a TCD heat is generated by supplying electrical power to a resistive filament. It is already discussed in chapter 2 that it loses its heat mainly by conduction and in less extent by convection and radiation.
Dimensionless numbers are widely used in literature dealing with flow phenomena. In this paragraph an outline about how to use these numbers in order to get an expression for the heat transfer is discussed. It will, however, be shown that it doesn't lead to an exact quantitative understanding of the convective heat transfer.
In order to find the desired expression, the total heat transfer is considered to be a linear function of the difference between the filament temperature and the average temperature of the gas.

$$P_{TOT} = \alpha_T(T_F - T_{AV}) \tag{44}$$

where the proportional factor, α_T, is called the heat transfer coefficient. T_{AV} is the average temperature of the flow and is here defined as:

$$T_{AV} = \frac{\int u(r)\rho C_p T(r)dA}{\int u(r)\rho C_p dA} = \frac{\int u(r)T(r)dA}{\int u(r)dA} \tag{45}$$

where u(r) is the velocity in the cell which is a function of the radius and A is the cross-sectional area of the cylindrical section of the cell.

The second form is only valid if the product of the density and the specific heat, ρC_p, is independent of the temperature.

The heat transfer coefficient, α_T, is determined by different physical processes and so a function of a number of quantities (8,9).

If the heat conduction, convective heat transfer, the influence of the flow pattern and the occurrence of vortexes are considered to be the phenomena affecting the total heat transfer, the problem can be defined using eight quantities.

These are the heat conductivity, the specific heat, the density and the viscosity as the property quantities of the gas. Also the velocity of the gas and the temperature of the filament and the length and the radius of the cell as the geometrical quantities.

At this stage the influence of radiation is neglected and it is assumed that the flow is incompressible.

By Buckingham's theorem, the connection between these eight quantities should reduce to a relationship between four dimensionless ratios.

Very useful dimensionless numbers in this context are the Nusselt, Prandl and Reynolds numbers. A fourth dimensionless ratio can be defined by the length-diameter ratio of the cell. The Nusselt number is defined as:

$$Nu = \alpha_T r_F/\lambda \tag{46}$$

The Nusselt number represents the ratio between the total heat transfer and the heat transfer by conduction.

Under the assumptions mentioned earlier, the Nusselt number can be written as a function of the three other dimensionless numbers.

$$Nu = f(Re, Pr, L/r_W) \qquad (47)$$

Many authors have sought for an explicit form for the total heat transfer as a function of these numbers (8,9,10). There is considerable evidence that:

$$Nu = aRe^B Pr^C (L/r_W)^D \qquad (48)$$

with a, B, C, and D constants and $0 \leq B \leq 1$, $0 \leq C \leq 1$ and $0 \leq D \leq 1$.
For numerous heat transfer problems, these constants are given in tabular form. Most exponents are determined considering a flow with a high Reynolds number ($Re > 100$). There is also an enormous lack of agreement concerning the values of these components. However, when making an estimation of the influence of a process on the heat transfer these numbers can be useful. In case a general expression for the heat transfer is desired this technique lacks universality and accuracy. For that reason, dimensionless numbers won't be used anymore in the sequel of this report.

7.3.2 The momentum and energy equations

By solving the momentum and energy equations of the flow in the cell the ratio of the convective heat transfer and the heat transfer by conduction can be determined.

The momentum equation for an incompressible stationary flow with constant viscosity is given by the Navier-Stokes equation:

$$\rho(\underline{u}.\nabla)\underline{u} = -\nabla p + \eta\nabla^2\underline{u} \tag{49}$$

Where p is the pressure, $\underline{u}$ is the velocity vector as a function of the place, η is the dynamic viscosity and ∇ is the differential operator.

The momentum equation for the flow in an annulus (two concentric cylinders) reduces in cylindrical coordinates to:

$$\frac{\partial p}{\partial x} = \eta\left(\frac{1}{r}\frac{\partial}{\partial r}\left(r\frac{\partial u}{\partial r}\right)\right) \tag{50}$$

x is the length coordinate (parallel to the annulus axis) and r is the radial coordinate (perpendicular to the axis).

This equation is only valid in the laminar region where the flow has an established velocity profile (see Fig. 9). Because angular and radial velocity components are equal to zero in this region, the velocity has only a component in the direction parallel to the axis. The magnitude of this velocity is a function of r and x.

Using the appropriate boundary conditions this equation (50) can be solved analytically. The boundary conditions are given by:

$$u = 0 \quad \text{if} \quad r = r_F \tag{51a}$$

and

$$u = 0 \quad \text{if} \quad r = r_W \tag{51b}$$

The dimensionless solution of the momentum equation with the above boundary conditions is given by:

$$u'(r') = \frac{2}{M}(1-r'^2+B\ln r') \tag{52}$$

with $$B = \frac{R^{*2}-1}{\ln R^*} \tag{52a}$$

and $$M = 1+R^{*2}-B \tag{52b}$$

and $$R^* = r_F/r_W \tag{52c}$$

All parameters marked with a ' are dimensionless. The velocity, u, is made dimensionless by dividing it by the mean velocity, u_{MEAN}, and the radial coordinate, r, is made dimensionless by dividing it by the radius of the outer cylinder, r_W.

All parameters marked with a * are a ratio between two constants (also dimensionless).

$$u' = u/u_{MEAN} \quad (0 < u' < 1) \tag{53}$$

and

$$r' = r/r_W \quad (R^* < r' < 1) \tag{54}$$

A velocity (profile) is required in case the energy equation of the flow has to be solved.

In case the heat conductivity, λ, of the gas is constant the energy equation is given by:

$$\rho c_p \frac{\partial T}{\partial t} + \rho c_p u \,\mathrm{grad} T = \lambda \nabla^2 T + \phi + 2\eta \underline{D}:\underline{D} \qquad (55)$$

$$\begin{array}{ccccc} 1 & 2 & 3 & 4 & 5 \end{array}$$

1 is the instationary heat transfer term

2 is the convective heat transfer term

3 is the heat conduction term

4 is the heat source term

5 is the viscous dissipation term

The viscous dissipation term consists of the product of matrices whose elements are vectors. These vectors are derivatives of the three components of the velocity vector.

This equation can also be reduced in case cylindrical coordinates are used and the same assumptions are made as for the momentum equation. That implies that the temperature profile will be solved in the region in which the velocity and temperature profiles are established. The heat source term can be neglected if a fixed filament temperature and a fixed wall temperature are taken as a boundary condition. If also the viscous dissipation term is neglected the energy equation will be given by:

$$\frac{1}{r}\left(\frac{\partial}{\partial r}\left(r\frac{\partial T}{\partial r}\right)\right) + \frac{\partial^2 T}{\partial x^2} = \frac{u(r)}{\alpha_D}\,\frac{\partial^2 T}{\partial x^2} \qquad (56)$$

Where α_D is the molecular thermal diffusity of the gas which is equal to $\lambda/\rho c_p$.

Because of the non-linear convective term this equation cannot be solved analytically.

It is however possible to find a temperature profile by assuming that all the heat from the filament is transferred to the wall by conduction. Because of the low Reynolds numbers the flow will only have a slight influence on the established temperature profile. This means that the real profile and the profile found when only considering heat conduction will almost be similar. A linear equation is found considering the temperature drop δT across a small distance δr to be linear with the thermal resistance per unit of radius and that no heating-up of the gas will occur.

$$\frac{\delta T}{\delta r} = \frac{A}{2\pi r} \tag{57}$$

Where A is a constant and can be determined by choosing proper boundary conditions. In order to find a dimensionless expression for the temperature profile, the boundary conditions are defined as:

$$T' = T^* \qquad \text{if} \quad r' = 1 \qquad (r = r_W) \tag{58a}$$

and

$$T' = 1 \qquad \text{if} \quad r' = R^* \qquad (r = r_F) \tag{58b}$$

and

$$T^* = T_W/T_F \tag{59}$$

T is made dimensionless by dividing it by the filament temperature, T_F, so,

$$T' = T/T_F \qquad (T^* < T' < 1) \tag{60}$$

The solution of the above differential equation plus its boundary conditions is given by:

$$T'(r') = \frac{1}{\ln R^*}(\ln r' - T^*\ln(r'/R^*)) \tag{61}$$

Fig. 9A and Fig. 9B show the velocity and temperature as a function of the radius for various ratios of the filament radius and the wall radius (R^*). In paragraph 7.4 the analytical determined velocity and temperature profiles will be used to find an expression for the convective heat transfer as a function of the flow in the cell.

Paragraph 7.5 discusses the usage and results of a computer program that is used to solve the non-linear momentum and energy equations for the flow in the HP cell. These solutions made it possible to calculate the convective heat transfer exactly.

In both cases the rate of axial transferred energy per second, P_{CV} is calculated using the energy-flux equation given by:

$$P_{CV} = \int_{R_F}^{R_W} \rho c_p u(r,x=L)T(r,x=L)\,dA - \int_{R_F}^{R_W} \rho c_p u(r,x=0)T(r,x=0)\,dA \qquad (62)$$

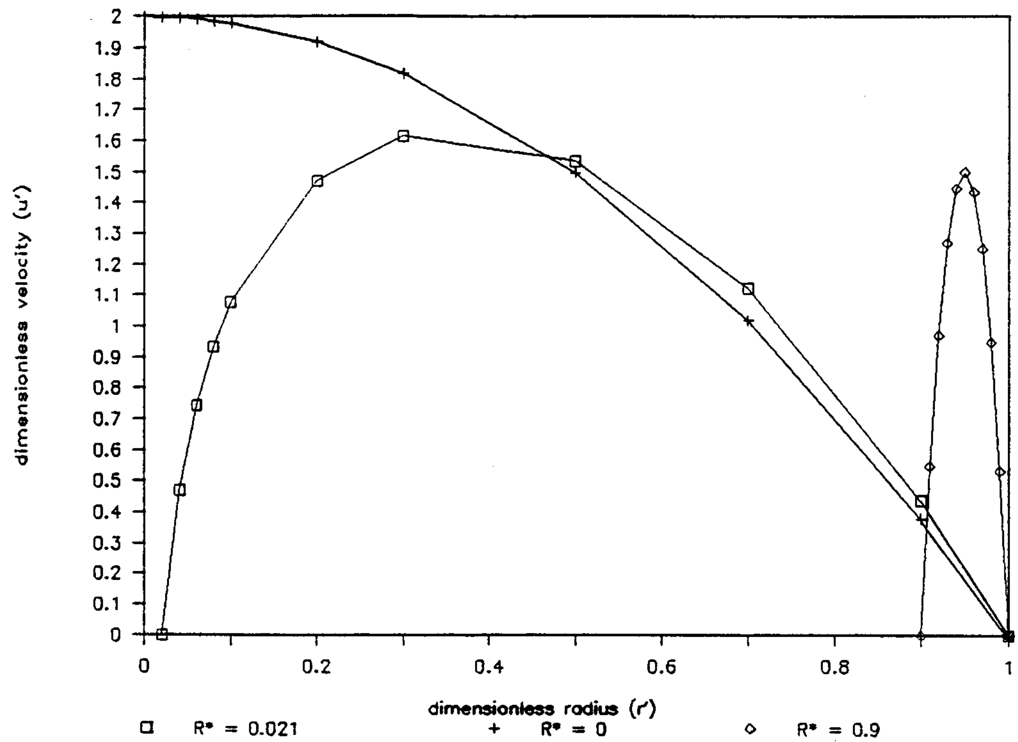

Fig. 9a Velocity profile between two concentric cylinders for various ratios of the cylinder diameters (R^*)

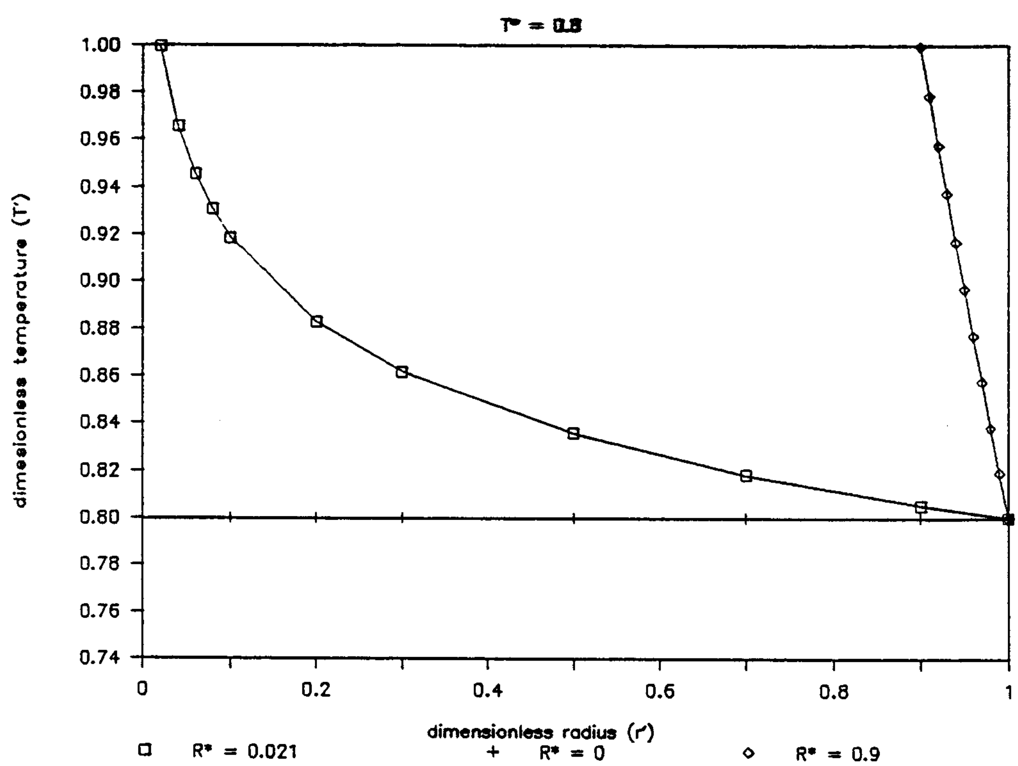

Fig. 9b Temperature profile between two concentric cylinders for various ratios of the cylinder diameters (R^*).

7.3.3 The analytical solution

In order to make it possible to calculate the convective heat transfer some assumptions concerning the velocity and temperature profiles at the inlet have to be made.

When the gas enters the interface connecting the column and the cell it will gradually adopt the temperature of this interface. According to eq. 43 it will adopt this temperature within a very short region because of the low Reynolds number of the flow.

Block and interface will approximately have the same temperature because of the high heat conductivity of the materials the block and the cell are made of. Therefore the gas will enter the cell having the same temperature as the block. The results which will be shown in the next paragraph will give further justification for this approach.

In this chapter the same values for the operating point parameters will be used as in chapter 2. This implies that the gas at the inlet is considered to have a uniform temperature of 440 K.

When the gas enters the cell it is forced to go a winding way before it reaches the filament channel. This means that the velocity profile at the inlet will differ from the ideal laminar profile described in eq. 52.

For reasons of convenience a flat velocity profile at the inlet will be assumed. This means that the velocity across the cross-section of the inlet will be assumed to be uniform, in other words everywhere equal to the mean velocity.

The results of the numerical solution which will be discussed in the next paragraph will show that the velocity profile assumed at the inlet is of minor influence as long as the mean velocity is kept constant.

The energy-flux equation given in the preceding paragraph shows that the specific heat and the density of the gas affect the magnitude of the

convective heat transfer in case these quantities are functions of the temperature. It is already mentioned in chapter 2 that the specific heat, c_p, of helium remains constant with temperature up to 6000 K (11). For this reason c_p will be treated as a constant when calculating the heat transfer. Eq. 8 gives an expression for the gas density, ρ, as a function of the temperature. It is derived using Gay-Lussac's law which holds for an ideal gas so $\rho(T)=\rho_0T_0/T$ (T in degrees K). ρ_0 being the density of helium at temperature T_0, mostly chosen to be 273 K.
The heat flow entering the cell can be written as:

$$P_{IN} = 2\pi\rho_0T_0c_pu_{MEAN,IN}r_W^2\int_{R^*}^{1} r'dr' \tag{63}$$

where $u_{MEAN,IN}$ is the mean velocity of the flow at the inlet of the cell. After solving the integral, P_{IN} can be written like:

$$P_{IN} = \pi\rho_0T_0c_pu_{MEAN.IN}r_W^2(1-R^{*2}) \tag{64}$$

For the calculation of the heat flow leaving the cell, the velocity profile given in eq. 52 will be used. The temperature profile at the outlet is of no importance. It drops out of the integral because the density is linear with 1/T.

$$P_{OUT} = 2\pi\rho_0T_0c_pu_{MEAN,OUT}r_W^2\int_{R^*}^{1} \frac{2}{M}(r'-r'^3+Br'\ln r')dr' \tag{65}$$

where $u_{MEAN,OUT}$ is the mean velocity of the flow at the outlet of the cell. The solution of this integral is given by:

$$P_{OUT} = \pi\rho_0T_0c_pr_W^2u_{MEAN,OUT}\frac{1}{M}(1-2R^{*2}(1-\tfrac{1}{2}R^{*2})-B(1-R^{*2}+2R^{*2}\ln R^*)) \tag{66}$$

with M and B already defined in the preceding paragraph.

Using eq. 52a for B and eq. 52b for M the above equation simplifies to:

$$P_{OUT} = \pi\rho_0 T_0 c_p r_W^2 u_{MEAN,OUT}(1-R^{*2}) \tag{67}$$

The difference between P_{OUT} and P_{IN}, P_{CV}, satisfies:

$$P_{CV} = \pi\rho_0 T_0 c_p r_W^2 (1-R^{*2})(u_{MEAN,OUT}-u_{MEAN,IN}) \tag{68}$$

As a result of the calculations it is found that the heat content per unit length, the energy density, is constant. The convective heat transfer is a function of the difference in mean velocity, only. This is a consequence of the fact that the density of helium is taken to be linear with 1/T.

In the thermal entrance region where the gas is partially heated up, the mean velocity increases because the gas expands. Here, the heat flow will change. The change in mean velocity can be calculated using the mass law.

$$\Phi_{M,IN} = \Phi_{M,OUT} \tag{69}$$

The mass flow, Φ_M, can be written like:

$$\Phi_M = 2\pi\rho_0 u_{MEAN} r_W^2 \int_{R^*}^{1} \rho'(r')u'(r')r'dr' \tag{70}$$

where ρ is made dimensionless by dividing it by ρ_0, the gas density at 273 K. Because $\rho(r)$ is a linear function of 1/T, the calculation of this integral at the outlet of the cell will yield an analytical unsolvable integral. It is possible to solve it by means of a mathematical (software) package or by using a table of integrals. When using one of these it will be shown that the solution of this integral can be represented by a couple of logarithmic Euler integrals which values are given in tabular form for various ratios of the integral boundaries.

This, however, won't provide us of a general and clear expression of the mass flow as a function of the cell parameters, T^* and R^*.

Another way to find an expression for the difference in mean velocity is by calculating the average temperature at the inlet and the outlet of the cell, assuming no flow. Relating this average temperature to an average density and mean velocity creates a way to find an average velocity. Because the gas expands the most close to the heated filament but flows the least close to filament the contribution of the expansion won't be as large as will be assumed in the following calculations. From eq. 70 it can be seen that it only gives a correct solution in case the temperature differences in the cell are zero. Only in that case the product of the density and the velocity is equal to the integral of the product of the density and the velocity. Recognizing this deviation the difference in the mean velocity can be found using:

$$\frac{T_{MEAN,OUT}}{T_{MEAN,IN}} \approx \frac{u_{MEAN,OUT}}{u_{MEAN,IN}} \tag{71}$$

Where $T_{MEAN,OUT}$ and $T_{MEAN,IN}$ are the average temperatures at the outlet and the inlet of the cell which can be calculated using (assuming no flow):

$$T_{AV} = \frac{2 \cdot T_F}{(1-R^{*2})} \int_{R^*}^{1} T'(r')r'dr' \tag{72}$$

Using the above equation it can be found easily that the average temperature at the inlet is T^*T_F, or T_W, as expected.

Assuming that R^{*2} is small compared to unity the average temperature at the outlet shows to be:

$$T_{MEAN,OUT} = \frac{T_F}{\ln R^*}\left(-\frac{1}{2}+\frac{T^*}{2}+T^*\ln R^*\right) \tag{73}$$

For obtaining this result all terms in the solution of the integral containing R^{*2} were neglected.

Combining eq. 72 with the obtained average temperatures gives:

$$u_{MEAN,OUT}-u_{MEAN,IN} = \frac{(T^*-1)u_{MEAN,OUT}}{(T^*(1+2\ln R^*)-1)} \tag{74}$$

while,

$$u_{MEAN,OUT} = \frac{F_{V,OUT}}{\pi(R_W^2-R_F^2)} \tag{75}$$

where $F_{V,OUT}$ is the volumetric flow at the outlet, the convective heat transfer as a function of the flow is found to be:

$$P_{CV} = \rho_0 T_0 c_P \frac{(T^*-1)}{T^*(1+2\ln R^*)-1} F_{V,OUT} \tag{76}$$

It is already mentioned that this expression is only exact in case the temperature difference between the filament and the block nears zero. So, using:

$$1-T^* \equiv \Delta T' = (T_F-T_W)/T_W \ll 1 \tag{77}$$

and defining the heat content of helium, $\rho_0 T_0 c_P$, per unit of volume as Q_0, the convective heat transfer is found to be:

$$P_{CV} = \frac{-Q_0}{2\ln R^*} \Delta T' F_{V,OUT} \qquad (78)$$

The final step will be to derive an expression for the increase in voltage across the filament, V_{CV}, due to the convective heat transfer losses as a function of the flow.

Using:

$$\frac{V_{CV}}{V_F} = \frac{P_{CV}}{2P_F} \quad \text{if } V_{CV} \ll V_F \text{ and } P_{CV} \ll P_F \qquad (79)$$

where P_{CV} is the increase in supplied power due to the convective heat transfer which value is defined already in eq. 78.

V_F is the voltage across the filament and P_F is power supplied to the filament necessary to get the cell in thermal equilibrium if only considering heat conduction.

Using, $V_F = \sqrt{(P_F R_F)}$ and $P_F = G_H(T_F - T_W)$ where R_F is the filament resistance and G_H is the heat conductance, V_{CV} is found to be:

$$V_{CV} = \frac{-Q_0}{4T_W \ln R^*} \sqrt{((T_F - T_W)R_F/G_H)} F'_{V,OUT} \qquad (80)$$

where $F'_{V,OUT}$ is the volumetric flow in m^3/s.

Or as a function of the Reynolds number for the flow in the cell:

$$V_{CV} = \frac{-Q_0}{4T_W \ln R^*} \sqrt{((T_F - T_W)R_F/G_H)} \frac{\eta \pi r_W Re}{\rho} \qquad (81)$$

where η and ρ are the viscosity and the density at the average temperature at the outlet.

For infinitely small temperature differences between filament and block this expression should return the convective heat transfer exactly. It is very well possible that the results given by these expressions are several times larger than the actual ones in case the temperature difference is as big as the actual difference of 110 K.

The voltage change as a function of the volumetric flow can be written like, using the values for the HP cell:

$$\frac{dV_F}{dF_V} = 4.6\ 10^{-4} \quad \text{Volts/(ml/min)} \tag{82}$$

It has to be noticed that this expression is found by assuming that V_{CV} is directly proportional with the temperature difference between filament and wall up to 110 K. It is already mentioned that this will not be exact because $\Delta T/T_W$ is no longer much smaller than 1.

From eq. 71 and eq. 74 it can be calculated that the average temperature at the outlet of the HP cell is 3% higher than the average temperature at the inlet of the cell. This means that the average gas temperature at the outlet will be approximately 453 K. The viscosity of helium at this temperature is $2.65\ 10^{-5}$ kg/m s and its density is 0.108 kg/m^3. Using these values in the above equation V_{CV} for the HP cell turns out to be:

$$V_{CV} = 6.4\ 10^{-3}\ Re \tag{83}$$

Where,

$$Re = 4.33\ 10^{6}\ F'_V \tag{84}$$

if F_V' is the volumetric flow in m^3/s or,

$$Re = 7.22\ 10^{-2}\ F_V \tag{85}$$

if F_V is the volumetric flow in ml/min.

Finally, the relative changes in the filament signal and dissipated power as a function of the flow can be derived:

$$\frac{\Delta V}{V} = 1.6\ 10^{-4}\ \Delta F_V \tag{86}$$

and

$$\frac{\Delta P}{P} = 3.3\ 10^{-4}\ \Delta F_V \tag{87}$$

7.4 The numerical solution

7.4.1 Introduction

The literature dealing with methods for solving differential equations numerically is countless. Most methods are either optimized or only applicable for a specific problem.

A method which is widely applicable is the finite elements analysis (FEA) method (12, 13, 14, 15).

The FEA package available at the Eindhoven University of Technology consists of FORTRAN modules which have to be imbedded in the correct sequence by CALL statements in the main program by the user.

An additional feature of this package is the possibility of plotting the results of the computations. The results will for example consist of a velocity vector field of the flow in the cell or the temperature distribution in the cell. It will also be possible to calculate other derivatives like the pressure distribution or the streamlines of the flow in the cell.

An example of a SEPRAN program is given in appendix 1.

7.4.2 The main program

The main program consists of modules which make it possible to solve the stationary non-linear momentum and heat equations of the flow in the cell. The boundary conditions like the velocity profile at the inlet, the temperature of the flow at the inlet or the filament and the block temperature can be varied very easily.

The exact velocity and the exact temperature as a function of the place in the cell are obtained by solving the momentum and the energy equation iteratively. This is required because the solutions for the temperature and the velocity are coupled. This means that an estimation for the velocity has to be used in order to solve the energy equation. Its solution will affect the solution of the non-linear momentum equation because the density and the viscosity are temperature dependent. Once the temperature as a function of the place in the cell is obtained, the density and viscosity as a function of the place in the cell have to be adjusted to the local temperature. In a next call the momentum equation has to be solved again in order to find the new values for the velocity. With the values obtained for the velocity the energy equation can be solved again and so on, till both the solution of the momentum and the energy equation are stable. The number of calls necessary to obtain this stable solution depends upon the initial estimation of the velocity profile. In case of low Reynolds numbers ($Re < 10$) a good approximation is given by the solution of the linear momentum equation. Because density, viscosity and thermal conductivity are adjusted to the local temperature, the accuracy of this method is only limited by the available numerical accuracy of the computer used.

The boundary conditions necessary to solve the momentum equation are already mentioned in paragraph 7.1. Concerning the boundary conditions of the energy equation a constant energy flux from the filament to the block as well as constant wall and filament temperatures can be chosen for boundary conditions. For the HP 5890 A cell the filament operates in a constant temperature mode. The block temperature is kept fixed at the set point value. Because of the high heat conductance and the high heat capacitance of the block material it seems correct to take a fixed block temperature to serve the goal of these calculations.

Velocity profile at the inlet, temperature of the gas at the inlet and mean velocity of the flow at the inlet are the input variables the program asks for every time it is run.

7.4.3 Plots of the flow

Fig. A to Fig. G in chapter 13 show some plots of the flow in the cell. Information on the variables along the axes is always plotted in the upperleft corner of the main box. The x axis is actually the radial axis because cylindrical coordinates are used. The y axis is in fact the length axis. This means that when the x and y vectors are in the upperleft corner, the radius increases downwards in the vertical way and the length increases to the right in the horizontal way.

It is tried to explain more clearly in Fig. 10 what is exactly shown in the plots of chapter 13. A complete cross-sectional plot of the considered cell is given in this figure.

The computations made, considered the complete cell as it is drawn. The boundary conditions mentioned in the previous paragraph were used. In the computations the cell was considered as a 3-dimensional non-rotating annulus. Only the part of the cell enclosed by box A is plotted in the figures of chapter 13. This implies that neither a part of the filament nor a part of the block is plotted.

Only the flow between filament and wall in the lower half of the cell is presented. In Fig. C to Fig. G only the part enclosed by box B is plotted. It is exactly one tenth of the total cell and is here called the entrance of the cell (which is not the same as the entrance region!). It is done to attain a higher resolution in this region. It's in this region that the temperature and velocity profiles reach their final shape.

It is also for the same reason that the plots are expanded in the radial direction, compared to the axial direction. In Fig. B and Fig. G the cell is expanded 100 times in the radial direction (relative to the axial direction) and in Fig. A and Fig. C to Fig. F 10 times.

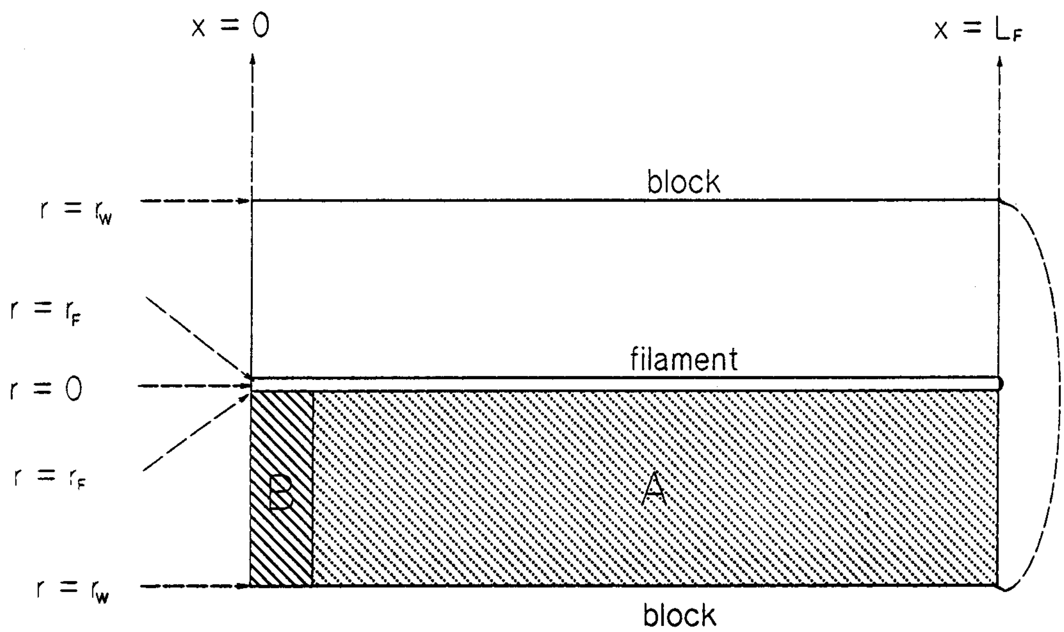

Fig. 10 Explanation of the plots of the flow shown in chapter 13.

Fig. A to Fig. C show plots of the velocity in a vector field presentation. Only in Fig. A all the meshpoints necessary to generate a computational grid are equidistant. In Fig. B and Fig. C the density of these points is much higher close to the filament and the wall. It is here that the highest temperature and velocity gradients occur.

The density of the velocity vectors is thus not connected with a volumetric or mass flow. Only the length of the vector, which is a standard for the magnitude of the local velocity or the direction of the vector, which is the direction of the local velocity, are meaningful.

Fig. A shows the velocity vector field in the isothermal cell when the velocity profile at the inlet of the cell is flat. The Reynolds number for the flow is 0.3. Isothermal means that there is no temperature difference between filament and wall (block).

Fig. B shows the velocity field at the entrance of the cell if the profile at the inlet satisfies the theoretical profile for a fully developed flow in an annulus. It is used to check the program. Since the cell is isothermal the velocity profile shouldn't change as a function of the length coordinate, because it possessed its final profile already at the inlet. It can be seen that none of the vectors changes direction.

Fig. C shows the velocity vector field at the entrance of an isothermal cell if the entrance profile is flat. It can be seen that the hydrodynamic entrance length, L_{EH}, is approximately 2 times the radius. The Reynolds number is now 0.4.

Fig. D to Fig. G present the pressure and temperature distributions in the cell. This is done by presenting isobars in Fig. D and by isotherms in Fig. E to Fig. G. The density of computational meshpoints was again higher closer to the filament and the wall. This was again done because of the larger gradients close to the filament and the wall.

Fig. D shows some isobars at the entrance of the cell if the velocity profile satisfies the final velocity profile of the flow in a pipe with a diameter equal to the radius of the cell. The Reynolds number is 0.4.

The lines perpendicular to the filament and the wall are the isobars. Adjacent isobars are 0.9 Pa lower in pressure when moving towards the outlet of the cell. The lines parallel to the filament and the wall are the streamlines of the flow. Here, the cell is isothermal.

Fig. E shows the isotherms when the filament is at 550 K and the block is at 440 K. Adjacent isotherms are 11 degrees lower in temperature when moving from the filament side towards the block side. The gas entering the cell is at 293 K. The Reynolds number is 0.3 and the velocity profile at the inlet is flat.

Fig. F shows a similar picture for a 10 times higher Reynolds number (Re = 3). It shows that L_{EH} is about three times larger.

In Fig. G the temperature of the gas at the inlet is 440 K and Re=0.3. It will be shown in the next paragraph that this is a more realistic temperature for the gas entering the cell. The thermal entrance length, L_{ET}, is approximately 2 times the radius of the cell.

7.4.5 Determination of the entrance lengths

In the calculations made in the previous paragraphs the temperature of the gas entering the cell was considered to be 440 K. In order to justify this choice the flow in the entrance of a cylindrical pipe (without filament) is considered. The pipe is at 440 K. The gas entering the pipe is considered to have a 150 degrees K lower temperature. A flat velocity profile is taken as the velocity profile at the inlet. By varying the mean velocity, L_{EH} and L_{ET} can be found as a function of the Reynolds number.

Fig. 11a shows the result of these computations. It shows the hydrodynamic entrance length as a function of the Reynolds number, which is now based upon the diameter of the pipe. Thermal and hydrodynamic entrance lengths are found to have the same magnitude within 10%. The entrance lengths are determined, using a fine computational mesh at the entrance of the pipe. The length the flow needs to establish its velocity or temperature profile reflects the entrance lengths.

For the Reynolds number occurring in the cell ($Re < 1$) these entrance lengths show to be less then 3 times the diameter of the pipe. This means that an interface between column and cell with a temperature of 440 K and a length of at least 3 times its diameter will increase the temperature of the gas leaving the column to 440 K. It seems thus reasonable to assume that the gas which enters the cell is at block temperature.

In Fig. 11b the ratio between the value of the numerically determined entrance length and the magnitude of the entrance length according to theory (eq. 42 and eq. 43) are shown.

For Reynolds numbers larger than 200, this ratio nears 1, which means that only for these Reynolds numbers agreement between numerically determined and theoretical value is found. It has, however, no consequences for the way the convective heat transfer will be calculated.

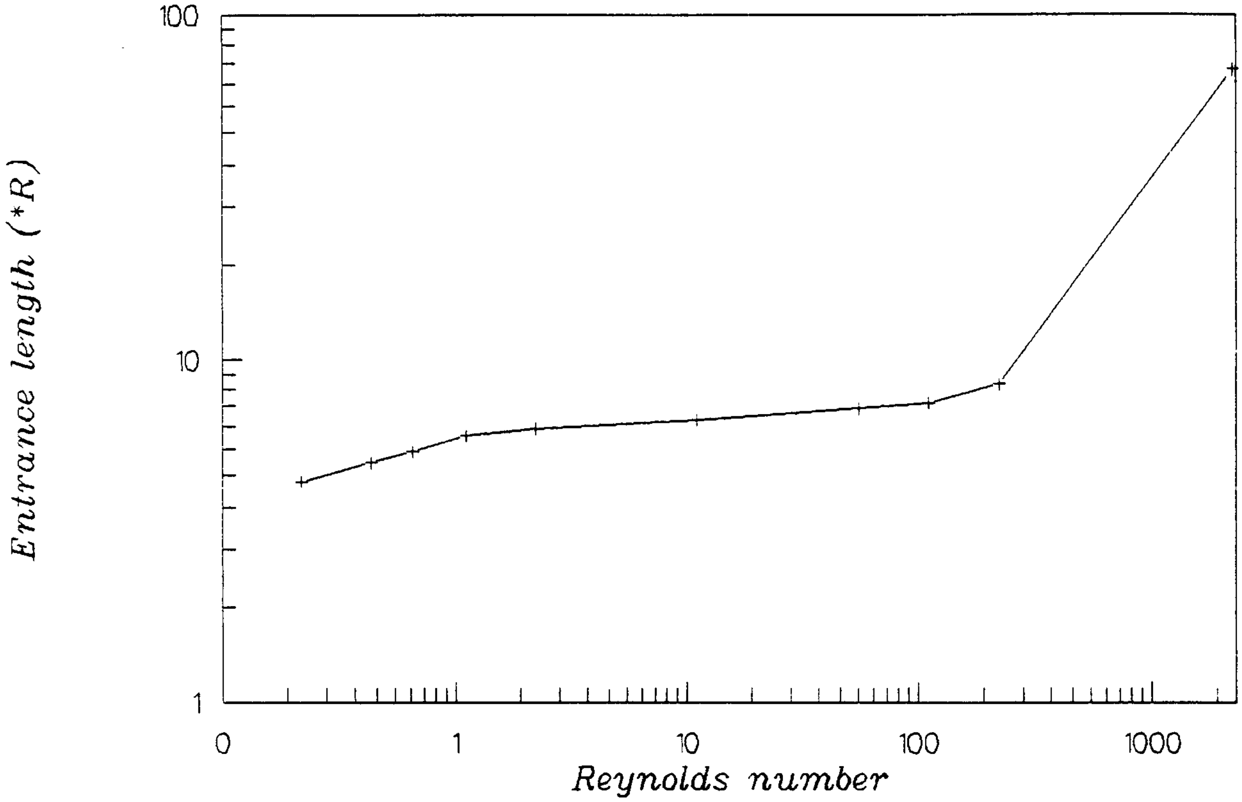

Fig. 11a Hydrodynamic entrance length of the flow in a cylindrical pipe.

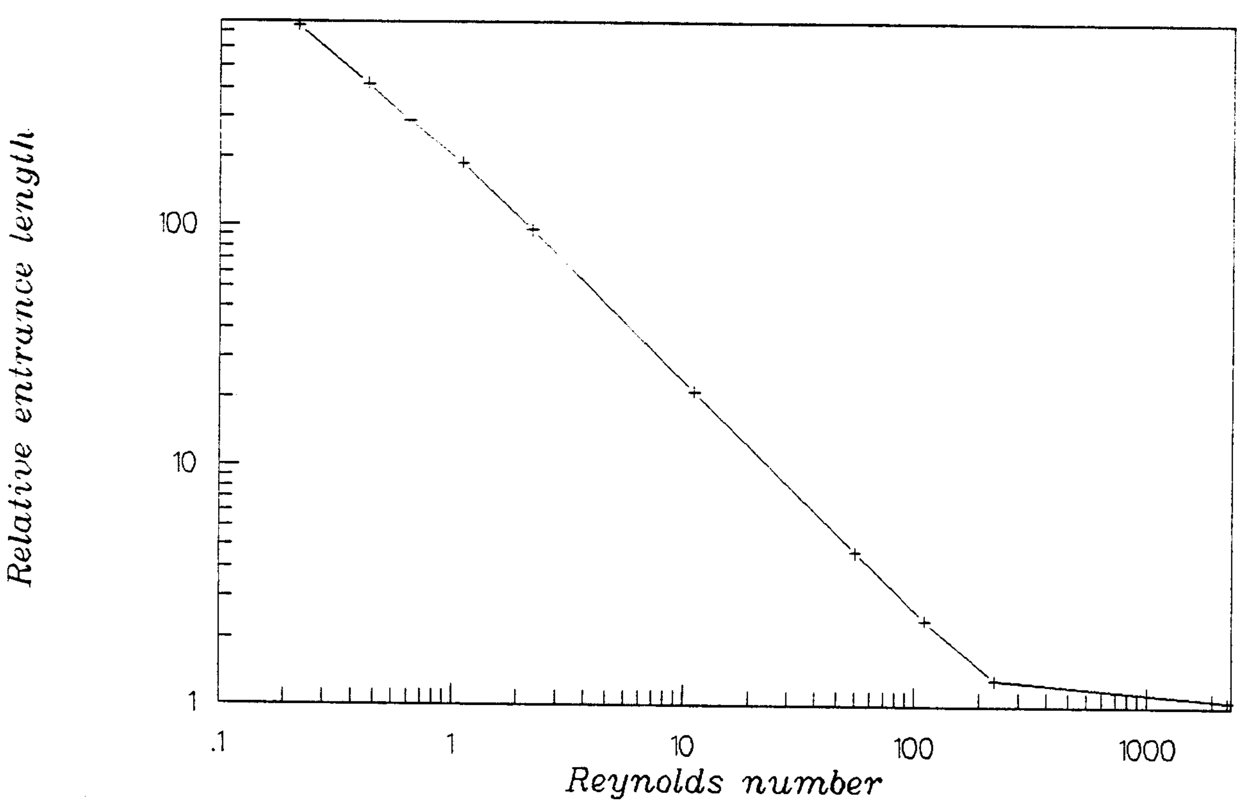

Fig. 11b Relative entrance length in a cylindrical pipe.

7.5.6 The convective heat transfer

Finally, the convective heat transfer, P_{CV}, as a function of the Reynolds number was determined. The values for the density and the viscosity were determined at 453 K, in order to make the results comparable with the results obtained from the analytical approach.
In order to investigate the influence of the profile the convective heat transfer as a function of the Reynolds number is determined for two different velocity profiles at the inlet of the cell. One of the profiles considered is the flat profile. The other profile equals the profile of the final flow in an isothermal cell. Its velocity as a function of the radius is given in eq. 52.
Fig. 12 shows the results for the two inlet profiles. It shows that the velocity profiles at the inlet have a very little effect on the convective heat transfer. For $0.25 \leq Re \leq 0.9$ the convective heat transfer is approximately given by:

$$P_{CV} = 4.85\ 10^{-4}\ Re \tag{88}$$

According to eq. 79 it shows that voltage change across the filament, due to the additional heat transfer because of this convective heat transfer, ΔV_{CV}, satisfies:

$$\Delta V_{CV} = 1.5\ 10^{-3}\ Re \tag{89}$$

Using eq. 85 it can finally be found that the relative voltage change and the relative change in the power dissipated as a function of the flow can be written as:

$$\frac{\Delta V_{CV}}{V_F} = 3.84\ 10^{-5}\ F_V \tag{90}$$

and

$$\frac{\Delta P_{CV}}{P_F} = 7.7\ 10^{-5}\ F_V \tag{91}$$

F_V is the volumetric flow in ml/min.

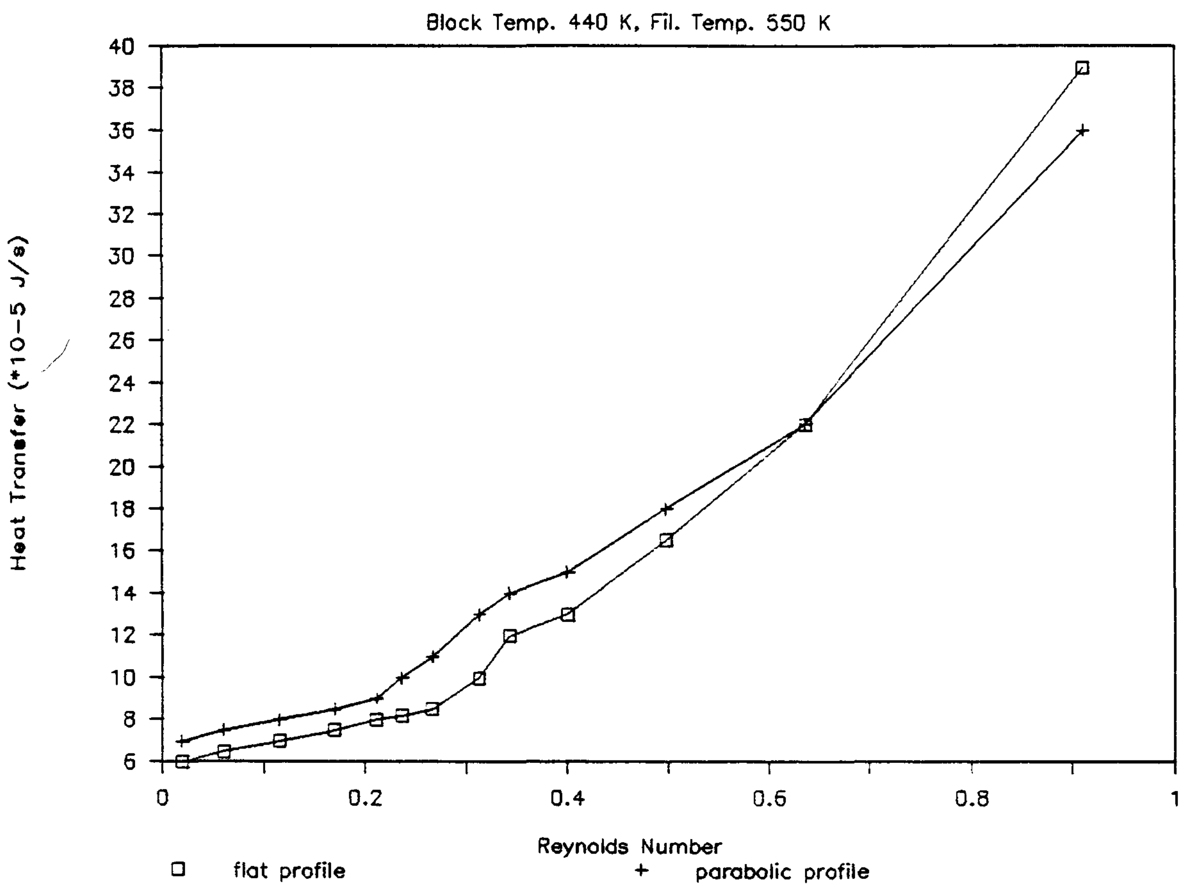

Fig. 12 Computated convective heat transfer for 2 different velocity profiles at the inlet.

8 The flow in the HP cell

The HP 5890 A cell is designed in a quite unconventional way. Normally a TCD cell exists of 2 (or 4) filaments all part of a Wheatstone bridge circuit. Along 1 (or 2) filament(s) pure carrier gas is flowing. This gas is called the reference gas and it is conducted through a reference column in the oven. The bridge is supposed to be in balance in case no sample gas leaves the column. This is especially useful in case the oven temperature is programmed. The cell output and the reference cell output are applied to a bridge circuit. This circuit makes it possible to monitor the difference of these outputs. The total bridge output shows a steady baseline.
Fig. 13 shows a schematic of the HP cell being used. It has three inlets at the bottom of this picture and 1 outlet at the top.

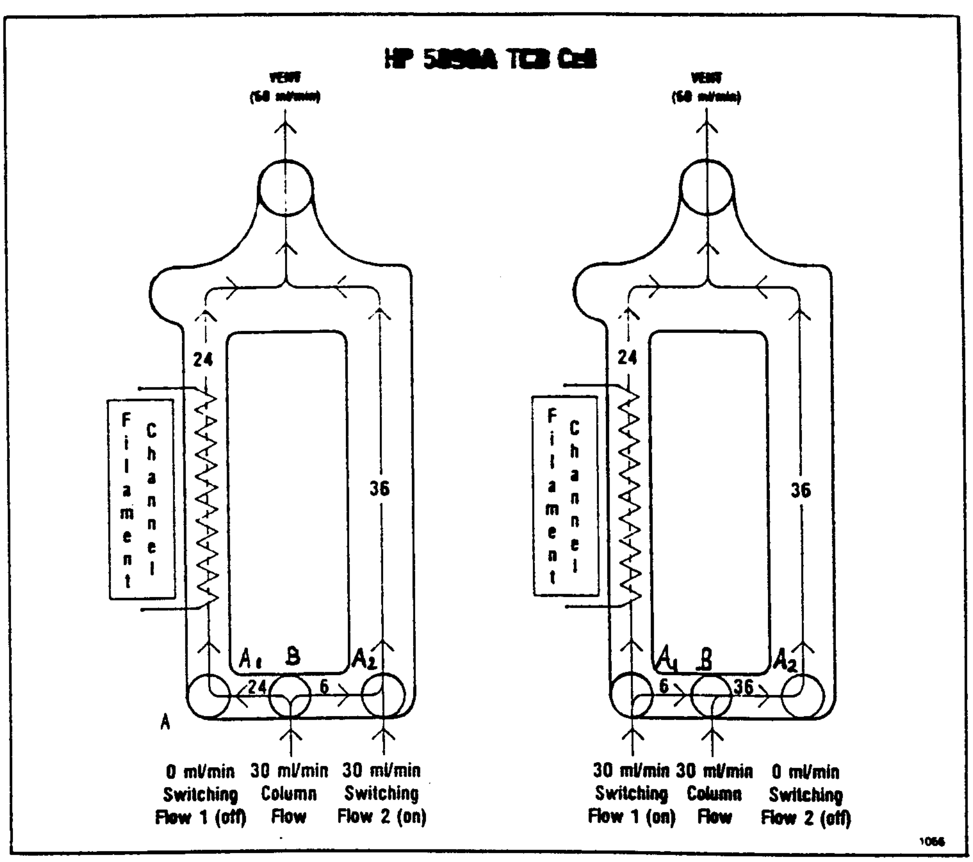

Fig. 13 Schematic section of the HP 5890 A cell.

The gas entering through one of these inlets can follow 2 different paths to the outlet. Only in the left channel a TCD filament is present.

Pure carrier (reference) gas supplies are connected with the entrances A1 and A2. The column interface is connected with entrance B, in the middle. Here, column gas (carrier plus possible sample gas) enters the cell.

The reference gas enters either through the left inlet A1 (right picture) or through the right inlet A2 (left picture). Its flow is forced to switch from one inlet to the other by switching a valve between the reference gas column and A1 and A2. This valve switches with a frequency of 5 Hz.

This has as a result that the column flow is forced to go either through the left (filament) channel or through the right channel. This means that during 0.1 seconds column gas passes the filament and after that 0.1 seconds reference gas, and so on.

Every second 5 pieces of the reference baseline are obtained and 5 pieces of the column gas signal are obtained.

The GC software is designed in such a way that the reference baseline is subtracted from the column gas signal in order to get a chromatogram with a steady baseline without drift due to changes in the oven temperature.

Because of the switching, the gas flow through the filament channel will change dependent on wether the reference gas enters at the left side or enters at the right side. In the next paragraphs a quantitative calculation of the changes in the flow as a function of the column and reference flow will be made.

Because the heat transfer as a function of the flow is known as a result of the previous chapter, the change in filament signal caused by the 5 Hz switching can be calculated.

It is already mentioned that the 5 Hz noise on the filament signal can be filtered out because the peak width of this noise is smaller than the width of the expected real peaks. A low pass (digital) filter with a 2.7 Hz bandwidth takes care of that.

Because the 5 Hz changes in the filament signal are easy to measure before they are filtered out, it creates the possibility of checking the expression derived for the convective heat transfer as a function of the flow in the filament channel.

A description of these measurements is given in chapter 9.

8.1 Electrical analogy of the flow in the cell

In Fig. 14 an electrical analogy of the flow in the cell is given in case the reference flow enters left (left picture) and in case the reference flow enters right (right picture). In contrast to Fig. 13 the reference flow enters at A1 in the left picture and at A2 at the right picture.

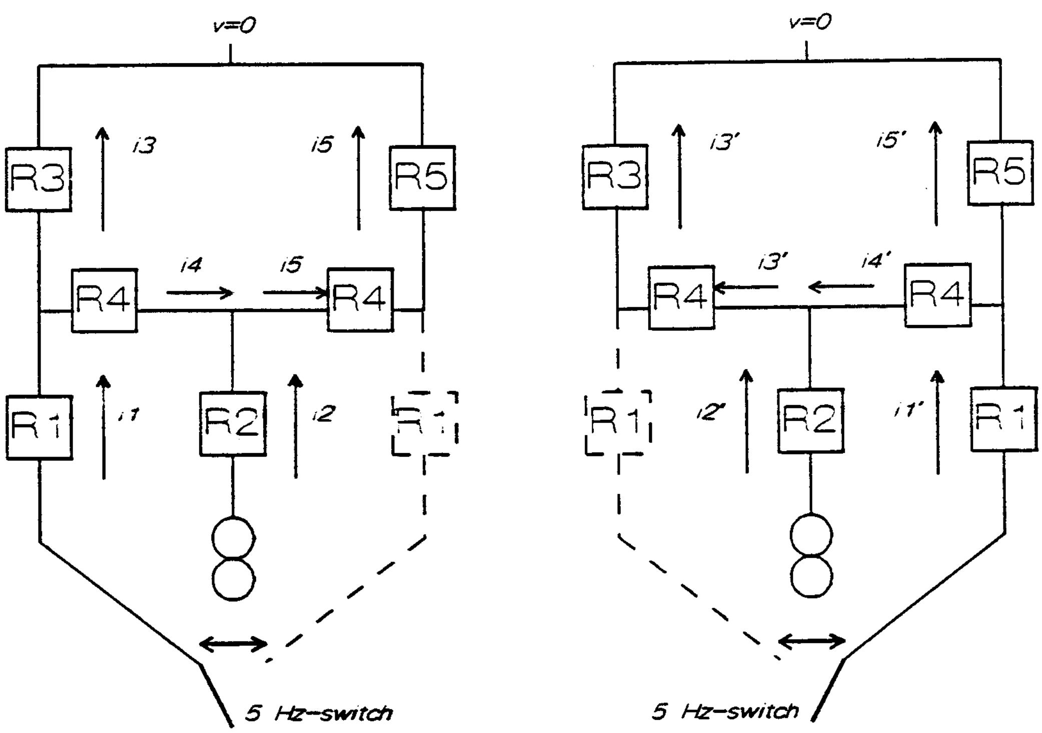

Fig. 14 Electrical analogy of the flow in the HP cell.

The magnitudes of the (flow) resistances are a function of the length and the radius of the channels and of the viscosity of the gas. This can be shown when a Hagen-Poiseuille flow is considered in all the (cylindrical) channels. A Hagen-Poiseuille flow is a laminar flow in an exact cylindrical pipe. This assumption is quite realistic because of the very low Reynolds numbers occurring. It is, however, not completely correct because the flow is disturbed after every curve in the channel circuit.

The mass flow, Φ_M, assuming a Hagen-Poiseuille flow in a cylindrical pipe is given by:

$$\Phi_M = \frac{-\rho\pi r^4 \Delta p}{8\eta\Delta L} \tag{92}$$

Where r is the radius of the pipe or channel, ΔL is the length of the pipe, Δp is the pressure drop across the length of the channel, ρ is the density of the gas and η is the dynamic viscosity of the gas.

From this it can be seen that the mass flow resistance R_{FLOW} equals:

$$R_{FLOW} = \frac{8\eta\Delta L}{\rho\pi r^4} \quad (\text{in } ms^{-1}) \tag{93}$$

It is assumed that the cell has an uniform temperature which is considered to be 440 K. At this temperature $\rho = 0.108$ kg/m^3 and $\eta = 2.59\ 10^{-5}$ kg/m s for helium. With $\Delta L = 1.27\ 10^{-2}$ m and $r_W = 3\ 10^{-4}$ m it is found that the (flow) resistance, R_3, of the filament channel equals $9.4\ 10^8$ (ms)$^{-1}$. Also with $L_4 = 3.05\ 10^{-3}$ m and $r_4 = 0.4\ 10^{-3}$ m, $R_4 = 7.2\ 10^7$ (ms)$^{-1}$ and with $L_5 = 1.27\ 10^{-7}$ m and $r_5 = 0.45\ 10^{-3}$ m, $R_5 = 1.84\ 10^8$ (ms)$^{-1}$.

It is assumed that the column and reference gas supplies can be treated as current sources because the resistance of the columns used in GC is orders of magnitude larger than the resistance of the cell. This means that a change in the cell resistance won't influence the mass flow leaving the columns.

Because of this the magnitudes of the flow resistances of the supply channels, R_1 and R_2, are not important when calculating the flow in the filament channel. Before making any calculations on the flow in the filament channel an estimation of the accuracy of this model was made. For that the program used in the previous chapter could be applied. One of its possibilities is to make a calculation of the pressure drop across the cell as a function of the Reynolds number of the flow in a cylindrical pipe or channel.

Fig. 15 shows the result of these calculations. A flat velocity profile is used for the velocity boundary condition at the inlet. The calculated pressure drop is divided by the theoretical pressure drop according to the Hagen-Poiseuille resistance.

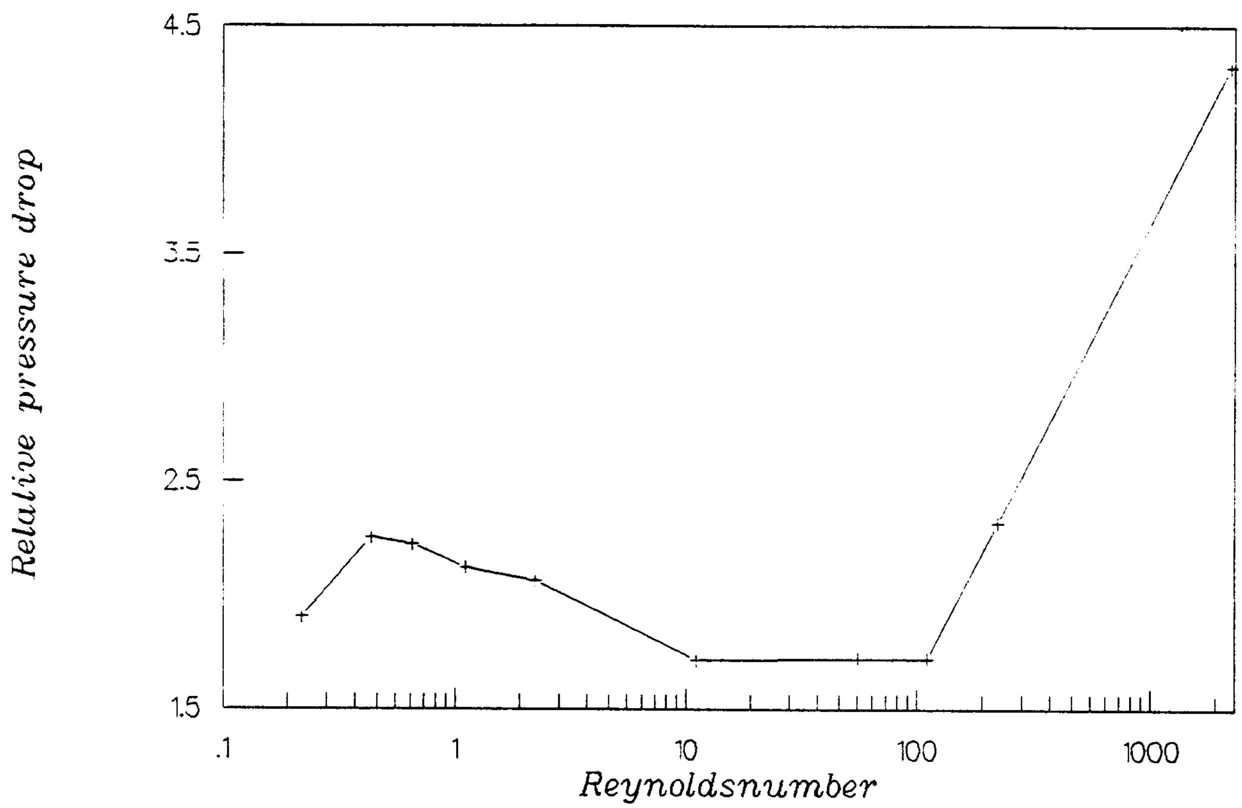

Fig. 15 Pressure drop in a cylindrical pipe as a function of the Reynolds number of the flow. The results obtained from the computations made are divided by the theoretical pressure drop assuming a Hagen-Poiseuille flow.

It can be seen that the actual pressure drop caused by the disturbance at the inlet is about 2 times the theoretical pressure drop for an undisturbed laminar flow. This is true for $.1 \leq Re \leq 100$. This result justifies the assumption of the (ideal) laminar flow resistances in the channels considered because the actual values for Re don't exceed 2.

Three equations are applied to find an expression for the flow in the filament channel.

If the reference gas enters left, the resistance of the right reference supply channel (dashed lines in left picture) is assumed to be infinite (left picture of Fig. 14). The equations are than given by:

$$\Phi_{M1} - \Phi_{M3} - \Phi_{M4} = 0 \tag{94a}$$

$$\Phi_{M2} + \Phi_{M4} - \Phi_{M5} = 0 \tag{94b}$$

$$\Phi_{M3}R_3 - \Phi_{M4}R_4 - \Phi_{M5}(R_4+R_5) = 0 \tag{94c}$$

Where Φ_{Mi} is the mass flow in the i-th channel.

After solving these equations the mass flow in the filament channel is found to be:

$$\Phi_{M3} = \Phi_{M1}\frac{(2R_4+R_5)}{R_3+2R_4+R_5} + \Phi_{M2}\frac{(R_4+R_5)}{R_3+2R_4+R_5} \tag{95}$$

Three other equations are used to solve the mass flow in the filament channel when the reference gas enters right (right picture in Fig. 14). Again, the resistance of the other (left) reference supply channel (dashed lines in right picture) is assumed to be infinite. The three equations are given by:

$$\Phi_{M1}' - \Phi_{M4}' - \Phi_{M5}' = 0 \tag{96a}$$

$$\Phi_{M2}' - \Phi_{M3}' + \Phi_{M4}' = 0 \tag{96b}$$

$$\Phi_{M3}'(R_3+R_4) + \Phi_{M4}'R_4 - \Phi_{M5}'R_5 = 0 \tag{96c}$$

Now, apostrophes (') are used to emphasis that the mass flows in this configuration differ from the mass flows in the former situation.
It is found that Φ_{M3}' is given by:

$$\Phi_{M3}' = \Phi_{M1}\frac{R_5}{R_3+2R_4+R_5} + \frac{\Phi_{M2}(R_4+R_5)}{R_3+2R_4+R_5} \tag{97}$$

Because column flow and reference flow are independent of the total impedance of the actual cell, these flows are equal in both configurations.
Using the values for the resistances given earlier in this paragraph it can be found that:

$$\Phi_{M3} = 0.259\Phi_{M1} + 0.20\Phi_{M2} \tag{98}$$

and

$$\Phi_{M3}' = 0.145\Phi_{M1} + 0.20\Phi_{M2} \tag{99}$$

Because the flow is always adjusted and measured by means of a volumetric flowmeter in ml/min at room temperature (293 K) these equations can be written as:

$$\Phi_{M3} = 7.21\ 10^{-10}F_{V,REF} + 5.57\ 10^{-10}\ F_{V,COL} \tag{100}$$

and

$$\Phi_{M3}' = 4.04\ 10^{-10}F_{V,REF} + 5.57\ 10^{-10}\ F_{V,COL} \tag{101}$$

Where $F_{V,REF}$ is the volumetric reference flow in ml/min at room temperature and $F_{V,COL}$ is the volumetric column flow in ml/min at room temperature. The density of helium at 293 K is 0.167 kg/m^3.

And since $Re = \Phi/\pi r_W \eta$ it can be found that the Reynolds number for the flow in the filament channel as a function of the column and reference flow (in ml/min) is given by:

$$Re = 2.89\ 10^{-2} F_{V,REF} + 2.23\ 10^{-2}\ F_{V,COL} \tag{102}$$

and

$$Re = 1.62\ 10^{-2} F_{V,REF} + 2.23\ 10^{-2}\ F_{V,COL} \tag{103}$$

The helium in the filament channel is considered to be at 453 K when calculating its viscosity ($\eta = 2.65\ 10^{-5}$ kg/ms). The difference in Reynolds numbers as a function of the reference flow (in ml/min) is given by:

$$\Delta Re = Re - Re' = 1.26\ 10^{-2} F_{V,REF} \tag{104}$$

The difference in volumetric flow as a function of the reference flow is finally given by:

$$\Delta F_V = 0.175 F_{V,REF} \tag{105}$$

Fig. 16 shows the results of these calculations. The higher the reference flow the higher the difference in Reynolds number is.

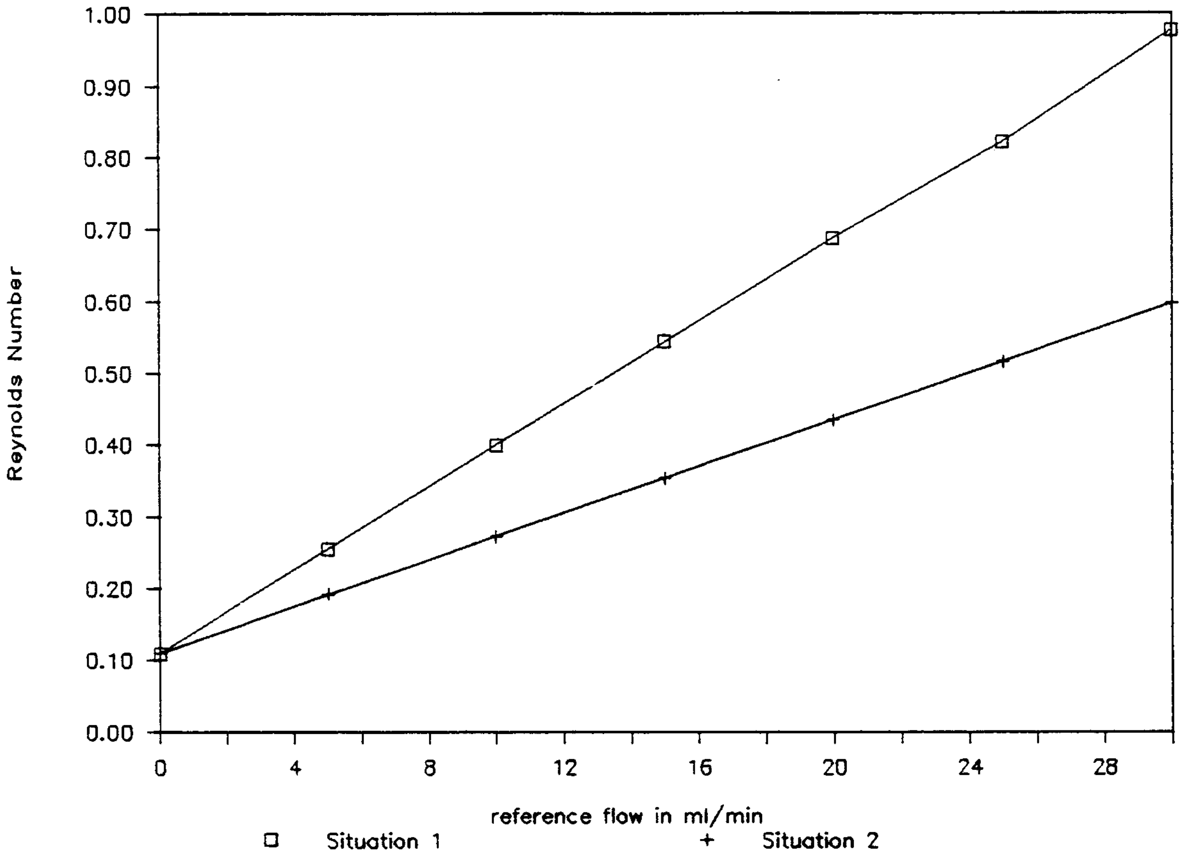

Fig. 16 Actual flow in the HP cell as a function of the reference flow rate in case the column flow is 5 ml/min. The upper line presents the flow in the filament channel in case the reference flow enters the cell through the left inlet and the lower line presents the flow in the filament channel in case the flow enters through the right inlet.

8.2 5 Hz noise

As a result of the previous paragraph and chapter 7, the magnitude of 5 Hz noise as a function of the column and reference flow (or Reynolds number for the flow in the cell) can be calculated. For this the column flow is assumed to be 5 ml/min and the reference flow is varied from 0 ml/min to 30 ml/min. The change in filament voltage due to convective heat transfer as a function of the Reynolds number was given by eq. (83):

$$V_{CV} = 6.4\ 10^{-3}Re$$

as a result of the analytical solution, and eq. (89):

$$V_{CV} = 1.5\ 10^{-3}Re \quad 0.15 \leq Re \leq 0.9$$

as a result of the numerical solution.
The 5 Hz signal in Volts as a function of the reference flow can be found using eq. 105. For the analytical approach it appears that:

$$\Delta V_{CV} = 8.1\ 10^{-5}F_V \tag{106}$$

and for the numerical approach:

$$\Delta V_{CV} = 1.9\ 10^{-5}F_V \tag{107}$$

Where F_V is the volumetric flow at room temperature in ml/min.
All these results are only valid for a column flow of 5 ml/min.

9 Experiments

9.1 Introduction

The main goal of the experiments performed is to show the influence of fluctuations in the flow rate on the filament signal and to get affirmation regarding the expressions derived in chapter 7 and chapter 8.
First it was tried to visualize this influence simply by monitoring the filament signal with an oscilloscope.
Next it was tried to determine the flow noise by means of a two-phase lock-in amplifier (LIA). It was tried to monitor the filament signal in the frequency range first from 4 to 10 and later from 4.5 Hz to 5.5 Hz by using a sweep signal as a reference signal for the LIA.
Finally the value of the 5 Hz noise component in the filament noise spectrum was determined using a frequency analyzer.
It is true that the 5 Hz fluctuations in the flow will cause noise on the filament signal but it has to be clear that this noise will be filtered out by the GC software. The measurements of the 5 Hz noise of the filament will make it possible to check the expressions derived in the previous chapters because it is now possible to measure the (5 Hz) noise as a function of the (5 Hz) flow fluctuations. In practice (random) fluctuations in the flow will occur which cannot be filtered out and so may limit the MDC.

9.2 Measurement of the noise with the a two-phase lock-in amplifier

9.2.1 Experimental Set-up

Fig. 17 shows the experimental set-up of a measurement of the flow noise in which a two-phase lock-in amplifier (LIA) forms the main part.

Two function generators were used to produce a sweep as the reference signal for the LIA. Fig. 18 shows the output signal of these function generators. The signal below (between 0 and 2 Volts) is the output signal of function generator 1. Its output voltage increases directly proportional to the time. This signal is the input signal for the second function generator and is connected with the sweep input channel of it.

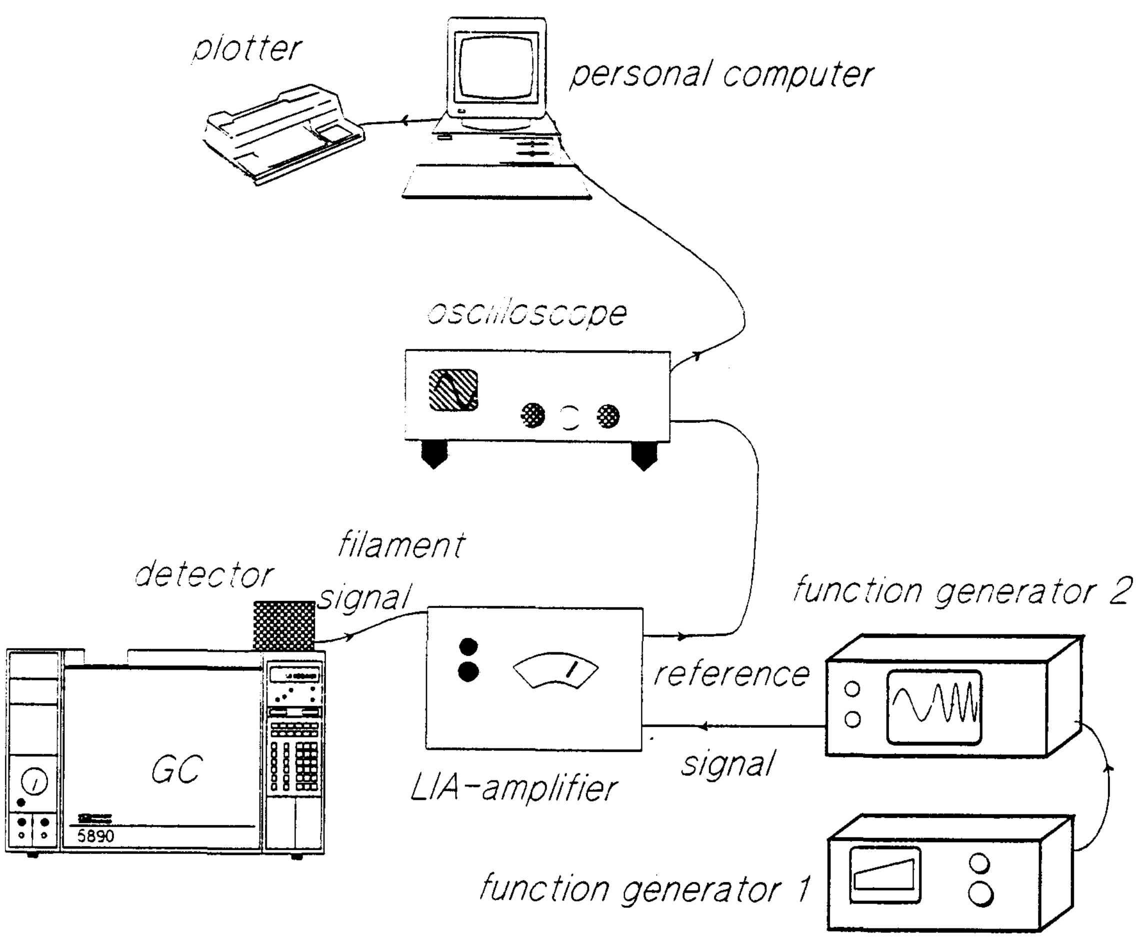

Fig. 17 Experimental set-up of the measurement of the flow noise by means of a lock-in amplifier.

The signal above shows the output signal of the second generator. The frequency of this signal increases from 4 Hz to 10 Hz within 4 seconds. The frequency change as a function of the time depends on the steepness of the ramp of its input signal. In this example the scan speed is 1.5 Hz per second. This signal is called the reference signal and is applied to the reference signal input channel of the LIA.

The second signal fed to the LIA is the signal obtained by measuring the voltage across the operating filament.

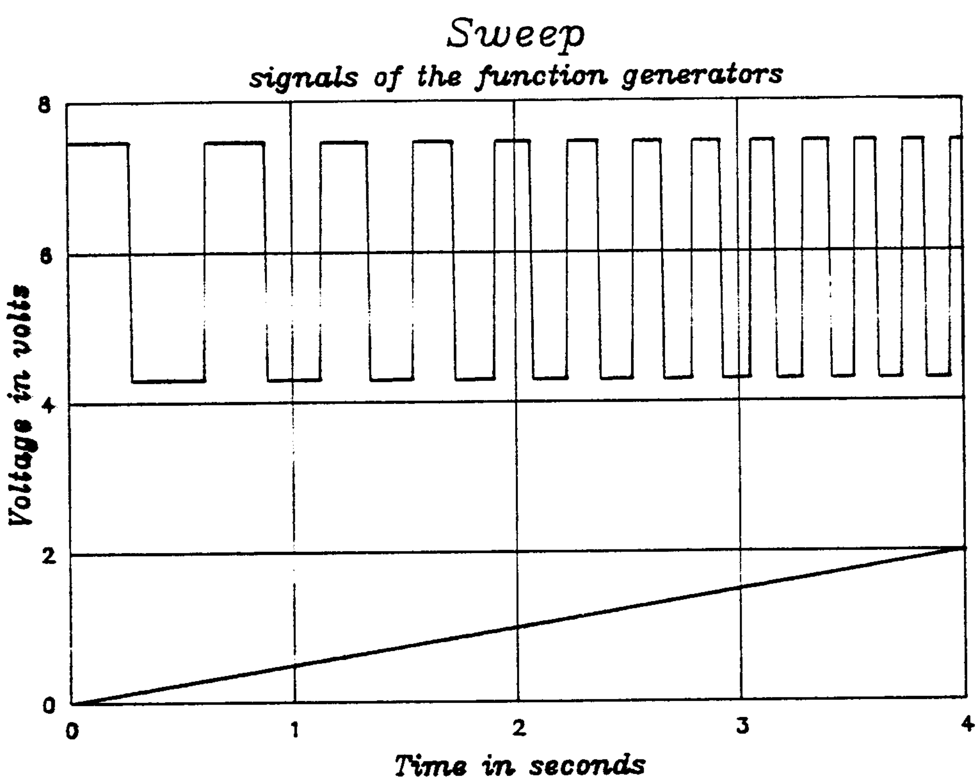

Fig. 18 Output signals of the function generators. The voltage of the function generator 1 increases directly proportional to the elapsed time (lower signal). Function generator 2 creates a sweep signal (upper signal).

The LIA first multiplies both signals and after that multiplies the result with a rectangle window. The remaining signal is the LIA output signal. In case both reference and noise signal have the same frequency (component) the LIA output signal will increase. The length of the time window has to be chosen by the user. It was taken to be 1 s.

In this way it is possible to obtain a frequency spectrum analyzer. Since the frequency of the reference signal changes the LIA scans the frequency noise spectrum of the filament signal between the begin and end frequencies of the reference (sweep) signal. By adjusting the signal of the first generator it was possible to analyze pieces of the filament signal noise spectrum from 0.01 Hz to 100 kHz. The output of the LIA was recorded by a digital oscilloscope. Finally, the noise spectra obtained were transmitted to a personal computer.

9.2.2 Measurements and Results

First, the whole noise spectrum of an operating filament was investigated. The temperature of the detector block was 180°C, the reference flow was 15 ml/min and the column flow was 5 ml/min.
According to the manual these flows induce an optimal performance of the detector when using capillary columns. The oven was off. Significant peaks were found at 5 Hz and at 50 Hz. A part of the results of these measurements are show in chapter 13.

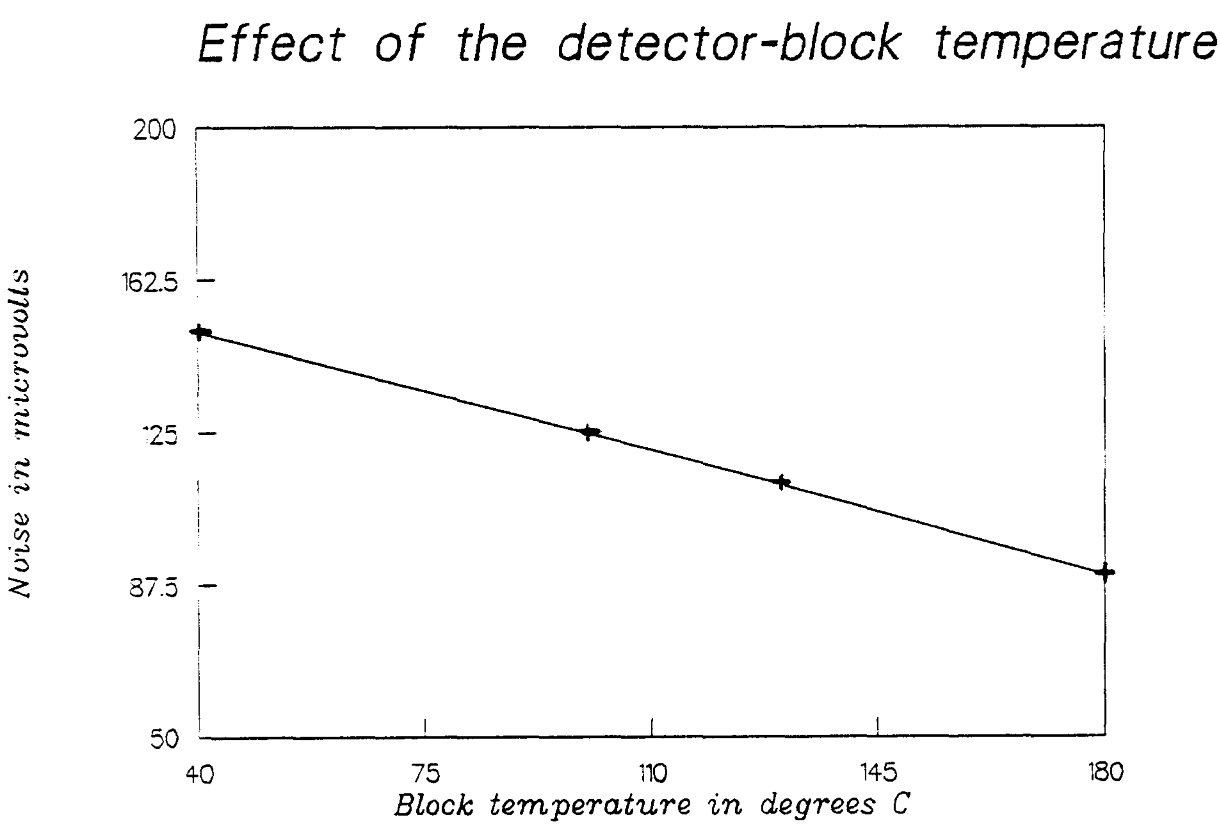

Fig. 19 Effect of the detector block temperature.

Fig. H1 and Fig. H2 show the part of the spectrum between 2 Hz and 8.7 Hz when the oven is off. The same part is shown when the oven is operating in

Fig. H3 and Fig. H4. It shows that there are two additional peaks in the spectrum at 3.9 Hz and 7.6 Hz. These peaks are small compared to the 5 Hz peak, but because the bandwidth of the GC filter is 2.7 Hz, the 3.9 Hz component in the filament signal may influence the MDC. The influence of the detector block temperature is shown in Fig. I1 to Fig. I4 in chapter 13. The spectrum between 4 Hz and 7.4 Hz is shown for various block temperatures. The flows were unchanged. The effect of the block temperature on the 5 Hz peak-height are summarized in Fig. 19. It shows that a higher block temperature decreases the magnitude of the 5 Hz-peak. This can be explained by the fact that the temperature difference between block and filament is kept fixed. Only the block temperature can be set by the user. The difference between the temperatures decreases as the setting of the block temperature is higher in order to avoid destruction of the filament. This means that the convective heat transfer will decrease because the average increase of the gas temperature is less.

Finally the scan speed was reduced by a factor 10 to 0.0044 Hz/s and the height of the 5 Hz peak as a function of the reference flow was determined. For these small scan speeds the height of the 5 Hz-peak becomes independent of the scan speed.

Fig. J1 to Fig. J6 show the spectra if the reference flow is varied from 0 ml/min to 30 ml/min. The results of these measurements are summarized in Fig. 20 (upper curve). The LIA output as a function of the reference flow can as a first approximation be written as:

$$V_{LIA} = 1.5\ 10^{-5}\ F_{V,REF}\ \text{[Volts]}\ (10\ \text{ml/min} \le F_{V,REF} \le 30\ \text{ml/min}) \quad (108)$$

This result will be used in paragraph 9.2.4 to derive an expression for the flow noise as a function of the flow fluctuations.

9.2.3 The configuration with the dead volumes

The volume of the two reference supply channels was increased by embodying a dead volume in each channel. It was expected that the maximum magnitudes of flow fluctuations in the cell would be diminished because the dead volumes act as capacitors.

Again the reference flows were varied from 0 ml/min to 30 ml/min. The block temperature was 180°C, the oven was off and the column flow was 5 ml/min. The scan speed was unaltered; 0.0044 Hz/s.

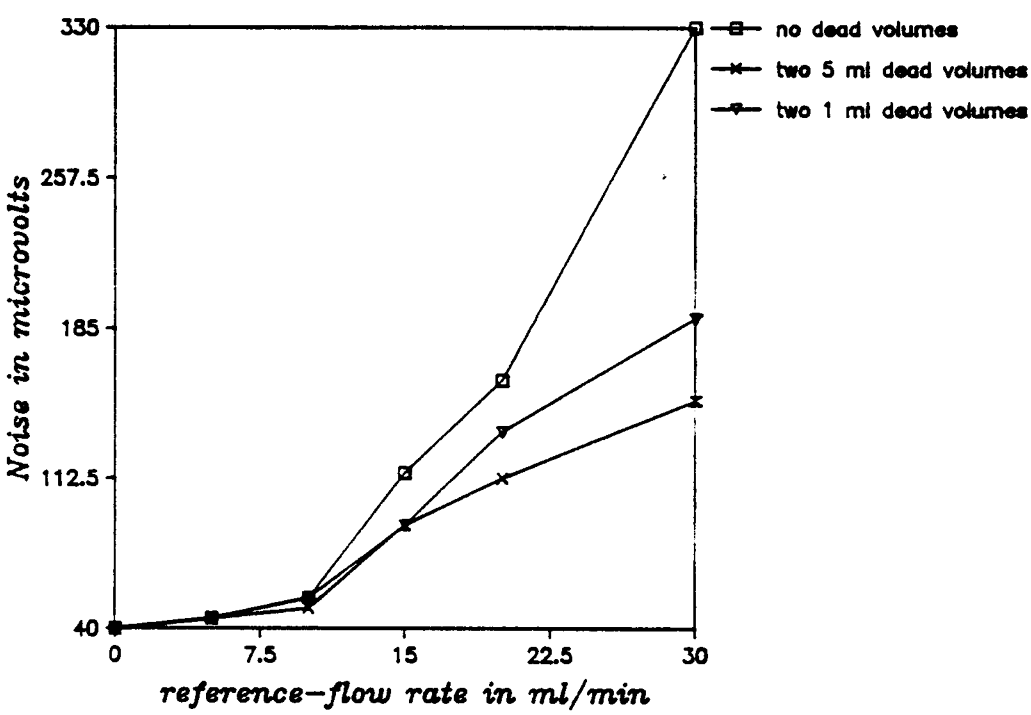

Fig. 20 LIA-output signal as a function of the reference flow in the HP 5890 A cell.

The noise spectra obtained are shown in Fig. K1 to Fig. K6 in chapter 13. The volumes of the dead volumes is 5 ml (the volume of the original supply channels is 0.1 ml). It is shown in Fig. 20 that the height of the 5 Hz-peak is approximately 2 times smaller.

The same measurements were done with two 1 ml dead volumes. The spectra are not shown. It is shown in Fig. 20 that the height of the 5 Hz-peak decreases approximately with a factor 1.5.

9.2.4 Interpretation of the results

In this paragraph it will be tried to find an expression for the convective heat transfer as a function of the reference flow using the results of the measurements done with the LIA.

The LIA output as a function of the time is given by:

$$V_{LIA}(t') = \frac{1}{2t_M} \int_{t'-2t_M}^{t'} V_F(t) V_{REF}(t) dt \tag{110}$$

Where t_M is the width of the rectangle window (also called the time constant of the LIA), V_F is the filament voltage and V_{REF} is the reference signal. In all the measurements performed the time constant was set to 1 second.

The filament signal has a dominant 5 Hz component which has approximately a square wave form. This signal can be written as a series of harmonic sinusoidal signals having frequencies of 5, 15, 25, 35 ....etc. Hz.

The only signal of interest in the frequency interval from 4.5 Hz to 5.5 Hz is the main (ground) 5 Hz sinusoidal signal which can be written as:

$$V_F(t) = V_{F0} \cos(2\pi f_p t + \omega) \tag{111}$$

Where V_{F0} is the amplitude of this signal and f_p is the frequency of the noise signal and ω is the phase of the signal.

The reason why a two-phase LIA is used in this experiment is because it also considers the 90 degrees out of phase component of the input signal. In this way it can be avoided that two signals having the same frequency give zero output because they are exactly 90 degrees out of phase.
The 90 degrees out of phase component can be written as:

$$V_F(t) = V_{F0}\sin(2\pi f_P t+\omega) \tag{112}$$

It will be clear that the phase is of no importance if both signals are considered because both signals can be composed exactly out of sinusoidal and cosinusoidal signals. For that the phase of the signal is no longer taken into account in the sequel of this paragraph.
The reference signal can be written as:

$$V_{REF} = V_{REF0}\cos 2\pi(f_P+\Delta f)t \tag{113}$$

Where V_{REF0} is the amplitude of the signal and Δf is the difference in frequency between the actual frequency and 5 Hz. Δf is a function of the time when using sweep signals.

$$\Delta f = \frac{(f_1-f_0)t+f_0 t_S}{t_S} - f_P \tag{114}$$

Where f_1 is the final frequency of the sweep signal (5.5 Hz), f_0 is the start frequency of the sweep (4.5 Hz) and t_S is the time the sweep lasts (200 s). It can be tried to solve the integral in eq. 110 as a function of the time, however, it will appear that the result has to be written as a series of Fresnel integrals. The side-lobes occurring in the plots can be explained by the behaviour of these integrals.

In this paragraph it will be tried to solve eq. 110 using a fixed frequency difference between input signal and reference signal.

If the input (filament) signal is presented by a cosine (with 0 phase) the result of the integral is given by:

$$V_{LIA} = \frac{V_F V_{REF}}{4t_M} \left[\frac{\sin 2\pi\Delta f t}{2\pi f t} + \frac{\sin 4\pi f_0 t}{4\pi f_0} \right]_{t'-2t_M}^{t'} \tag{115}$$

If the input signal is presented by a sine (with 0 phase) the result is given by:

$$V_{LIA} = \frac{V_F V_{REF}}{4t_M} \left[\frac{\cos 2\pi\Delta f t}{2\pi f} + \frac{\cos 4\pi f_0 t}{4\pi f_0} \right]_{t'-2t_M}^{t'} \tag{116}$$

After 100 seconds the frequency of the sweep is exactly 5 Hz. The LIA output for 5 Hz is thus determined between 98 and 100 seconds after the beginning of the sweep.

From eq. 113 it can be seen that the frequency changes $1\ 10^{-2}$ Hz within 2 seconds. An average frequency difference of $5\ 10^{-3}$ Hz during these two seconds is used in eq. 115 it is found that $V_{LIA} = 1.999 V_{F0} V_{REF}/4$. Using this frequency difference in eq. 116 it is found that $V_{LIA} = 6\ 10^{-2} V_{F0} V_{REF}/4$.

For the total output of the two-phase LIA it is found after taking the squareroot of the sum of the squares of both the results that:

$$V_{LIA} = V_{F0} V_{REF0}/2 \tag{117}$$

From the results shown in chapter 13 it can be seen that for 10 ml/min $\leq F_{V,REF} \leq$ 30 ml/min the V_{LIA} output is given by:

$$V_{LIA} = 1.5\ 10^{-5} F_{V,REF} \tag{118}$$

Since $V_{F0} = 3.5$ Volts it appears after combining eq. 116 and eq. 117 that:

$$V_{F0} = 0.8\ 10^{-5} F_{V,REF} \tag{119}$$

Now using eq. 79 and eq. 105 again it is finally found that the relative change in the dissipated power as a function of the reference flow can be written as:

$$\frac{\Delta P_{CV}}{P_F} = 3.5\ 10^{-5}\ \Delta F_V \tag{120}$$

ΔP_{CV} is the change in the transferred power caused by the change in volumetric flow in the filament channel.

9.3 Measurements of the noise with an oscilloscope

The main goal of the experiment described is to find affirmation concerning the convective heat transfer affecting the filament signal.

Therefore the signal of the operating filament was measured by means of an digital oscilloscope (NICOLET 3091). The oscilloscope signal could be plotted directly by means of a plotter connected with the scope.

The filament signal was measured connecting its power supply leads with the oscilloscope input leads.

The column flow was adjusted to be 5 ml/min and the reference flow could be varied. The temperature of the block was set to be 170°C (443 K).

Because the geometry and the quantities of this cell are the same as the geometry and quantities used for the calculations in the former chapters, the applied power was approximately 0.45 W and the voltage drop across the filament 2.81 V.

Fig. L1 to Fig. L3 in chapter 13 show the measured filament signal for a reference flow of 0 ml/min, 15 ml/min and 30 ml/min. The column flow was kept constant, 5 ml/min. The sensitivity setting of the analyzer was maximal.

Fig. L1 shows the filament signal in case there is no reference flow. The baseline shows no 5 Hz noise. The 50 Hz fluctuation on the signal is caused by the network.

Fig. L2 shows the signal in case the reference flow is 15 ml/min. The estimated magnitude of the 5 Hz noise is about 3 10^{-5} Volts.

Fig. L3 shows the signal in case the reference flow is 30 ml/min. The estimated 5 Hz fluctuation is about 6 10^{-5} Volts.

Linearizing these results it can be estimated that the voltage changes as a function of the reference flow are approximately equal to:

$$\Delta V_{OSC} \approx 2\ 10^{-6}\ F_{V,REF} \qquad (121)$$

where F_V is the volumetric flow in the cell in ml/min.

For the relative power changes as a function of the changes in the flow in the filament channel it can be found, using eq. 79 and eq. 105 that:

$$\frac{\Delta P_{CV}}{P_F} = 1\ 10^{-5}\ \Delta F_V \tag{122}$$

The lack in agreement between the result of the measurement with the LIA (eq. 120) and the result obtained with the oscilloscope can be explained on the one hand by the rough calculations made in the previous paragraph and on the other by the small voltages which had to be measured with the oscilloscope.

9.4 Measurements of the noise with a spectrum analyzer

9.4.1 Measurements and results

Finally the amplitude of the 5 Hz-peak signal is determined using a spectrum analyzer (TR 9042 ADVANTEST).
The signal of the filament was measured connecting the leads of it to the analyzer input leads. The bandwidth of the analyzer is 0.025 Hz when its frequency range is between 0 Hz (0.025 Hz) and 10 Hz. The frequency spectrum determined could be plotted by means of a plotter directly connected to the analyzer.
The column flow was set to be 5 ml/min. The reference flow was varied from 0 ml/min to 30 ml/min.
First the spectrum analyzer was scaled by measuring a defined 5 Hz sinusoidal signal generated by a function generator. The RMS value of this signal was determined with a suitable AC voltmeter to be 0.1 V. The frequency spectrum of this signal showed only one peak at 5 Hz and its height was exactly 0.1 V. Evidently, the spectrum analyzer shows the RMS value of the frequency components. This means that the 5 Hz frequency peak has to be multiplied by $\sqrt{2}$ to get the amplitude of the 5 Hz signal. The results of the measurements of the 5 Hz filament noise are shown in Fig. M1 to Fig. M7 of chapter 13.
The height of the 5 Hz-peak, V_{SA}, is approximately linearly dependent of the reference flow.

$$V_{SA} = 1.1\ 10^{-6}\ F_{V,REF} - 2\ 10^{-6} \qquad \text{(in Volts)} \qquad (123)$$

The amplitudes of the 5 Hz signal will be $\sqrt{2}$ times higher and by using eq. 79 and eq. 105 again shows that this result implies for the convective heat transfer as a function of the volumetric flow in the cell:

$$\frac{\Delta P_{CV}}{P_F} = 0.8\ 10^{-5}\ \Delta F_V \tag{124}$$

where F_V is the volumetric flow in the cell in ml/min.

This result shows reasonable agreement with the result obtained with the oscilloscope. The inaccuracy of the previous measurements makes it acceptable to consider the result obtained with the frequency analyzer as the most reliable experimentally found expression for the convective heat transfer as a function of the volumetric flow in the cell.

10 Results

As a first result it is proved that the fundamental (theoretical) detection limit of a Thermal Conductivity Detector differs approximately two orders of magnitude from the actual (practical) detection limit.
It is found that fluctuations in the flow in the cell can limit the signal to noise ratio of this detector.
For that an expression for the heat transfer in the cell as a function of the flow , was derived after solving the mass, momentum and energy equation of the flow in the cell. This was done in two ways, considering a 3.5 μl cell operating with a 110 K temperature difference between filament and block.
First, it was tried to solve these equations analytically after making the appropriate assumptions and simplifications. As a result it is found that the power transferred by convection, P_{CV}, as a function of the volumetric flow in the cell, F_V (in ml/min), can be written like: $P_{CV}/P_F = 3.3\ 10^{-4} F_V$, if P_F is the total applied power to the filament. An exact expression is found by solving the mass, momentum and energy equations numerically. It was found that $P_{CV}/P_F = 7.7\ 10^{-5}\ F_V$.
It is very well acceptable that the disagreement between these results is caused by the assumptions and simplifications made when solving the equations analytically. The results obtained are not completely confirmed by the results of the measurements of the flow noise. For that the flow noise of a cell (HP 5890 A TCD) having the same geometry and quantities as the cell used in the theoretical model, was measured in three different ways. The main noise-monitoring equipment in the experimental set-up consists either of a lock-in amplifier, an oscilloscope or a spectrum analyzer.
The cell consists of two parallel flow channels. Only in one channel a filament is present. The way it is operated induces 5 Hz fluctuations in the flow in the filament channel. The value of these fluctuations are directly

proportional to the reference flow rate. The 5 Hz signal was measured as a function of the reference flow.

As a result of comparing the flow in the cell with the current in a analog electrical circuit it is found that the fluctuations in the flow, ΔF_V in the filament channel can be written as: $\Delta F_V = 0.175 F_{V,REF}$. Where $F_{V,REF}$ is the reference flow. Finally knowing the flow fluctuations as a function of the reference flow and the 5 Hz (noise) signal as a function of the reference flow the desired expression for the flow noise as a function of fluctuations in the flow in the cell could be found experimentally.

From the measurements of the noise with a oscilloscope and a spectrum analyzer, caused by known (5 Hz) fluctuations in the flow, it was found that $\Delta P_{CV}/P_F \approx 1\ 10^{-5} \Delta F_V$. Where ΔP_{CV} is now the change in dissipated heat caused by the fluctuations in volumetric flow, ΔF_V (in ml/min). The result of a measurement with a lock-in amplifier is: $\Delta P_{CV}/P_F \approx 3.5\ 10^{-6} \Delta F_V$.

These results imply that flow fluctuations will limit the actual MDC (1 PPM) of this cell if they exceed approximately 1 10^{-4} ml/min, assuming 1 PPB to be the fundamental detection limit.

It further appears that the values for the thermal and hydrodynamic entrance lengths for the actual Reynolds number for the flow in the cell exceed the values obtained with the boundary layer theory, many times. Because this theory deals with boundary layers having an almost constant thickness, this disagreement is not very surprising. It may be clear that there cannot be spoken about boundary layers when the entrance lengths are very short, in other words, for very low Reynolds numbers. It is however very important to notice that the developed regions are at least 15 times larger than the entrance regions.

Another useful result is that it is shown that the temperature of the gas which reaches the part of the cell which contains the filament will be at block temperature.

11 Conclusions

The conclusions which can be drawn from the results are:

It must be possible to improve the detection limit of a Thermal Conductivity Detector by reducing its actual noise level.

The thermal time constant of the HP 5890 A cell does not affect the width of the peaks eluting from the column.

The 3.5 μl HP 5890 A cell is not compatible with capillary columns.

The heat transferred in the TCD cell by convection has a negligible effect on the TCD response.

The heat transferred by convection is approximately a linear function of the flow in the cell.

(Random) fluctuations in the convective heat transfer caused by fluctuations in the flow will limit the Minimum Detectable Concentration (MDC) of the considered TCD if they exceed 1 10^{-4} ml/min (approximately 0.001% of the volumetric flow in the cell for normal flows).

The energy density of the helium gas in the cell, meaning the energy per unit of cell length is constant in the entire cell. The mean velocity of the helium gas in the cell, increases only in the thermal entrance region of the cell.

The thermal conductivity of the gas in the thermal developed region of the cell is the only gas parameter determining the total transferred heat. Assuming a uniform filament and block temperature the cell behaves like an ideal Thermal Conductivity Detector in this region.

12 Recommendations

In order to find the actual (main) source of noise which determines the actual detection limit two processes have to be investigated further.
It is already mentioned in paragraph 6.3 that the influence of an unsteady wall temperature has to be studied on further.
As a result of this report it is proved that fluctuations in the flow have an effect on the filament signal. The actual fluctuations occurring in the cell may limit the present detection limit. These fluctuations in the flow can be caused by the actual (atmospheric) pressure fluctuations.
The magnitude, spectral density and the bandwidth of the pressure fluctuations have to be determined before any statement about the importance can be made. Also the transfer function of the cell meaning the influence of the pressure fluctuations on the flow has to be taken in account.
Preheating the gas could be a solution to eliminate the influence of the flow fluctuations on the filament signal. This means that part of the filament close to the inlet of the cell (or a second filament) takes care of establishment of the temperature profile.
The other larger part of the filament (or the second filament) is now in the developed region of the flow and is thus insensible to changes in the flow. This part (or filament) operates as an ideal Thermal Conductivity sensor.
Before this concept can be turned into reality some problems have to be eliminated.
When using a single filament consisting of two parts, the material of the part which takes care for the preheating has to have a negligible temperature coefficient of resistivity because it is also part of the sensor. It is also very well possible that the joining of two different filaments both having a thickness of a few μm will cause some great difficulties.
When using two separate filaments it has to be realized that the filaments

close to their connections with the supply leads won't have a uniform temperature. It is not mentioned in this report thus far that the filament will lose some energy by heat conduction through the leads and that the leads will approximately have the same temperature as the block.
This means that the established temperature profile of the first filament will be disturbed again when the flow passes the end of the first (preheating) filament and reaches the beginning of the second (sensing) filament. This means that the signal of the sensor will be flow dependent again.

13 Figures

-Fig. A to Fig. G

SEPRAN plots of the flow in the cell

-Fig. H(1-4), I(1-4), J(1-6) and K(1-6)

Plots of the Lock-in Amplifier output.

-Fig. L1 to Fig. L3

Advantest Spectrum Analyzer output of the filament noise of the HP 5890 A cell.

-Fig. M1 to M7

Advantest Spectrum Analyzer frequency spectrum plots of the filament signal.

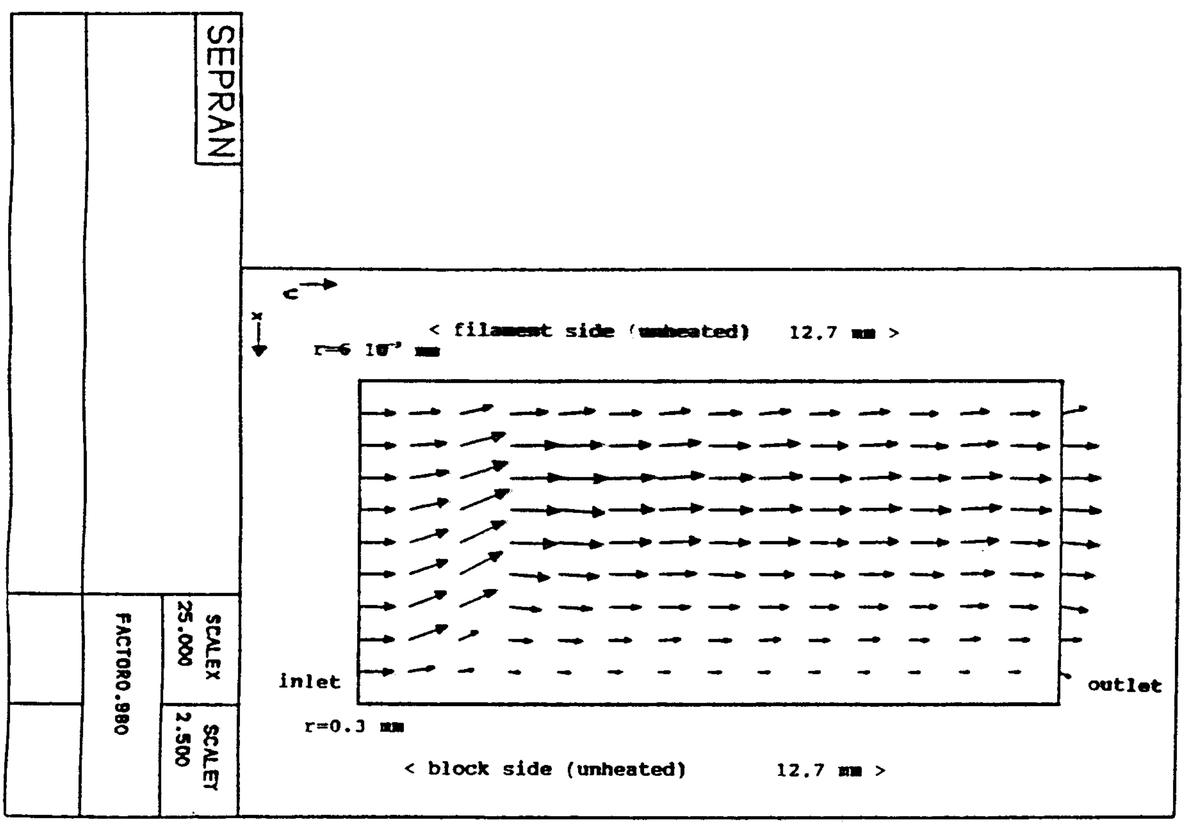

Fig. A Velocity profile in the unheated cell. The filament is at the upper side (r=6 10^{-3} mm)

The block is at the lower side (r=0.3 mm). The cell is expanded 10 times in the radial direction relative to the axial direction. Re=0.4.

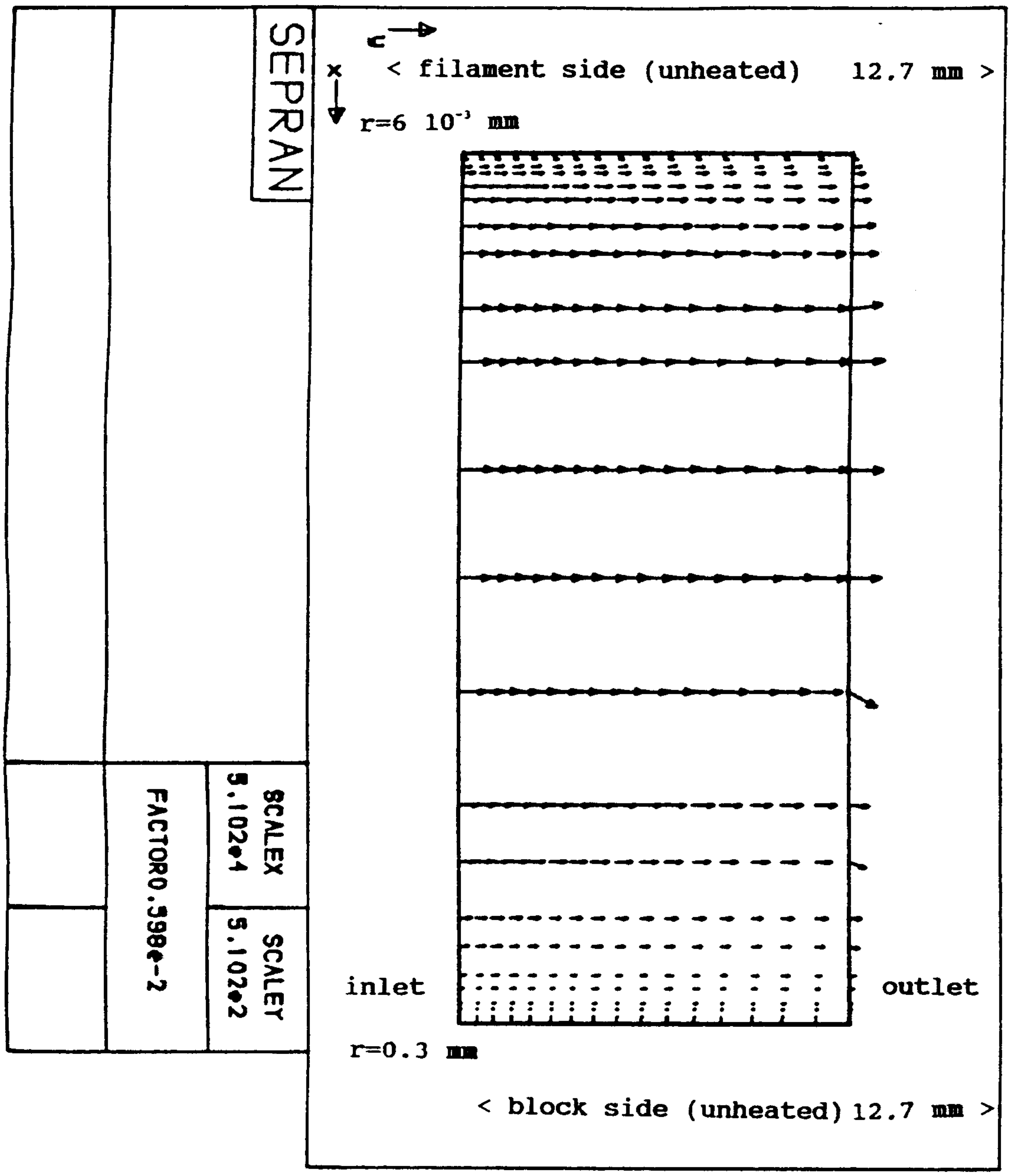

Fig. B Velocity profile in the cell when the velocity profile at the inlet satisfies the theoretical profile. (100 times expanded in radial direction relative to axial direction). Re=0.4.

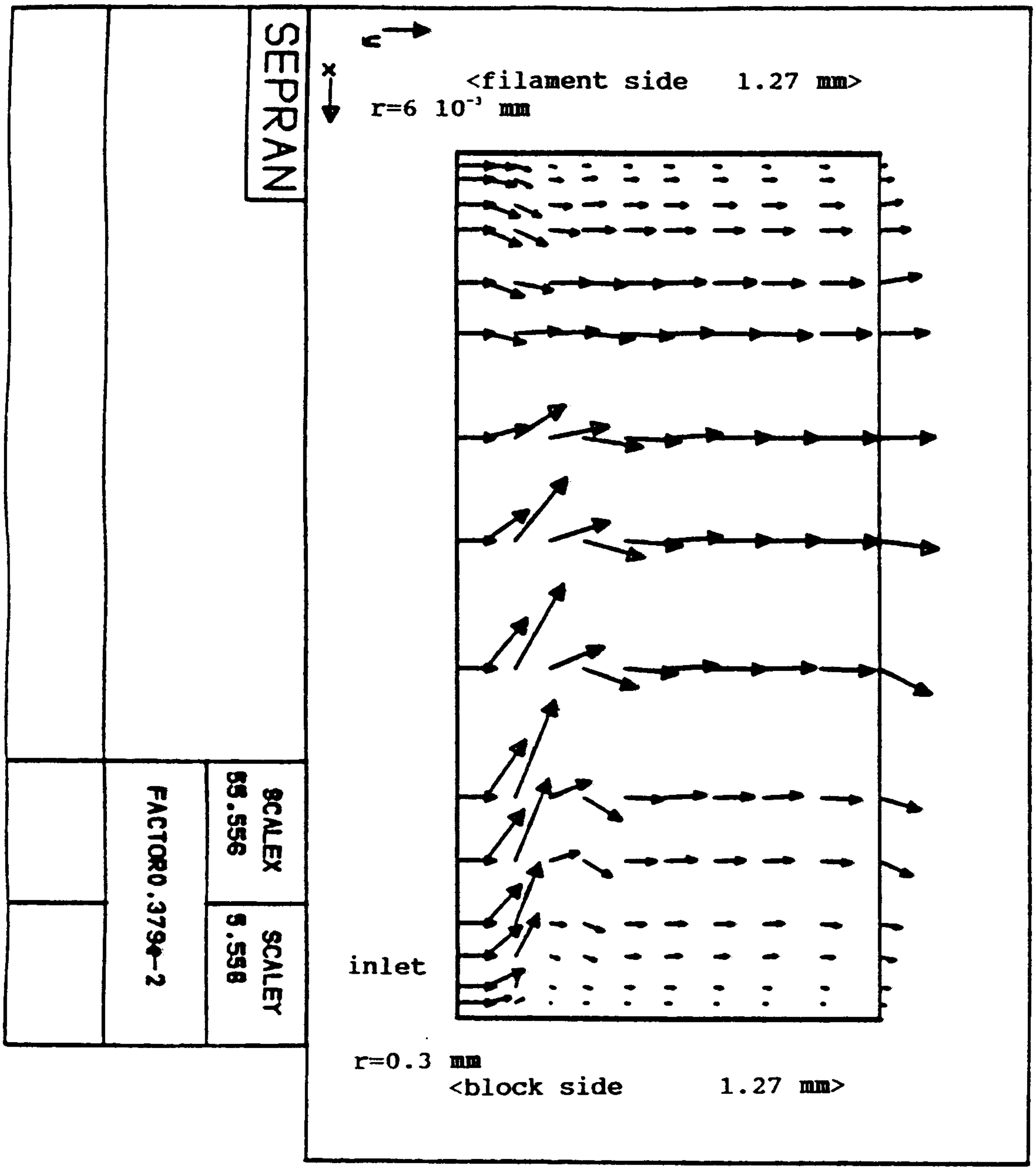

Fig. C Velocity profile in the entrance of the cell (0.1 times the total length of the cell) when the velocity profile at the inlet is flat. 10 times expanded in the radial direction relative to the axial direction. Re=0.4.

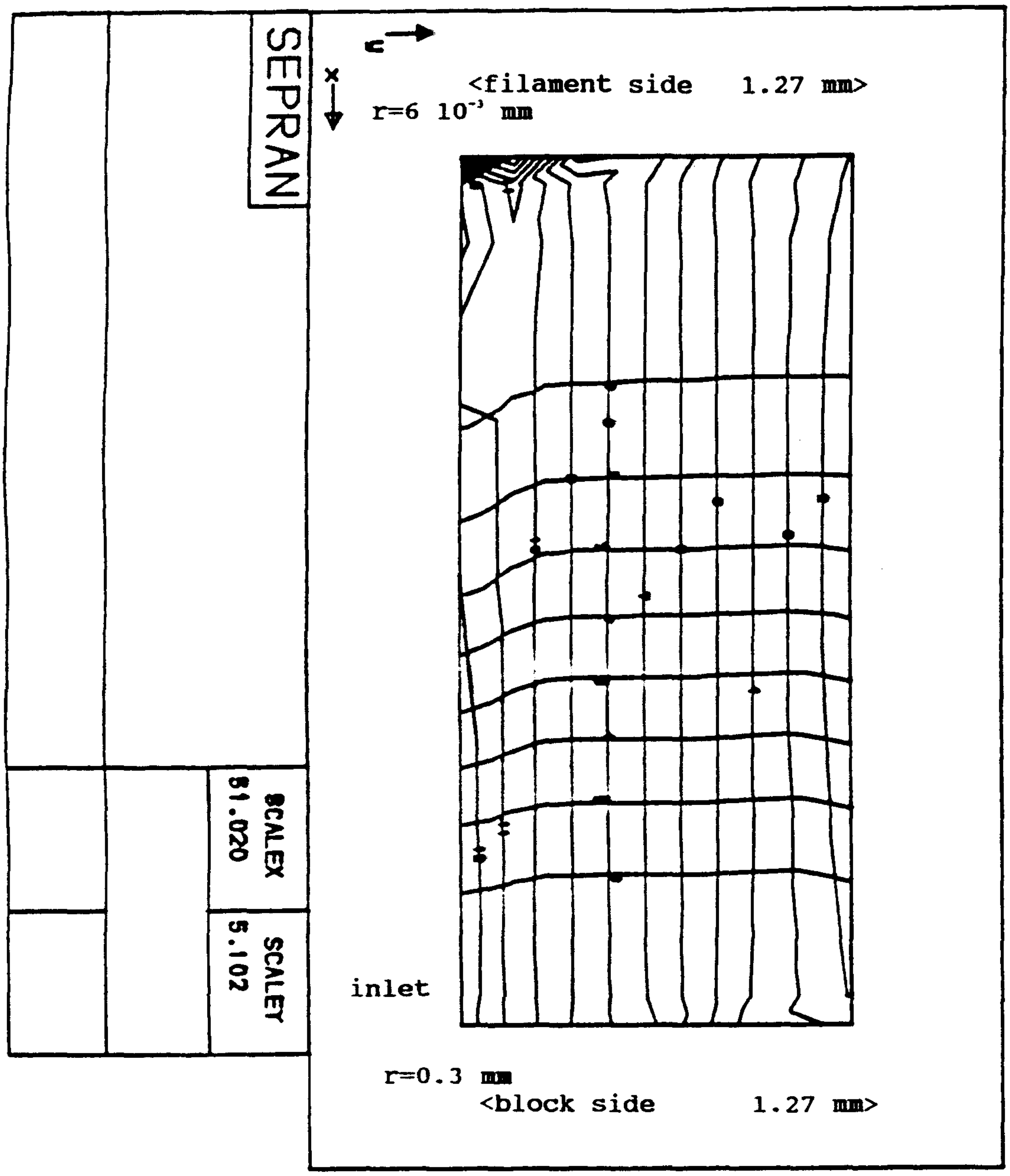

Fig. D Isobars and streamlines in the entrance of the cell when the velocity profile is parabolic. 10 times enlarged in the radial direction relative to the axial direction. Re=0.4

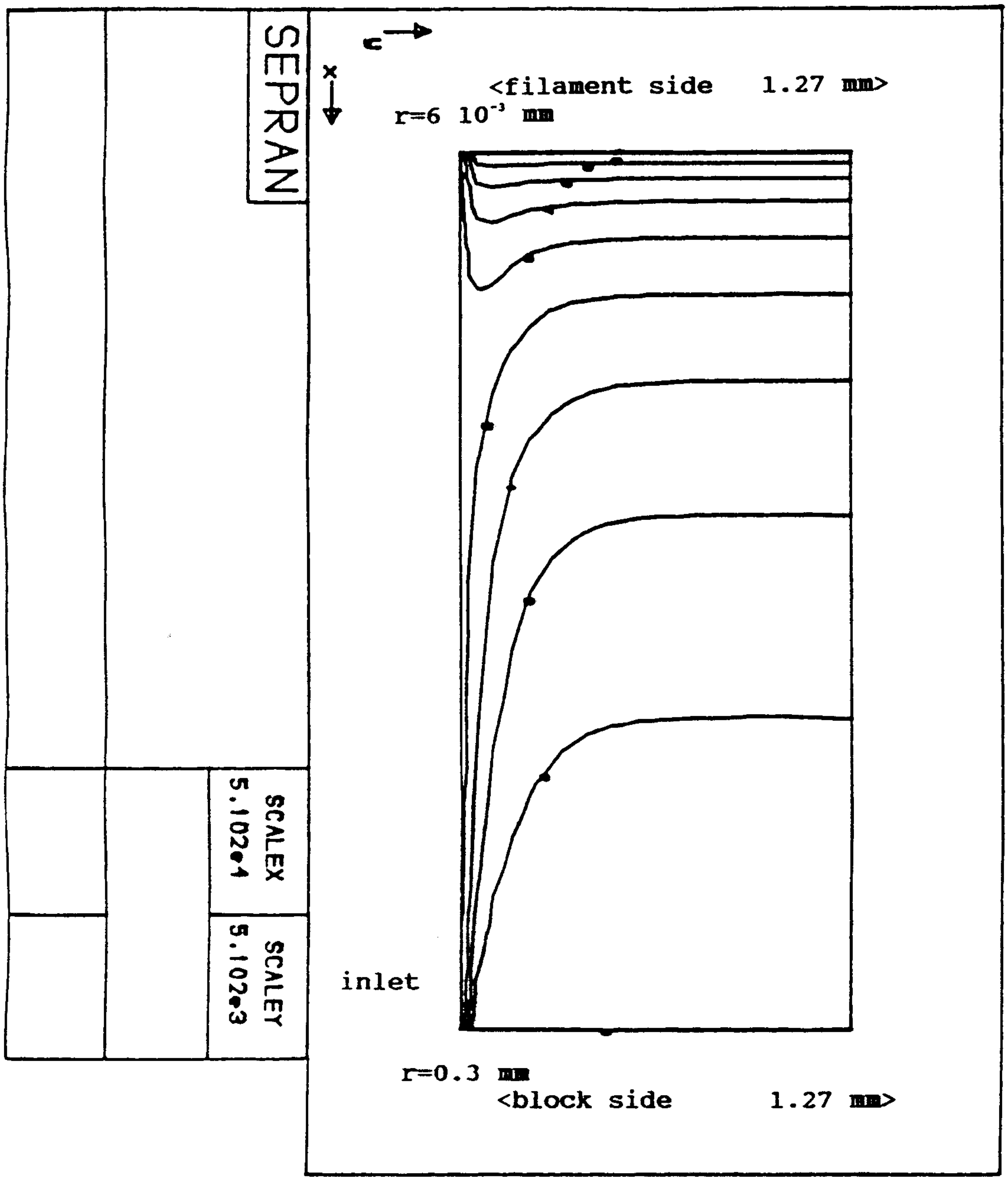

Fig. E Temperature profile at the entrance of the of the cell. The temperature of the incoming helium is 293 K. The filament is at 550 K and the block is at 440 K. Adjacent isotherms are 11 degrees K lower in temperature, when moving towards the wall. 10 times expanded in the radial direction relative to the axial direction. Re=0.3.

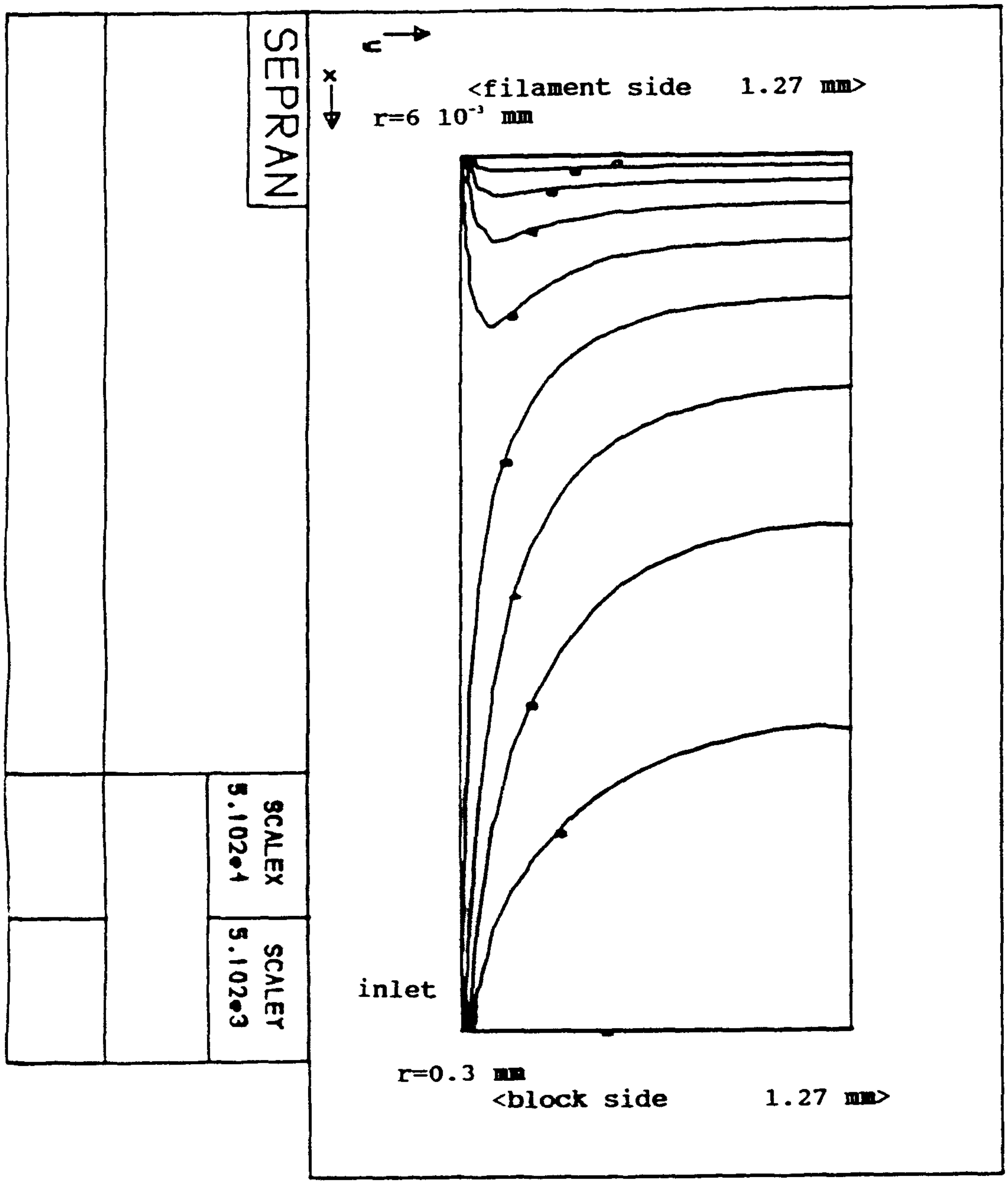

Fig. F Temperature profile at the entrance of the cell. The temperature of the incoming helium is 293 K. The filament is at 550 K and the block is at 440 K. Adjacent isotherms are 11 degrees K lower in temperature, when moving towards the wall. 10 times expanded in the radial direction relative to the axial direction. Re=3.

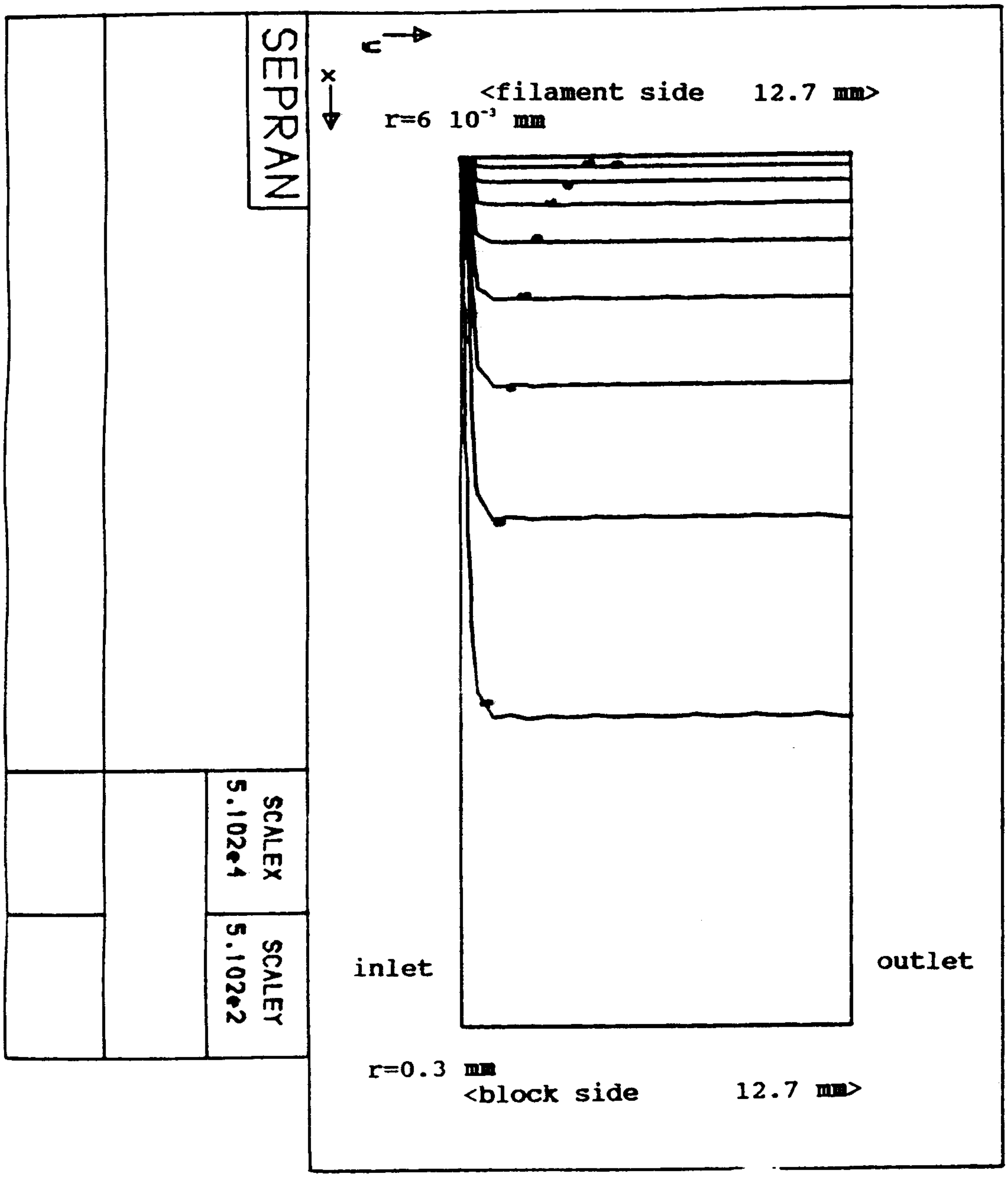

Fig. G Temperature profile in the entire cell. The temperature of the incoming helium is 440 K. The filament is at 550 K and the block at 440 K. Adjacent isotherms are 11 degrees K lower in temperature, when moving towards the wall. 100 times expanded in the radial direction relative to the axial direction. Re=0.3.

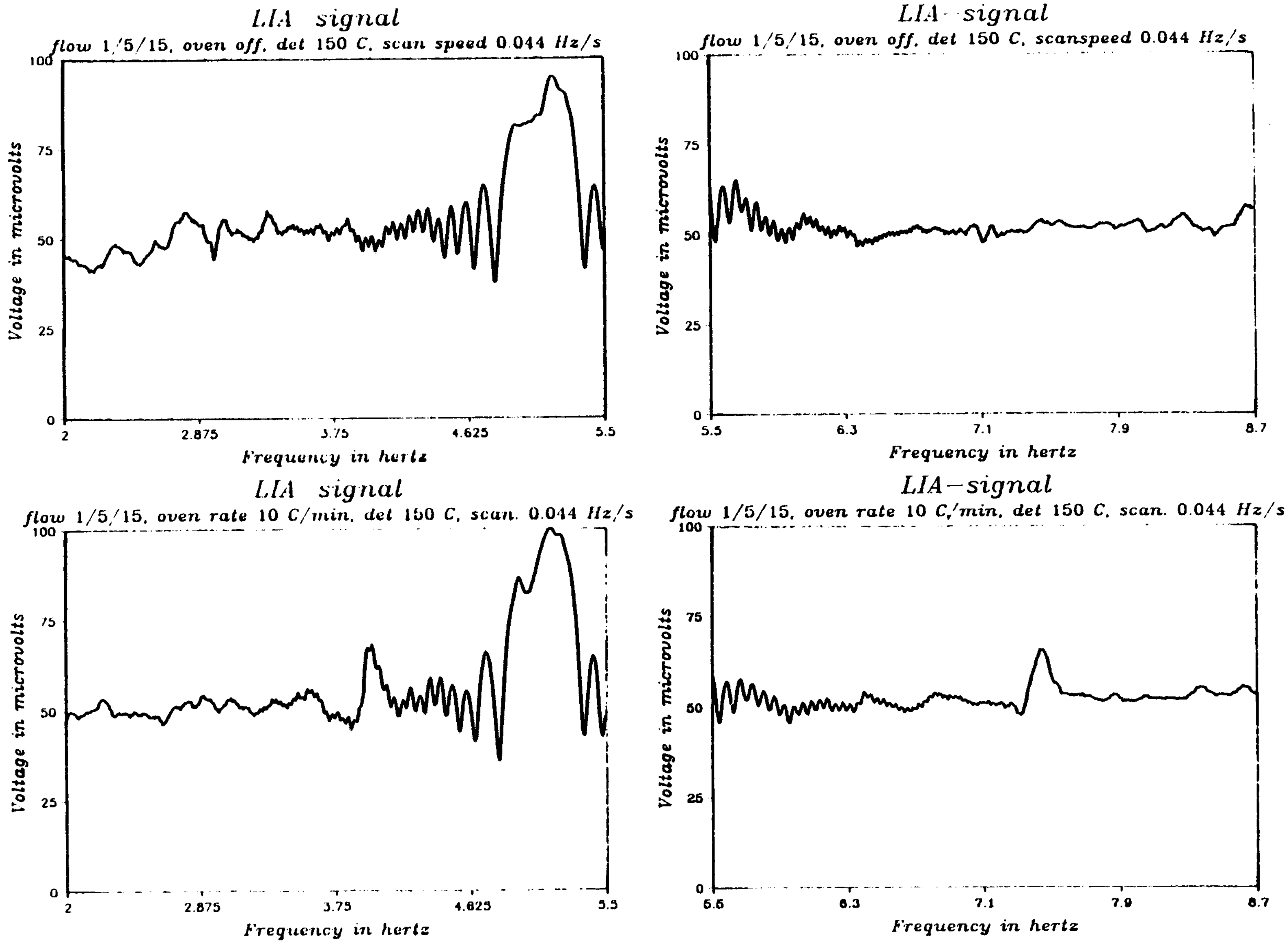

Fig. H(1-4) LIA-output and the effect of the oven temperature. A 3.9 Hz peak and a 7.6 Hz peak appear in the spectrum.

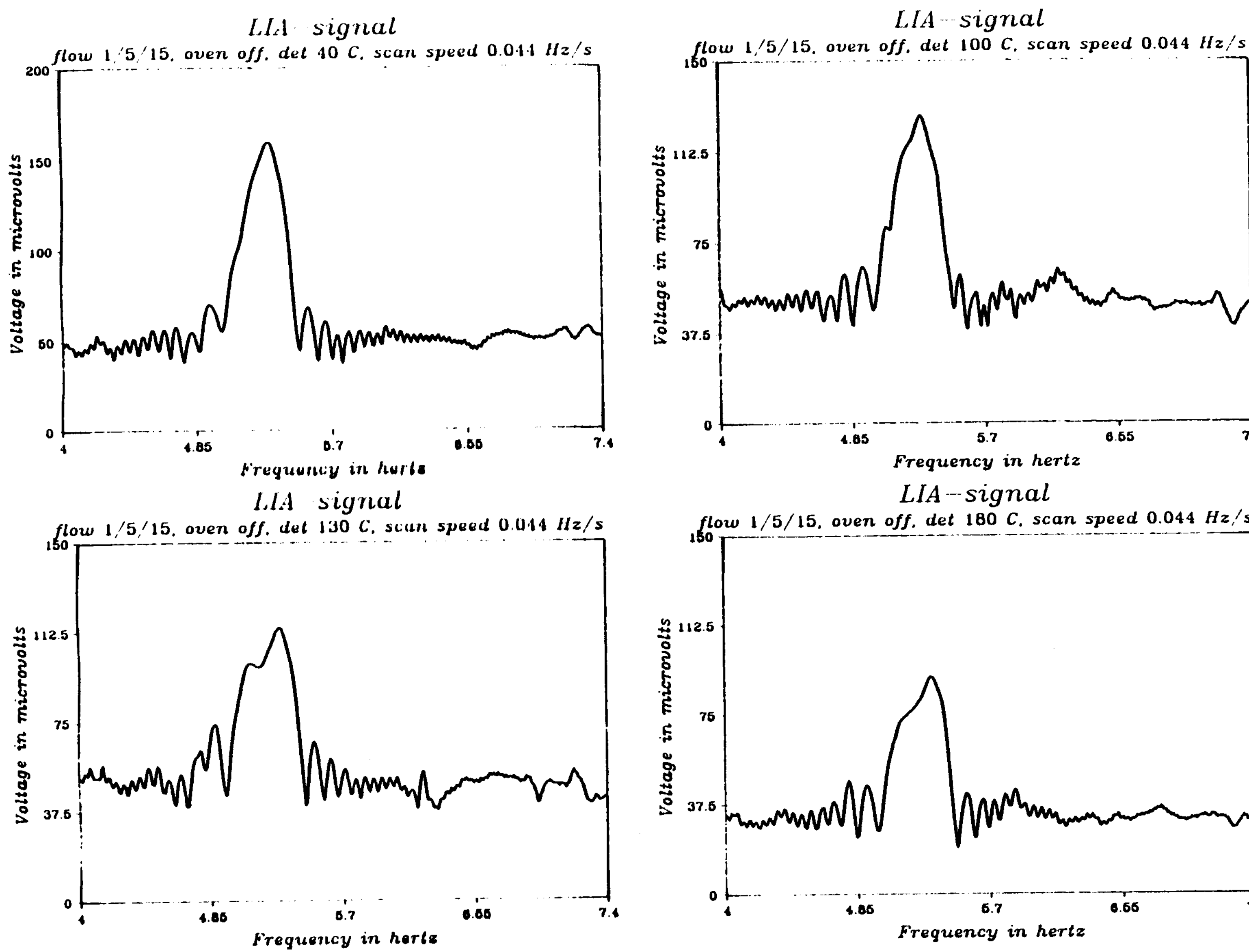

Fig. I(1-4) Effect of the detector block temperature.

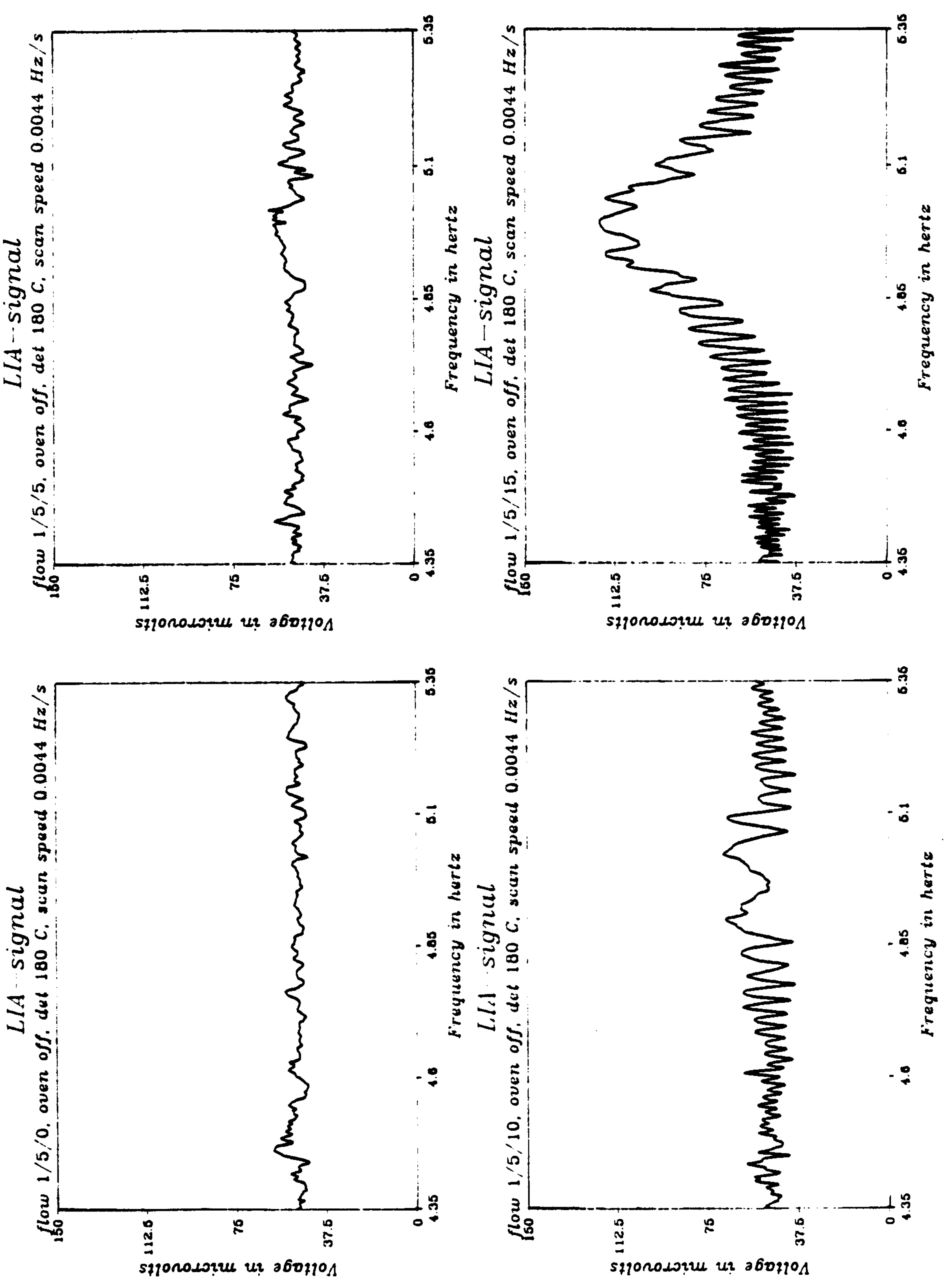

Fig. J(1-4) Effect of the reference flow rate on the 5 Hz filament noise. The reference flow varies from 0 ml/min (Fig. I1) to 15 ml/min (Fig. I4). No dead volumes are embodied in the reference gas supply channels.

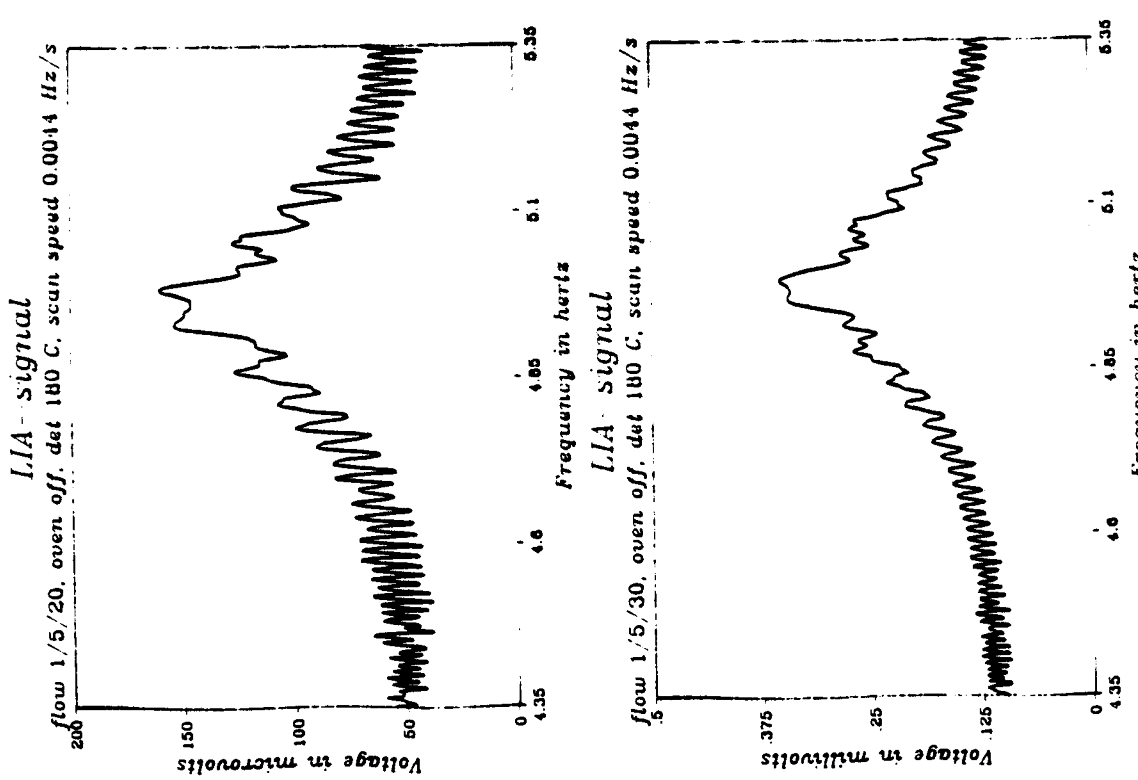

Fig. J(5-6) Effect of the reference flow rate on the 5 Hz filament noise. The flow varies from 25 ml/min (Fig. I5) to 30 ml/min (Fig. I6).

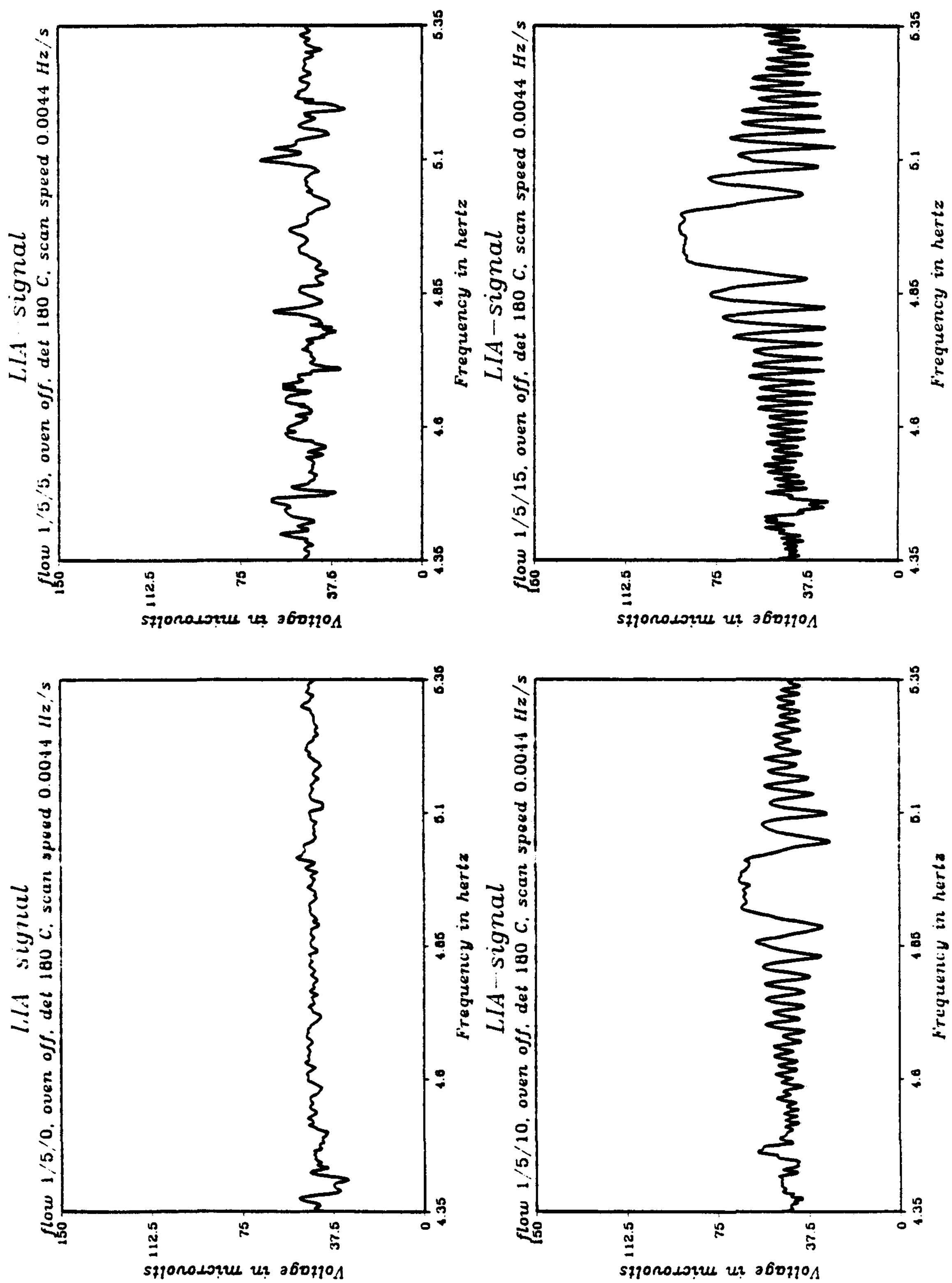

Fig. K(1-4) Effect of the reference flow rate on the 5 Hz filament noise when two dead volumes are embodied in the reference gas supply channels. The flow varies from 0 ml/min (Fig. K1) to 15 ml/min (Fig. K4).

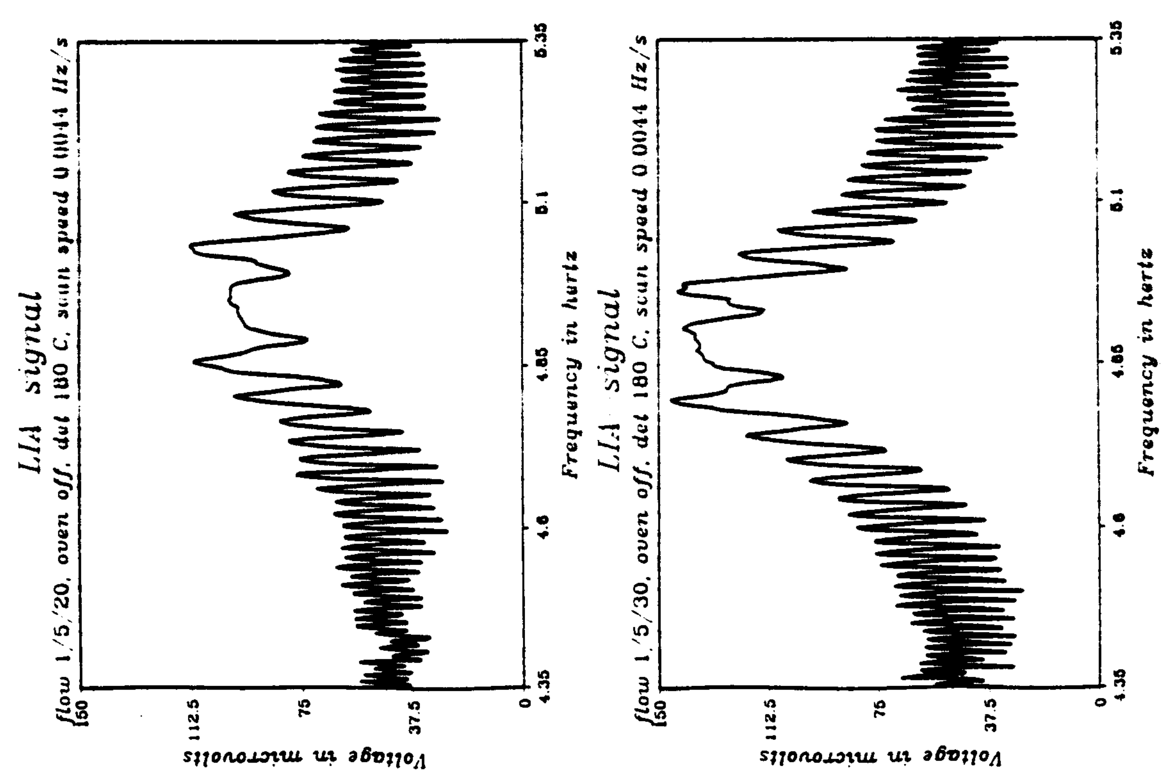

Fig. K(5-6) Effect of the reference flow rate on the 5 Hz filament noise when two dead volumes are embodied in the reference gas supply channels. The flow varies from 20 ml/min (Fig K5) to 30 ml/min (Fig. K6).

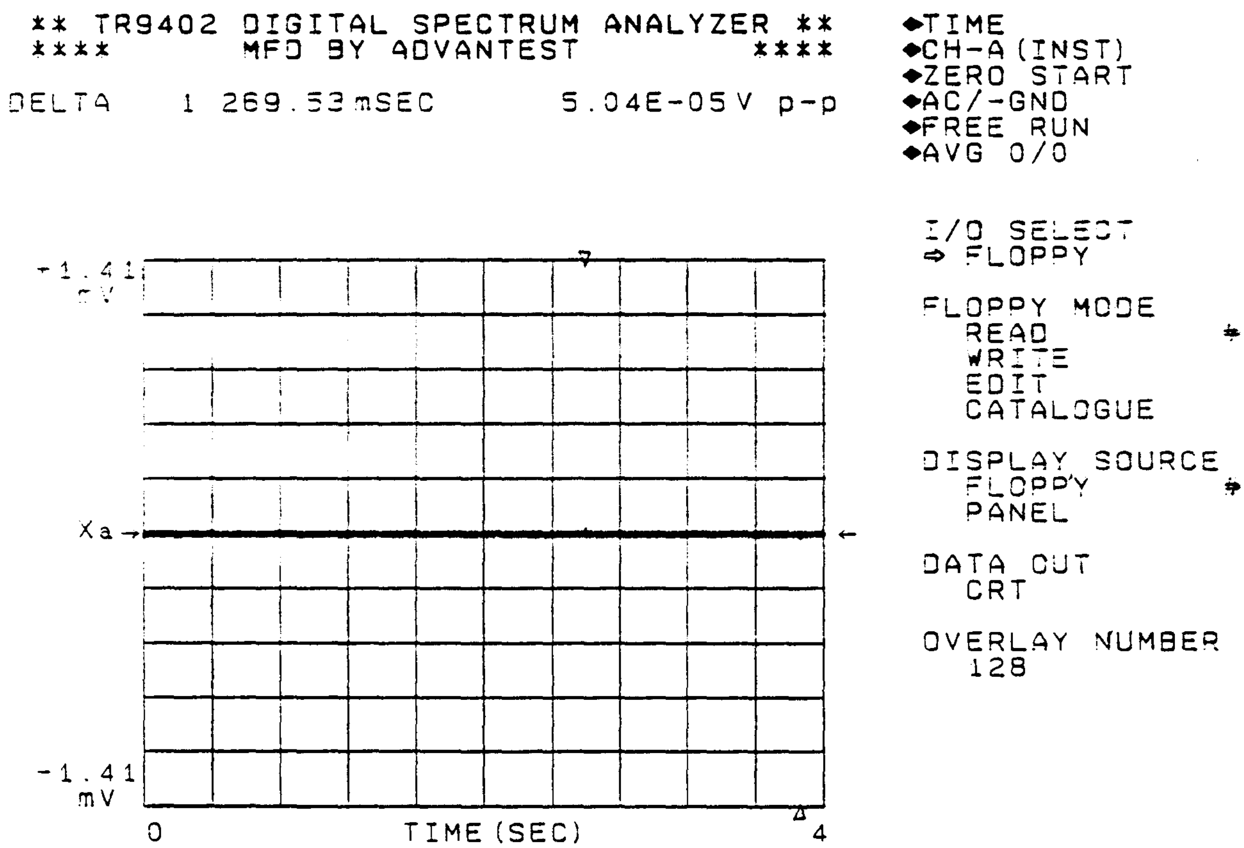

Fig. L1 Filament signal in case there is no reference flow. The column flow is 5 ml/min.

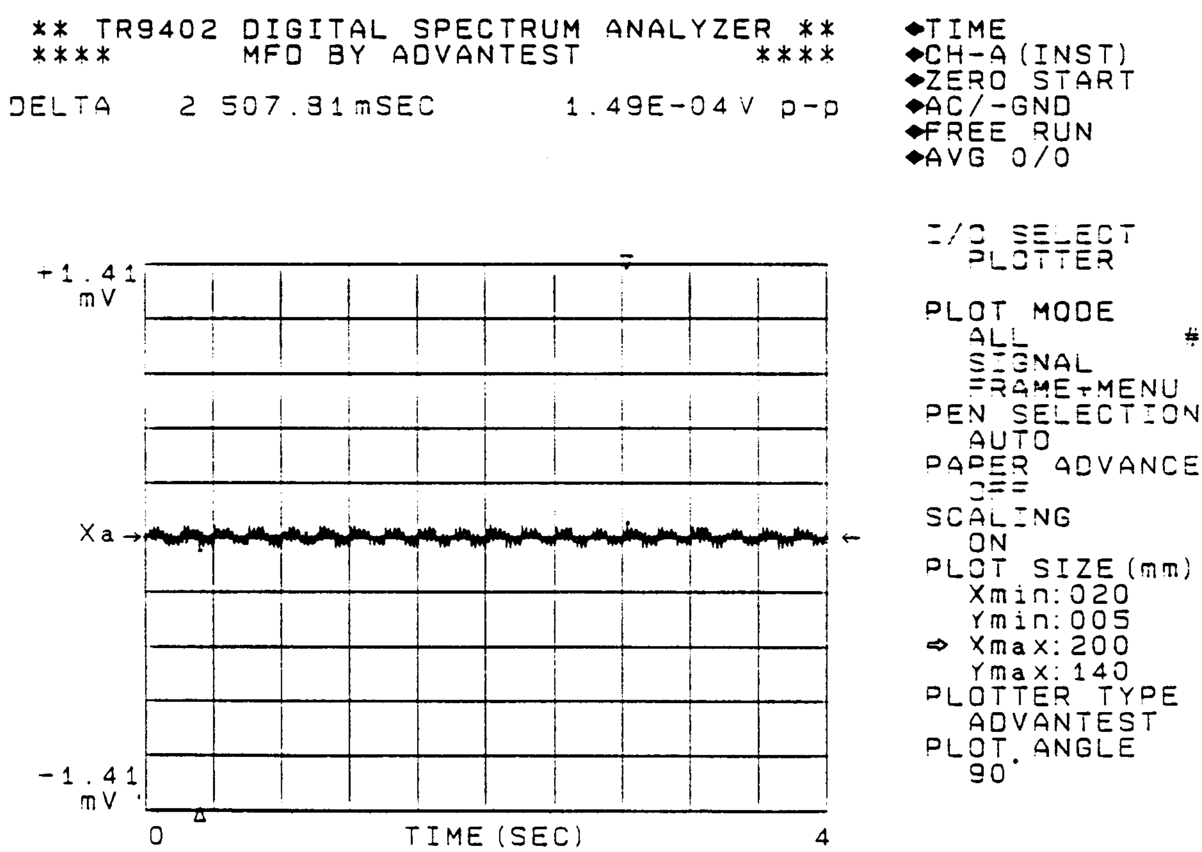

Fig L2. Filament signal in case the reference flow is 15 ml/min. The column flow is 5 ml/min.

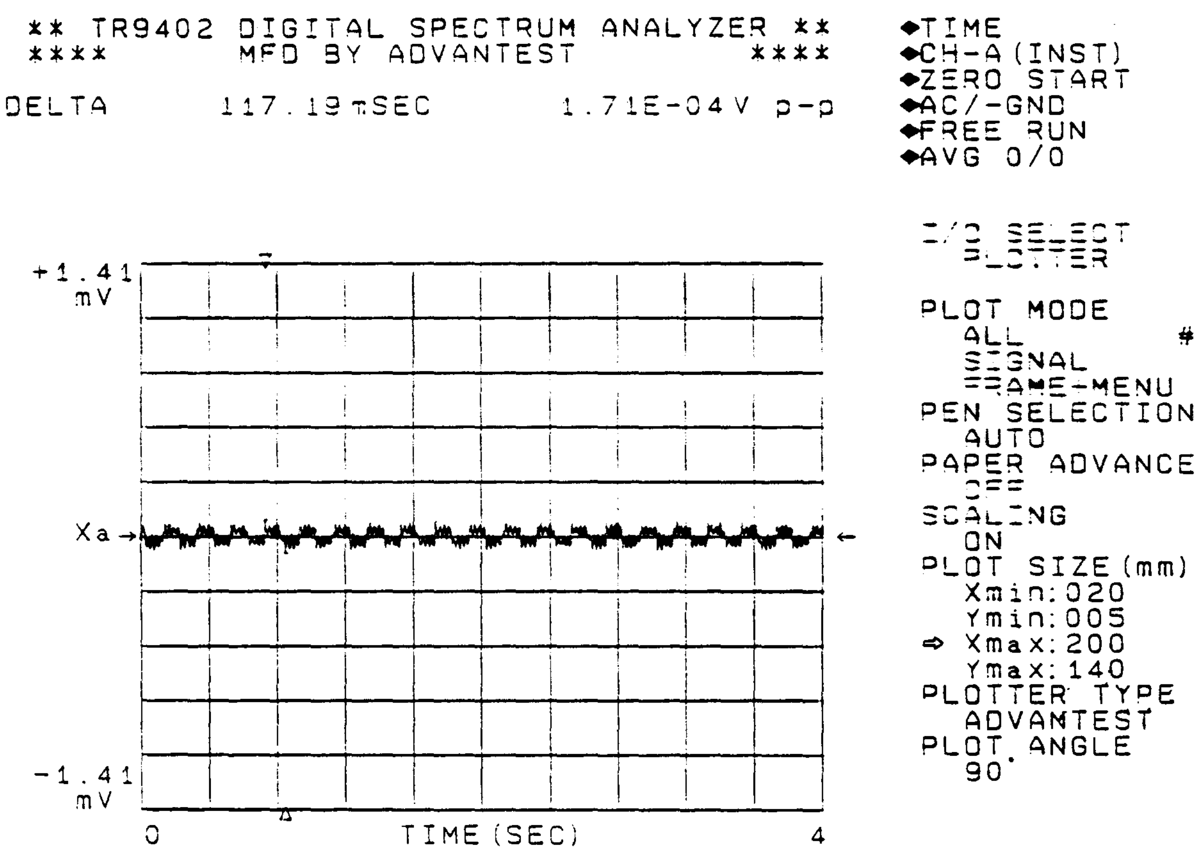

Fig. L3 Filament signal in case the reference flow is 30 ml/min. The column flow is 5 ml/min.

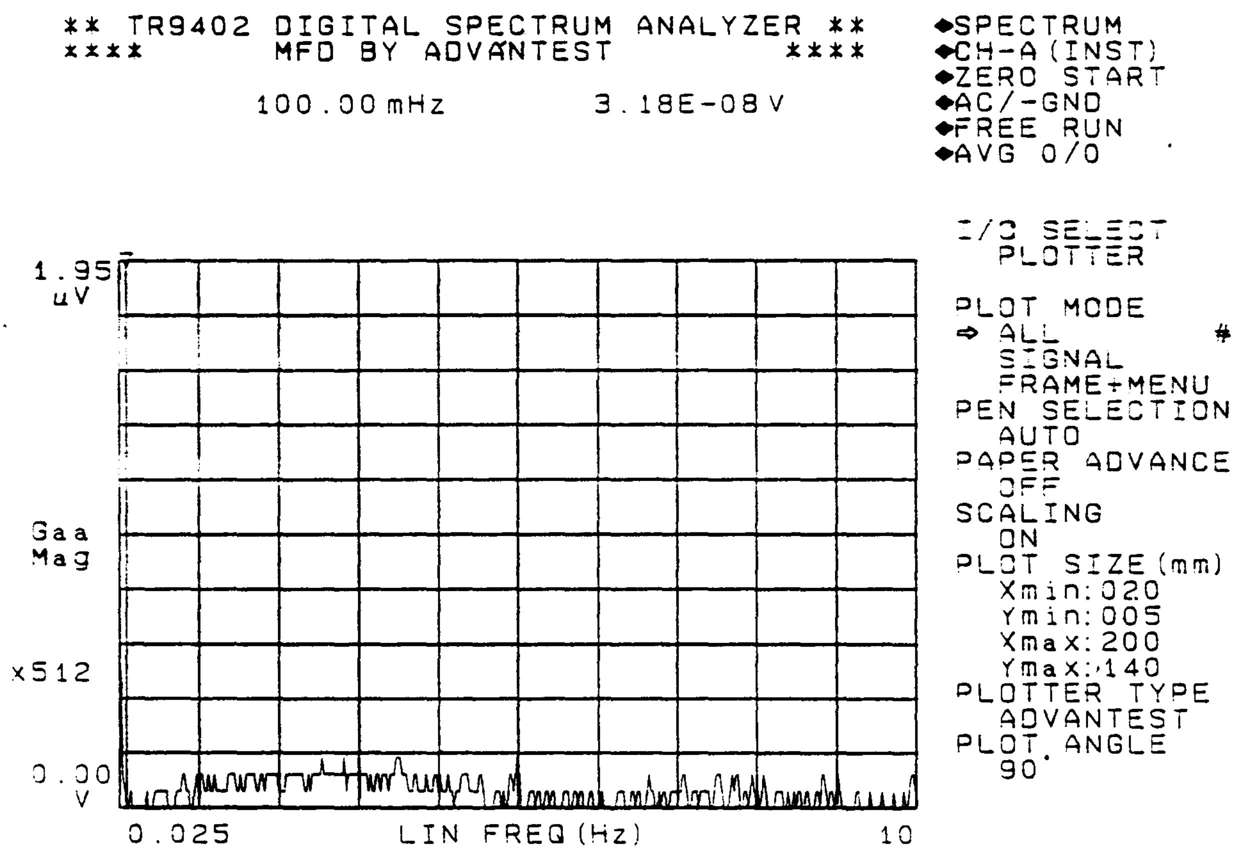

Fig. M1 Frequency spectrum of the filament noise if the reference flow is 0 ml/min.

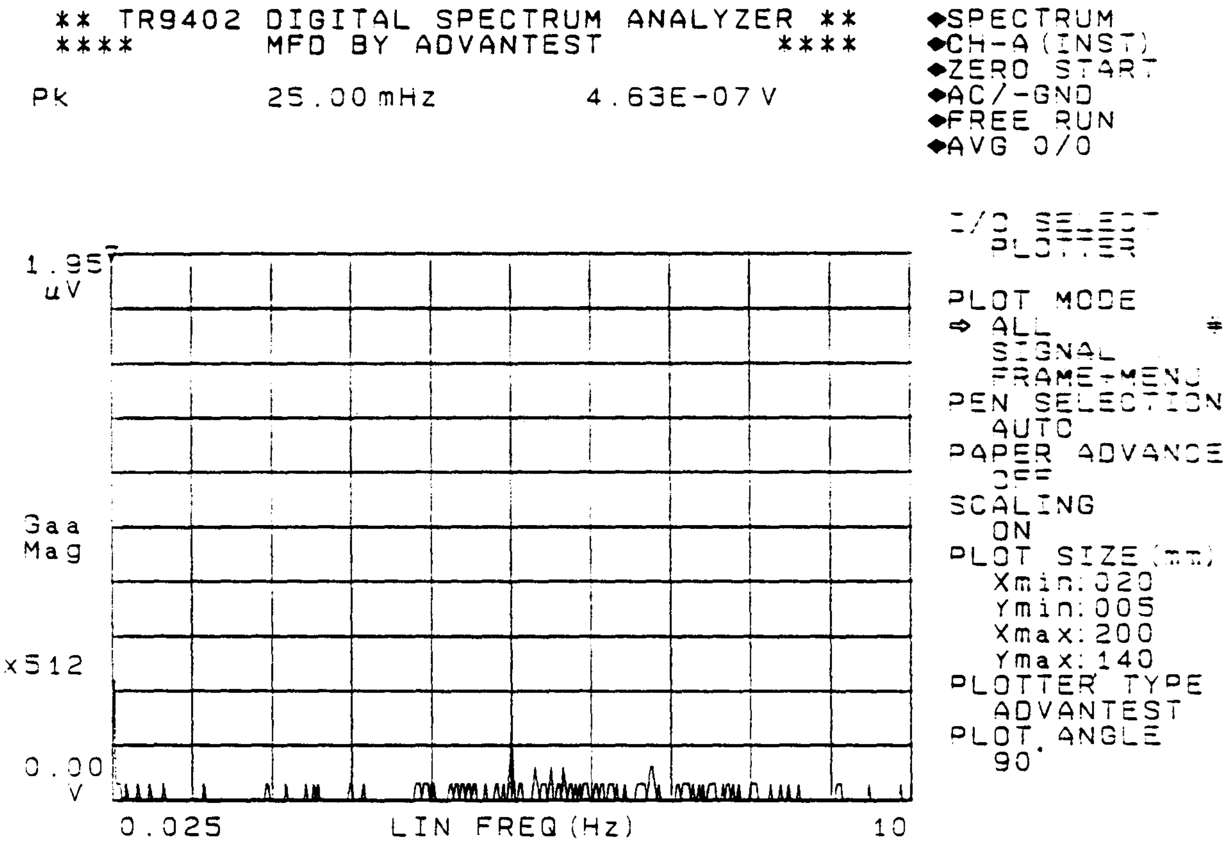

Fig. M2 Frequency spectrum of the filament noise if the reference flow is 5 ml/min.

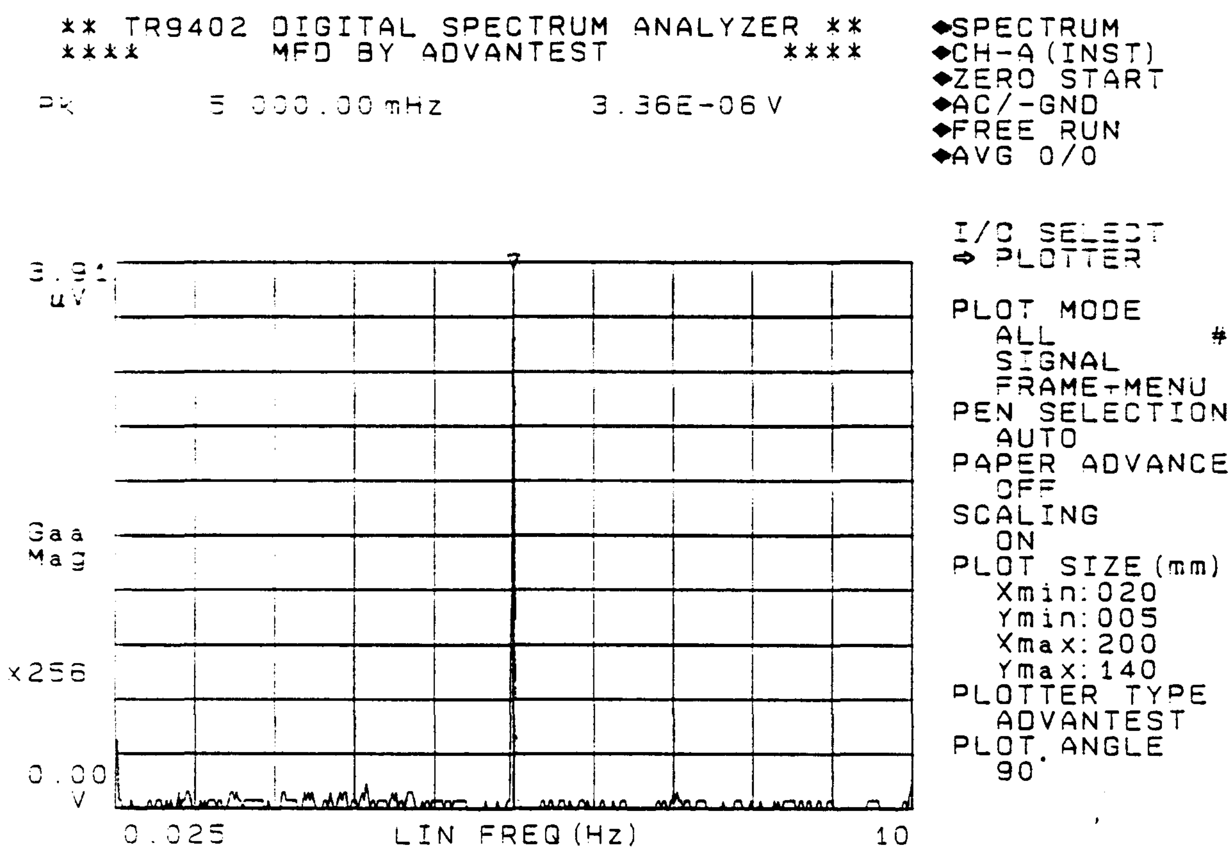

Fig. M3 Frequency spectrum of the filament noise if the reference flow is 10 ml/min.

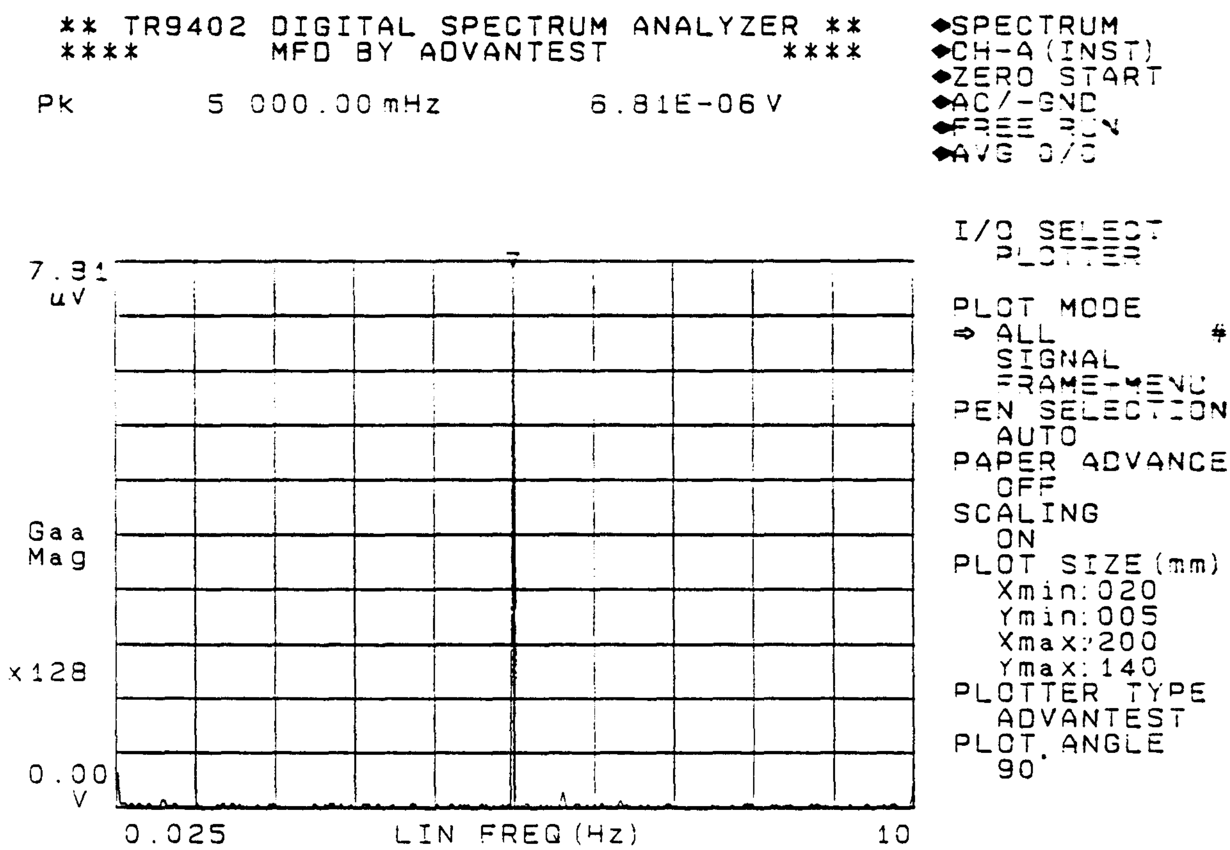

Fig. M4 Frequency spectrum of the filament noise if the reference flow is 15 ml/min.

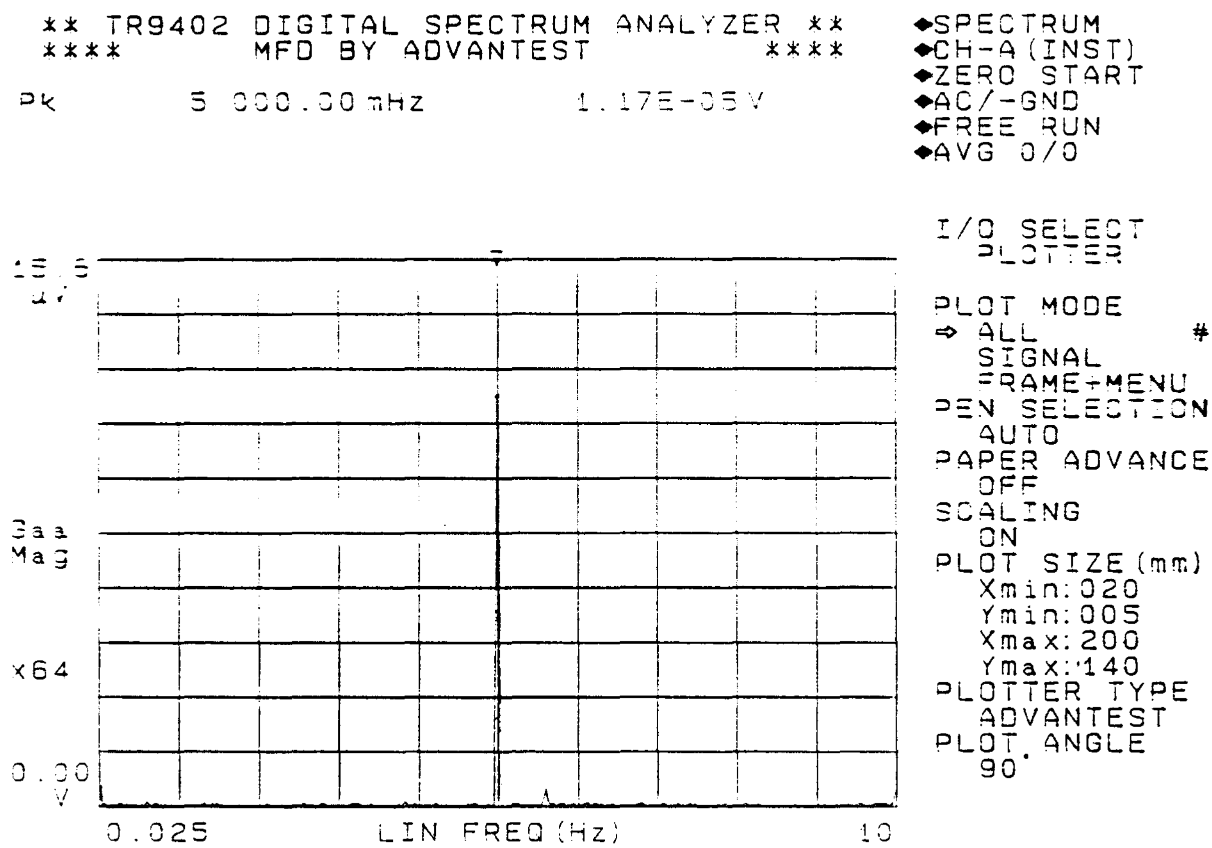

Fig. M5 Frequency spectrum of the filament noise if the reference flow is 20 ml/min.

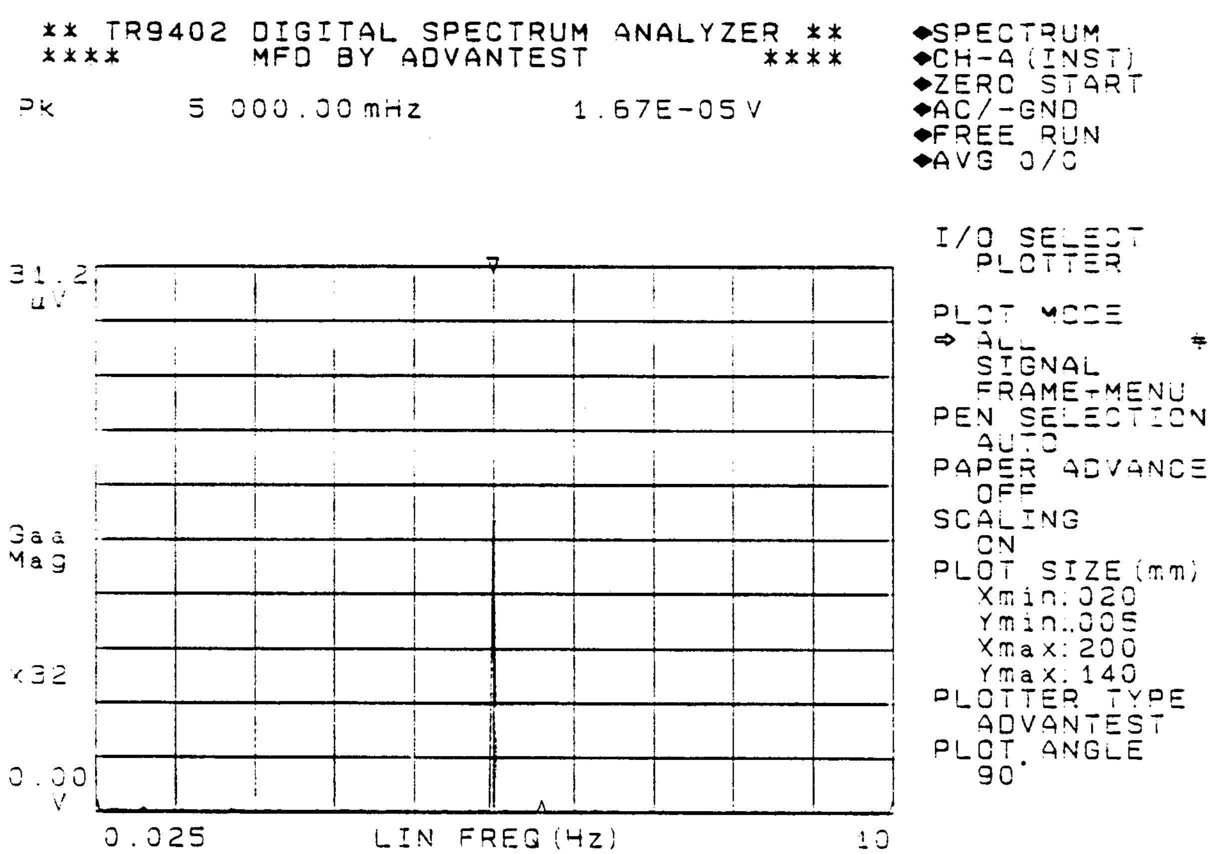

Fig. M6 Frequency spectrum of the filament noise if the reference flow is 25 ml/min.

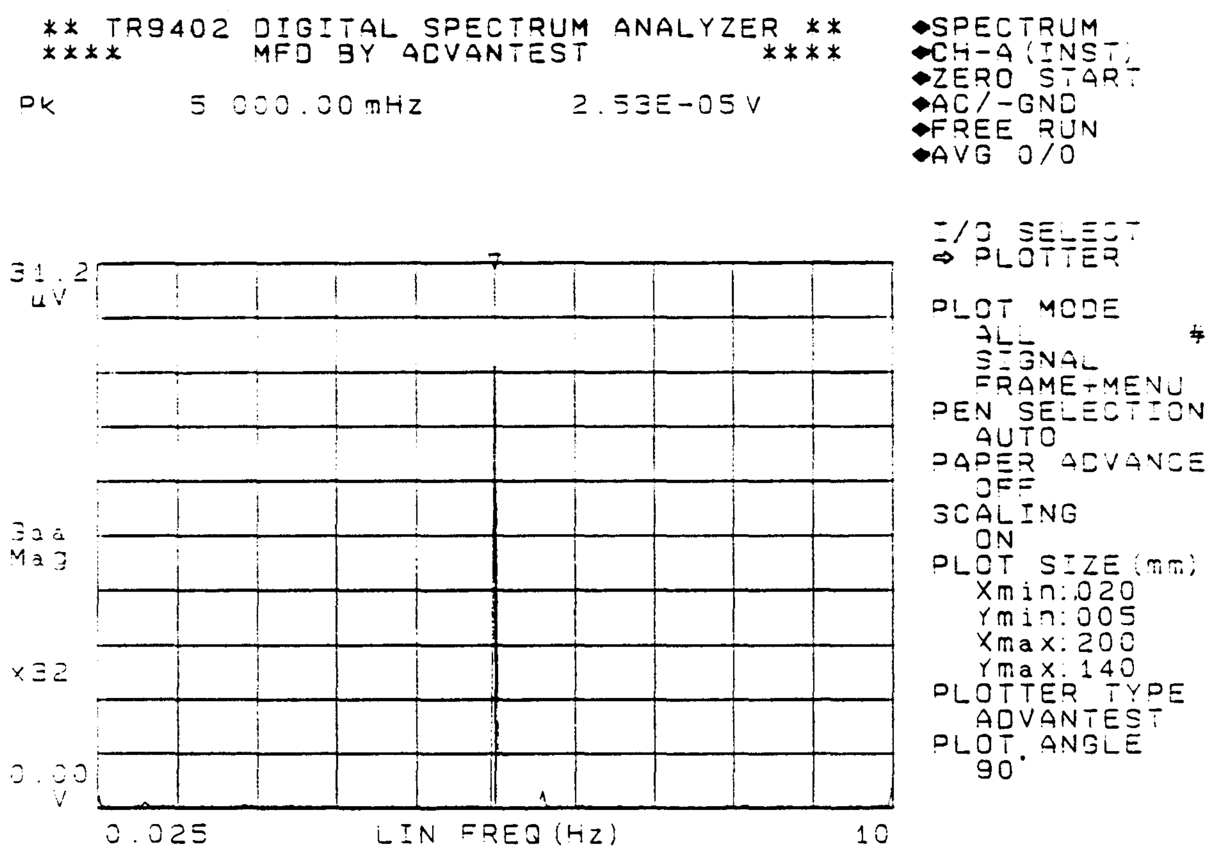

Fig. M7 Frequency spectrum of the filament noise if the reference flow is 30 ml/min.

14 References

1 Thermophysical properties of matter, Vol. 3, Thermal Conductivity, Y.S. Touloukian, P.E. Liley, S.C. Saxena, IFI/Plenum, NY-Washington, 1970, pp. 33, 345-346.

2 A. Wassiljewa, Phys. Zeitschrift, no. 22, vol. 5, Nov., 737, 1904.

3 Inleiding Meten 2 voor N2.2., J.A. Poulis, C.H. Massen, Internal lecture notes of the Eindhoven University of Technology, pp. 57-60.

4 Advances in Chromatography, Vol. 2, Edited by J.C. Giddings and R.A. Keller, Marcel Dekker Inc., New York, 1966, pp. 206-208.

5 Thermal Conductivity, Vol. 2, R.P. Tye, Academic Press, London-New York, 1969, pp. 88.

6 Detection Limits of Thermal Conductivity and Photo-ionization Detectors in High Speed Narrow Bore CGC, v. Es, C. Cramers and J. Rijks, Journal of HRC, vol. 12, may 1989, pp. 303-307.

7 Introduction to Heat and Mass Transfer, E.R.G. Eckert, Mc Graw Hill, New York, 1963, pp. 101-102.

8 Methods of Experimental Physics, Fluid Dynamics, Vol. 13A, Academic Press, New York, 1981.

9 An Introduction to Fluid Mechanics and Heat Transfer, J. M. Kay, Cambridge, 1963.

10 Transport Phenomena, R. Byronn Bird, W.E. Stewart, E.N. Lightfoot, John Wiley and Sons Inc., New York, 1960.

11 Thermophysical Properties of matter, Vol. 6, Specific Heat of Nonmetallic Liquids and Gases, Y.S. Touloukian, T.

Makita, IFI/Plenum, New York, Wilmington, 1970, pp. 24.

12 An analysis of the finite element method, G. Strange and G.J. Fix, Prentice Hall, 1973

13 Applied finite element analysis, L.J. Segerlind, Wiley, London, 1976.

14 Finite element solution of boundary value problems; Theory and Computation, O. Axelsson and V.A. Barker, Academic Press, 1984.

15 Fundamentals of the finite element method, H. Grandin Jr., Macmillan, New York, 1986.

16 SEPRAN Analysis by Guus Segal; a condensed report of the user manual of SEPRAN, Internal lecture note of the Eindhoven University of Technology, 1989.

15 Appendices

Appendix 1: SEPRAN finite elements analysis program

```
*******       This program solves the Navier-Stokes equation iterativelly
              after using the velocity obtained by solving the linear
              Stokes equation as a first approximation.
              The results are presented in a velocity vector field plot.
              Finally, isobars and streamlines are computated and plotted.
      program main
      implicit double precision(a-h,o-z)
c     by T.Dassen
*******       defining work arrays
      dimension kmesh(100),kprob(100),intmat(5),matr(5)
      dimension isol(5),irhsd(5),iwork(10),work(10),iuser(100)
      dimension user(100),contln(20),isol1(5),ipres(5),
     v        istrm(5)
      kmesh(1)=100
      kprob(1)=100
      iuser(1)=100
      user(1)=100
      contln(1)=20
*******       generating and plotting the computational mesh
      call start(0,2,0,0)
      call mesh(0,iinput,rinput,kmesh)
*******       defining the boundary condition for the velocity
      call probdf(0,kprob,kmesh,iinput)
      jmetod=2
      value=funcbc(ichois,x,y)
      call commat(jmetod,kmesh,kprob,intmat)
      call bvalue(0,2,kmesh,kprob,isol,0d0,1,3,1,0)
      call bvalue(0,2,kmesh,kprob,isol,0d0,6,6,1,0)
      call bvalue(1,2,kmesh,kprob,isol,value,1,2,2,0)
      call bvalue(0,2,kmesh,kprob,isol,0d0,3,3,2,0)
      call bvalue(0,2,kmesh,kprob,isol,0d0,6,6,2,0)
      do 10 i=1,10
      work(i)=0d0
      iwork(i)=0
 10   continue
      work(1)=1d-6
      work(2)=1.79              density of helium at T = 273 K.
      work(8)=2.65d-5             viscosity of helium at T = 273 K.
      iwork(7)=1
*******       solving the Stokes equation
      call fil100(1,iuser,user,kprob,8,iwork,work)
      call system(1,matr,intmat,kmesh,kprob,irhsd,isol,
     v          iuser,user,islold,ielhlp)
      call solve(0,matr,isol,irhsd,intmat,kprob)
      call prinrv(isol,kmesh,kprob,4,0,'solution')
      factor=0
      plotfm=15d0
      yfact=1d-1
      call plotvc(1,2,isol,isol,kmesh,kprob,plotfm,yfact,
     v          factor)
*******       solving the Navier-Stokes equation iterativelly
      iwork(3)=2
      iter=0
      do 20 j=1,10
      iter=j
```

```
      call copyvc(isol,isol1)
      call fil100(1.iuser,user,kprob,8,iwork,work)
      call system(-1,matr,intmat,kmesh,kprob,irhsd,isol,
     v         iuser,user,isol1,ielhlp)
      call solve(0,matr,isol,irhsd,intmat,kprob)
      call diffvc(0,isol,isol1,kprob,difmax)
      if (difmax.lt.1d-3) goto 30
20    continue
30    write(6,*)'the number of strokes is ',iter
      call prinrv(isol,kmesh,kprob,4,0,'solution')
*******          plotting the velocity vector field
      call plotvc(1,2,isol,isol,kmesh,kprob,plotfm,yfact,0)
      call deriva(ichois,1,ix,jdegfd,ivec,ipres,
*******          calculating isobars and streamlines of the flow
     v   kmesh,kprob,isol,isol,iuser,user,ielhlp)
      call prinrv(ipres,kmesh,kprob,4,0,'pressure values')
      call plotc1(1,kmesh,kprob,ipres,contln,-15,
     v         plotfm,yfact,0)
      call stream(1,ivec,istrm,0,psiphi,kmesh,kprob,isol)
      call prinrv(istrm,kmesh,kprob,4,0,'stroomfunctie')
*******          plotting the isobars and streamlines
      call plotc1(1,kmesh,kprob,istrm,contln,-10,
     v         plotfm,yfact,0)
      call finish(0)
      end
*******          self-defined velocity inlet profile
      function funcbc(ichois,x,y)
      implicit double precision(a-h,o-z)
      if (ichois.eq.1) then
      x=((x-0.15d0)/0.15d0)**2d0
      x=1-x
      funcbc=60d0*x
      endif
      end
```